FP7-ICT-611140 CARRE

Project co-funded by the European Commission
under the Information and Communication Technologies
(ICT) 7th Framework Programme

D.3.2. Sensors and Aggregators for Personal Sensor Data

UPDATE: Investigation of possibilities to develop sensors and algorithms for cardiorenal patient monitoring

V. Marozas, D. Stankevičius, S. Daukantas, A. Petrėnas, T. Mickus, D. Jegelevičius, A. Sološenko, D. Sokas, A. Third, A. Lukoševičius

October 2016

CARRE Contacts

Project Coordinator:	Eleni Kaldoudi	kaldoudi@med.duth.gr
Project Manager:	George Drosatos	gdrosato@ee.duth.gr

DUTH Democritus University of Thrace	Eleni Kaldoudi	kaldoudi@med.duth.gr
OU The Open University	John Domingue	john.domingue@open.ac.uk
BED: Bedfordshire University	Enjie Liu	Enjie.Liu@beds.ac.uk
VULSK: Vilnius University Hospital Santariskių Klinikos	Domantas Stundys	Domantas.Stundys@santa.lt
KTU Kaunas University of Technology	Arunas Lukosevicius	arunas.lukosevicius@ktu.lt
PIAP Industrial Research Institute for Automation & Measurements	Roman Szewczyk	rszewczyk@piap.pl

Disclaimer

CARRE is a Specific Targeted Research Project partially funded by the European Union, under FP7-ICT-2013-10, Theme 5.1. “Personalized health, active ageing& independent living”.

Document Control Page

Project	
Contract No.:	611140
Acronym:	CARRE
Title:	Personalized Patient Empowerment and Shared Decision Support for Cardiorenal Disease and Comorbidities
Type:	STREP
Start:	1 November 2013
End:	31 October 2016
Programme:	FP7-ICT-2013.5.1
Website:	http://www.carre-project.eu/
Deliverable	
Deliverable No.:	D.3.2
Deliverable Title:	Sensors and Aggregators for Personal Sensor Data: Update 1
Responsible Partner:	KTU – Dr. Saulius Daukantas
Authors:	V. Marozas, D. Stankevičius, S. Daukantas, A. Petrėnas, T. Mickus, D. Jegelevičius, A. Sološenko, D. Sokas, A. Third, A. Lukoševičius
Input from:	KTU, DUTH, PIAP, OU
Peer Reviewers:	G. Drosatos (DUTH), D. Stundys (VULSK), E. Liu (BED)
Task:	T 3.2. Sensors and Aggregators for Personal Sensor Data
Task duration:	10 months: 1 March 2014 to 31 January 2015
Work Package:	WP3: Data and metadata harvesting
Work Package Leader:	KTU – Arunas Lukosevicius
Due Date:	31 Jan 2015
Actual Delivery Date:	2 Feb 2015
Update #1:	8 Nov 2016
Dissemination Level:	PU
Nature:	P
Files and format:	Deliverable report: 1 pdf file Software source code: (1) Sensor aggregator responder v0.2: 2 zip files (Java code and Java binary); (2) Historical data retriever v1.0: 1 zip file (Python code); (3) Triple store v1.0: 1 zip file (Python code); (4) CARRE Multiparametric Scales Data Analyzer v1.0: zip file (Matlab code)
Version:	06
Status:	☐ Draft ☒ Consortium reviewed ☒ WP leader accepted ☒ Coordinator accepted ☐ EC accepted

Document Revision History

Version	Date	Modifications	Contributors
v01.0	7 Jul 2014	New content – outline	V. Marozas, A. Lukoševičius
v01.1	8 Jul 2014	New content – outline and aggregator structure	V. Marozas, A. Lukoševičius, D. Stankevicius
v01.2	8 Aug 2014	New content – revision of outline	V. Marozas
v01.3	16 Oct 2014	New content – revision of outline	A. Lukoševičius
v01.4	1 Nov 2014	New content – revision of outline	V. Marozas
v01.5	29 Nov 2014	New content – revision of outline	A. Lukoševičius
v01.6	07 Dec 2014	New content – new content added in different chapters	V. Marozas
v02.1	14 Dec 2014	New content – weight scales resolution experiment results	V. Marozas
v02.2	6 Jan 2015	New content added in chapter 2	S. Daukantas
v02.3	9 Jan 2015	New content in chapters 2.3 and 3.1	D. Stankevičius
v02.3	9 Jan 2015	New content in chapters 2.3 and 3.1	D. Stankevičius
v02.4	17 Jan 2015	New content in chapter 2.1	V. Marozas
v02.5	20 Jan 2015	Structure revision	A. Lukoševičius, V. Marozas
v02.6	21 Jan 2015	Structure changes, content revision and update	A. Lukoševičius, V. Marozas D. Stankevičius, S. Daukantas
V02.7	21 Jan 2015	Feedback and comments	E. Kaldoudi
v02.8	22 Jan 2015	Structure changes, content revision and update	V. Marozas, D. Stankevičius, S. Daukantas
v02.9	23 Jan 2015	Content added in subsections 4.1, 4.2, 4.3	A. Third
v03.0	25 Jan 2015	Content added in chapters 1, 2 and executive summary is written	D. Stankevičius, V. Marozas, A. Lukoševičius
v03.1	26 Jan 2015	Content added in chapter 2.1	D. Stankevičius, V. Marozas
v03.2	27 Jan 2015	Content added in chapter 3.3, schematics updated in chapter 4.1	A. Sološenko, S. Daukantas, D. Stankevičius
v03.3	27 Jan 2015	Content added in chapters 2.3 and 4.4	V. Marozas, D. Stankevičius
v03.4	28 Jan 2015	Content added in chapter 2.3	D. Stankevičius, V. Marozas
v03.5	31 Jan 2015	Reviewers' feedback added	V. Marozas
v04	02 Feb 2015	Formatting for QA conformance	E. Kaldoudi

Updated Document Revision History

v05.1	26 May 2016	Outline of updates	V. Marozas
v05.2	20 June 2016	Chapter 3.2 update	D. Stankevičius, V. Marozas,
v05.3	27 Sep 2016	Chapter 3.1 update	A. Petrėnas, A. Sološenko

v05.4	21 Oct 2016	Chapter 3.3 update	S. Daukantas, V. Marozas, D. Sokas, D. Jegelevičius, A. Lukoševičius
v05.6	29 Oct 2016	Reviewers' feedback added	V. Marozas
V06	30 Oct 2016	Formatting for QA conformance	E. Kaldoudi

Table of Contents

List of Figures

List of Tables

Executive Summary

This deliverable contains detailed information on sensors used for the acquisition of personal data as well as appropriate data aggregator architecture and implementation. After previous analysis of observables and data sources needed for monitoring of personal health data of patients having cardiorenal risks the most suitable sensor candidates from the market were selected. Four groups of monitoring sensors – for weight and body composition; for physical activity; blood glucose measurement; and cardiovascular state were tested and evaluated with the aim to compare testing results and to recommend the most reliable, unobtrusive, accurate and software-friendly ones for the use of patients in pilot sites. Since commercially available sensors do not cover fully all monitoring requirements, results of investigation of possibilities to develop new sensors and algorithms are presented as well. Among new developments is wristwatch for continuous monitoring of health parameters, an innovative algorithm for arrhythmia detection and smart scales for intermittent monitoring of body hydration and cardiovascular parameters. Architecture of aggregator for integration of all sensor data into CARRE semantic repository using cloud services was developed and details of implementation presented.

About CARRE

CARRE is an EU FP7-ICT funded project with the goal to provide innovative means for the management of comorbidities (multiple co-occurring medical conditions), especially in the case of chronic cardiac and renal disease patients or persons with increased risk of such conditions.

Sources of medical and other knowledge will be semantically linked with sensor outputs to provide clinical information personalised to the individual patient, so as to be able to track the progression and interactions of comorbid conditions. Visual analytics will be employed so that patients and clinicians will be able to visualise, understand and interact with this linked knowledge and also take advantage of personalised empowerment services supported by a dedicated decision support system.

The ultimate goal is to provide the means for patients with comorbidities to take an active role in care processes, including self-care and shared decision-making, and also to support medical professionals in understanding and treating comorbidities via an integrative approach.

Terms and Definitions

The following are definitions of terms, abbreviations and acronyms used in this document.

Term	Definition
AAMI	Association for the Advancement of Medical Instrumentation, is a nonprofit organization founded in 1967. Mission - supporting the healthcare community in the development, management, and use of safe and effective medical technology.
Accuracy	According to ISO 5725-1, Accuracy consists of Trueness (proximity of measurement results to the true value) and Precision (repeatability or reproducibility of the measurement)
AF	Atrial Fibrillation
AHI	Apnea-hypopnea index
API	Application Programming Interface
BHS	British Hypertension Society
BIA	Bioelectrical Impedance Analysis
BIS	Bioelectrical Impedance Spectrography
BIVA	Bioelectrical Impedance Vector Analysis
BLE	Bluetooth Low Energy
BP	Blood Pressure
BPM	Blood Pressure Monitor
Data source	Devices and sensors (e.g. weight scales, physical activity monitors), personal health record, electronic medical record, personalized information on lifestyle (e.g. Facebook, Twitter), sources of medical evidence and other medical authoritative information (e.g. PubMed), on-line patient educational sources (e.g. MedlinePlus)
Diastolic BP	Diastolic blood pressure – lower of the two numbers which shows the pressure in the arteries when the heart muscle is resting between beats and refilling with blood.
ECG	Electrocardiogram – graphical representation of electrical cardiac activity registered by using biopotential electrodes.
ESH	European Society of Hypertension
GET	HTTP method
GPS	Global Positioning System
HTTP	Hypertext Transfer Protocol
IPG	Impedance plethysmogram – graphical representation of mechanical cardiac activity registered by sensing impedance changes.
JSON	JavaScript Object Notation
LCD	Liquid Crystal Display
MET	Metabolic equivalent
NIBP	Noninvasive blood pressure. Mostly measured by two methods: auscultatory (manual), oscillometric (automatic)
Observable	Physical variable that can be measured or otherwise ascertained (e.g. biomarkers, biometric variables, biological signals and other non-biological factors e.g. environmental).
OGTT	Oral Glucose Tolerance Test

PAF	Paroxysmal atrial fibrillation is an episode of uncoordinated movement of the cardiac atria and irregular heart that occurs occasionally and then stops. Episodes can last from minutes to days before stopping and returning to normal “sinus” rhythm.
PAT	Pulse arrival time is associated with pulse wave velocity and is defined as the time interval between the R-wave of the QRS complex in the electrocardiogram and the particular point in the pulse pressure wave recorded at the distal artery.
PC	Personal Computer
POST	HTTP method
PPG	Photoplethysmogram - graphical representation of mechanical cardiac activity registered by using optical sensor.
PVC	Premature Ventricular Contraction
RDF	RDF (Resource Description Framework) is a standard model for data interchange on the Web.
Systolic BP	Systolic blood pressure – higher of the two numbers, which shows the pressure in the arteries when the heart muscle contracts.
SPARQL	An RDF query language. http://www.w3.org/2009/sparql/
SD	Standard deviation of measurements.
TBW	Total body water
URL	Uniform Resource Locator, a.k.a. a web address

List of Major Updates

This document is an update of Deliverable D.3.2. Sensors and Aggregators for Personal Sensor Data, originally submitted on January 2015.

Major updates include the following:

1. The structure of the Chapter 3 was changed.
2. Section 3.1 was updated with more details about the updated ECG signal analyser GUI. The updates concern with extension of functionality and stability of the software module. Also short description of implementation (porting to JAVA) of the developed algorithm in CARRE Life style aggregator is presented.
3. Section 3.2 was rewritten and updated with the information about the wrist worn device hardware implementation, the algorithm details for PPG based atrial fibrillation detection, performance evaluation of the algorithm and continuation of the development and exploitation.
4. Section 3.2 was also rewritten and updated with information about multiparametric weight scales hardware and software implementation. Software includes firmware of the multiprocessor device and personal computer application “Multiparametric Scales Data Analyzer” which is a GUI to analyse the GDF data files registered with the instrument.
5. New Section 3.3.6 provides analysis of medical regulatory requirements related to the developed devices. The related standards were identified and analysed.
6. New Section 3.3.7 presents a concept of modification to biomedical file standard. The proposed modification concerns general data format (GDF) security and subject data privacy.
7. Annexes 2 and 3 were added.

1. Introduction

This document is a report of the project Task 3.2 “Sensors and Aggregators for Personal Sensor Data”. It is based on previous project deliverables:

- D.2.2 “Functional Requirements & CARRE Information Model”, where patient risks and needed observables were analyzed and classified from the point of view of medical domain specifics and CARRE information model;
- D.2.3 “Data source identification and description”, where data sources were analyzed and review of all available appropriate sensors presented; and
- D.3.1 “Aggregator Module Generic Design”, where the concept of data aggregation of all data sources including personal sensors is presented.

The aim of Task 3.2 is to determine an appropriate set of sensors, evaluate their accuracy, reliability, robustness and security using testing results of available 3rd party candidates as well as to capture the semantics of monitoring data, i.e. to ensure semantic sensors data linking and aggregation into CARRE data repository. Section 2 of this report present testing and evaluation of selected 3rd party sensors and conclusions regarding their characteristics and applicability. Section 3 investigates possibilities to develop new sensors and algorithms needed to cover specific needs of monitoring which are not covered by commercially available sensors and also for data aggregator architecture and cloud services as well as for implementation issues. Finally, Section 4 presents the details of the development and implementation of the aggregators for the selected sensors.

Annex 1 gives links for downloading the actual D.3.3 deliverable which is the sensor aggregator software developed in T.3.2 (and described in detail in this report).

2. Testing and evaluation of the 3rd party sensors

2.1. Sensors for weight and body composition monitoring

2.1.1. Selected sensors for investigation

Based on previous investigation in Task 2.3, the following devices for weight and body composition monitoring have been preselected for investigation:

- iHealth HS5 Wi-Fi[1] (entitled as iHealth)
- Medisana BS 440 Connect[2](entitled as Medisana)
- Medisana Target Scale 2[3] (entitled as Targetscale)

As the list of observables has been updated and the total body water (TBW) parameter had been removed, two additional scales were included in investigation:

- Withings Smart Body Analyzer4 (entitled as Withings)
- Fitbit Aria Scale5 (entitled as Fitbit)

[1] http://www.ihealthlabs.com/wireless-scales/wireless-body-analysis-scale/ (Last accessed: 01/21/2015)

[2] http://www.medisana.com/en/Health-control/Personal-scales/Body-analysis-scale-with-Bluetooth-BS-440-connect.html (Last accessed: 01/21/2015)

[3] http://www.vitadock.com/targetscale/targetscale-benefits.html (Last accessed: 01/21/2015)

[4] http://www.withings.com/us/smart-body-analyzer.html (Last accessed: 01/24/2015)

[5] http://www.fitbit.com/aria (Last accessed: 01/24/2015)

2.1.2. Testing and evaluation methodology

The testing of the selected devices was accomplished by comparison to the reference device (see Figure 1). Three main parameters: weight (kg), Total Body Water (%) and Fat (%) were used for comparison. Professional Tanita TBF-300A Body Composition Analyzer (Tanita Corporation, Tokyo, Japan) was used for the reference measurements. Bio-impedance analysis measurements of this device are declared by manufacture to be within 5% of DEXA (Dual-energy X-ray absorptiometry), the gold standard.

There were performed 2 tests for weight (kg), fat (%) and Total Body Water (%) measurement accuracy estimation:

- Test No.1: 10 subjects (2 females), 30 measurements with each weight scale (Targetscale, Medisana, iHealth)
- Test No.2: 14 subjects (2 females), 42 measurements with each weight scale (Withings, Fitbit).

Each subject stood on the scale three times on each scale in series. Weight and fat percentage was measured. Personal information, such as the date of birth, height and sex was filled in to the user account at the beginning. Account information was synchronized with the scale prior to the measurement.

The 3rd test aimed to investigate linearity of body weight change detection by the devices. One subject participated in the experiment. The subject weight was increased linearly in the range of 0 – 1 kg with small additions (0.1 kg) of liquid to the small tank held by the subject. The test was repeated 3 times.

Bland – Altman diagrams[6] are used for visual presentation of testing results. The accuracy components (mean of differences and standard deviation) are summarized in table for numerical comparisons.

a) b) c)

Figure 1. Body composition scales: Medisana (a, top), Withings (a, bottom), Tanita (b, top), Targetscale (b, bottom), iHealth (c, top), Fitbit (c, bottom)

[6] Altman DG, Bland JM (1983). "Measurement in medicine: the analysis of method comparison studies". The Statistician 32: 307–317

2.1.3. Results of testing and comparison

The results of weight scales testing are presented by Bland - Altman diagrams (Figure 2 – Figure 4) and summary is presented in Table 1. In weight measurement, the lowest mean error is achieved by the Fitbit scale with error of 0.00±0.12 kg. However, its SD of error is slightly higher than the Withings scale. The Withings scale overestimates weight by 0.19±0.08 kg. The Medisana scale also shows good performance with error of -0.07 ±0.17 kg.The least accurate weight scale is the Targetscale. It overestimates weight by 0.42±0.15 kg. iHealth weight scale demonstrated average accuracy (0.21±0.28 kg).

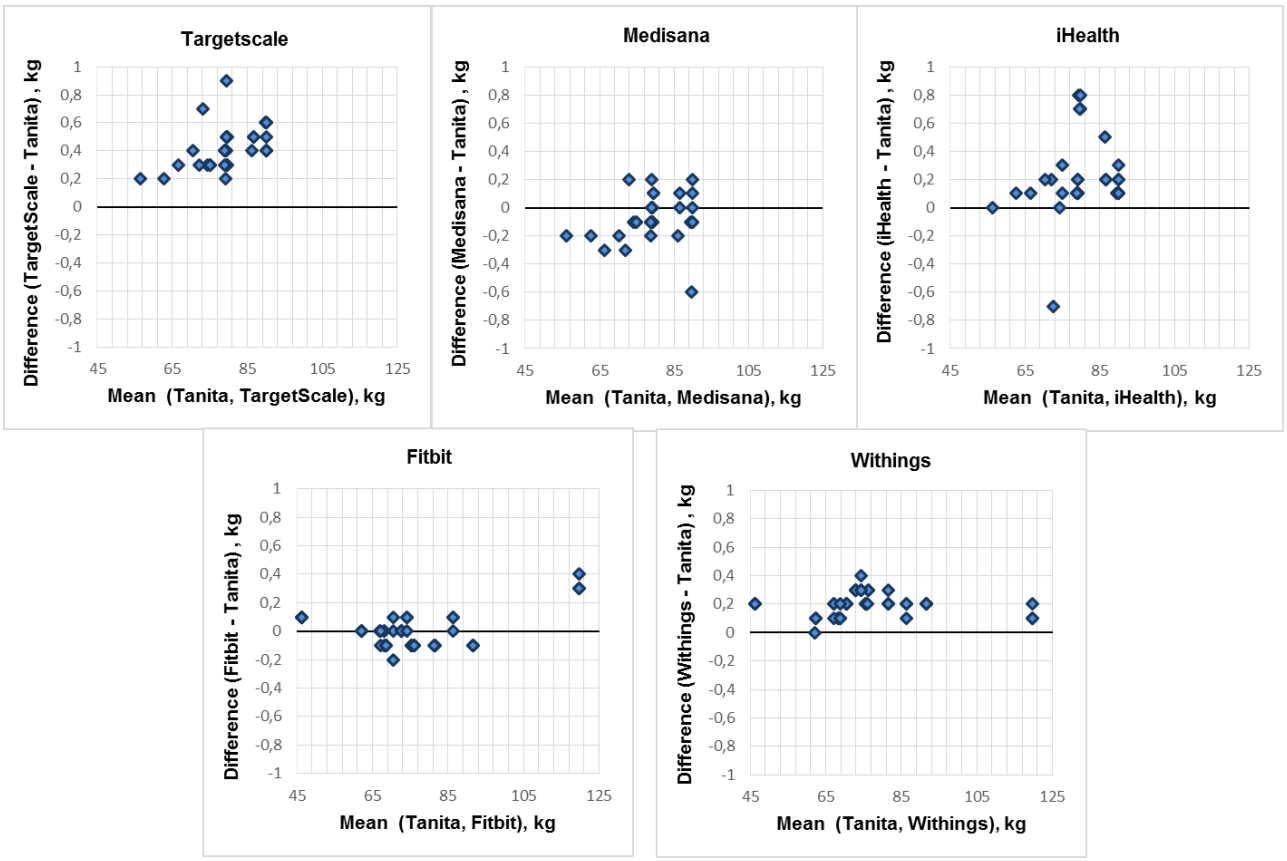

Figure 2. Testing results: weight

All tested body composition weight scales were able to estimate body fat percentage. The testing results in terms of Bland – Altman diagrams are presented in Figure 3. Fitbit and iHealth scales showed the best performance with error of 0.84±0.62% and 0.75±0.53% respectively. The mean error of Medisana scale is even lower (0.28%) but SD is much higher (2.42%) than the previous two. The worst performance was demonstrated by Targetscale (0.94±2.96%). The average performance was shown by Withings scale (1.72±1.25%).

Parameter “Total body water” was measured by only 3 out of 5 scales: Targetscale, Medisana, iHealth. Each of these scales demonstrates average performance. Targetscale and Medisana scale have low mean error (0.07% and 0.35% respectively) but high SD (1.97% and 2.19%, respectively). On the other hand, iHealth scale has lower SD (0.90%) but very high mean error (-4.00%).

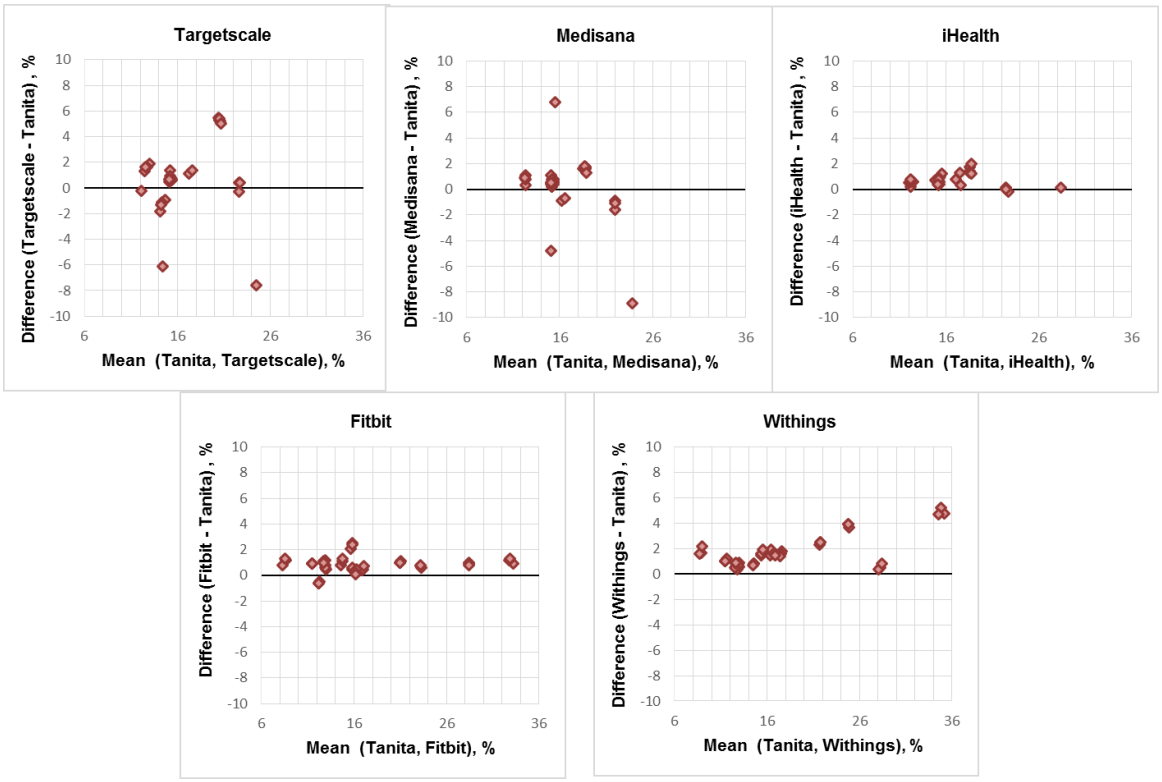

Figure 3. Testing results: fat

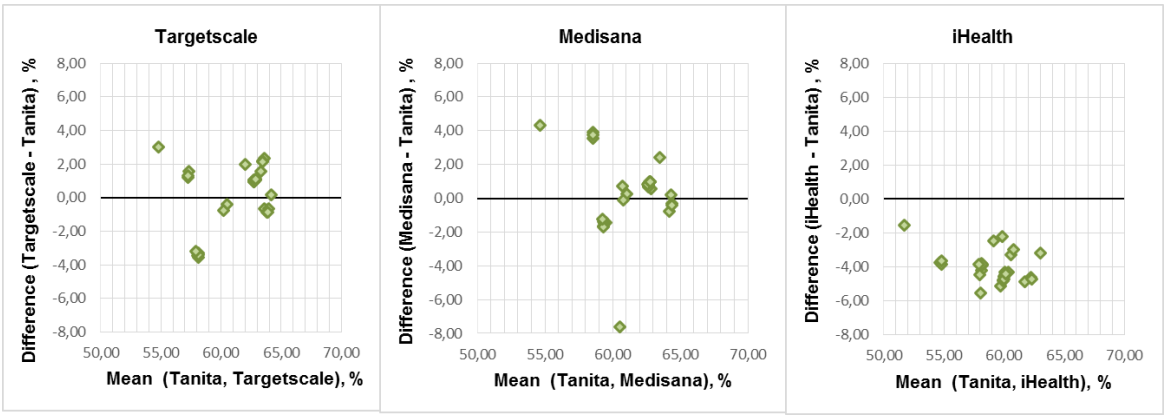

Figure 4. Testing results: Total Body Water (TBW)

Table 1. Comparison of weight scales						
Device	Error in weight, kg		Error in fat, %		Error in TBW, %	
	Mean	SD	Mean	SD	Mean	SD
Targetscale	0.42	0.15	0.94	2.96	0.07	1.97
Medisana	-0.07	0.17	0.28	2.42	0.35	2.19
iHealth	0.21	0.28	0.75	0.53	-4.00	0.90
Fitbit	0.00	0.12	0.84	0.62	N/A	N/A
Withings	0.19	0.08	1.72	1.25	N/A	N/A

The results of the 3rd test are presented in Figure 5. It can be observed that Medisana and Withings scales were unable to detect small changes (0.1 kg) of weight in several instances. However, these errors are within the manufacturers specifications. Therefore all these devices are suitable in weight change detection.

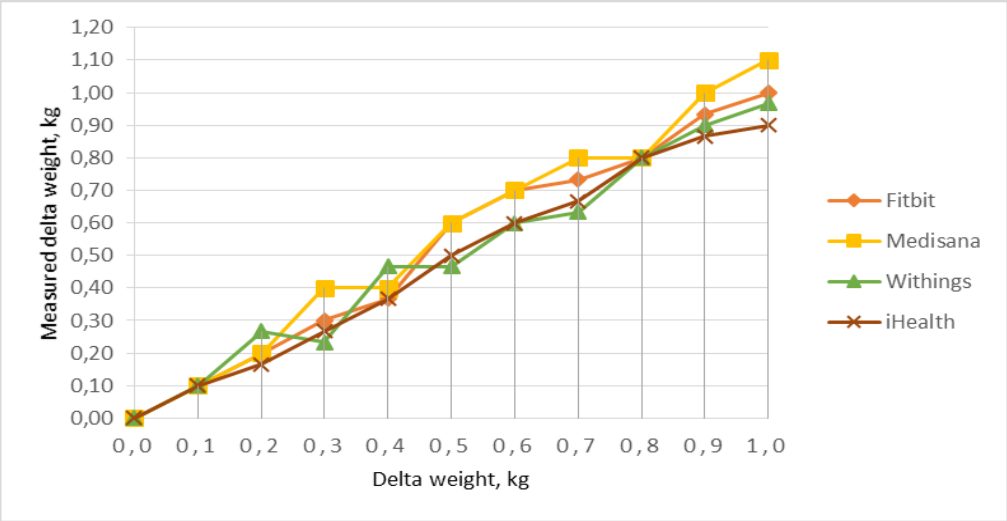

Figure 5. Body weight change detection

2.1.4. Conclusion

Accuracy of all devices for weight measurement is acceptable. Medisana scale (price 70 EUR) provides the largest amount of observables (including Total Body Water), but its usability requires improvement. iHealth scale (price 120 EUR) has the worst performance and inadequate mechanical design. Fitbit scale (price 130 EUR) is the most accurate, but it synchronizes only via Wi-Fi network. On the other hand, the accuracy of the Withings scale (price 150 EUR) is slightly worse than Fitbit, but it also measures heart rate, which is another important observable. Withings scale synchronizes via Wi-Fi network, or via Bluetooth, if Wi-Fi is not available.

In final conclusion:

- Fitbit scale is recommended if kidney related observables (such as weight) are more important than heart related observables, and there is a Wi-Fi network available at patient's home;
- Withings scale is recommended if heart related observables (such as heart rate) are more important than kidney related observables, or there is no Wi-Fi network available at the patient's home;
- Medisana scale is recommended if hydration related observables are important.

2.2. Sensors for physical activity monitoring

2.2.1. Selected sensors for investigation

Based on previous investigation in Task 2.3, the following devices have been preselected for investigation:

- Fitbit One[7] (entitled as One)
- Fitbit Flex[8] (entitled as Flex)

[7] http://www.fitbit.com/one (Last accessed: 01/09/2015)

[8] http://www.fitbit.com/flex (Last accessed: 01/09/2015)

- iHealth Wireless Activity and Sleep Tracker[9] (entitled as iHealth)
- Medisana VIFIT Connect[10] (entitled as Vifit)
- Samsung Gear Live[11] (entitled as Gear)

Also, the following smartphone apps have been selected:

- Samsung S Health[12] (entitled as Shealth)
- Moves[13] (entitled as Moves)
- Endomondo Sports Tracker[14] (entitled as Endo)
- Google My Tracks[15] (entitled as Tracks)

2.2.2. Testing and evaluation methodology

The testing of the selected devices was accomplished by comparison to the reference methods. Three main parameters: step count, distance traveled and energy consumption (calories burned) were used for comparison. The following testing equipment was used for the reference measurements:

- Cosmed K4b2 – portable system for indirect calorimetry measurement of energy consumption (in kcal) with additionally placed GPS sensor for distance measurements (m);
- KTU BII Cardiologger v6 attached to the waist was used to acquire accelerometer signal. Later on, interactive peak detection based step counting algorithm (implemented in Matlab, Mathworks Inc.) was used for step count calculation.

One of the test subjects is presented in Figure 6 with all testing equipment on.

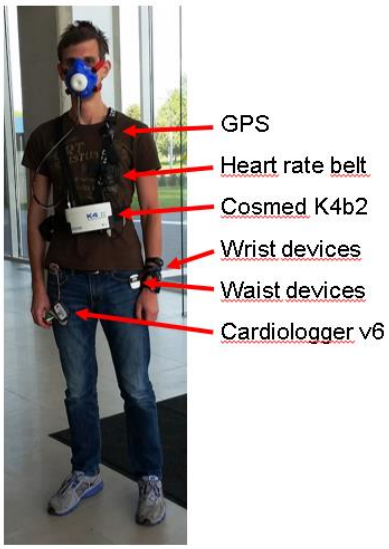

Figure 6. Mounting of testing equipment and sensors on the subject

[9] http://www.ihealthlabs.com/fitness-devices/wireless-activity-and-sleep-tracker/ (Last accessed: 01/09/2015)

[10] http://www.medisana.com/en/Sport/Activity-Tracker/ViFit-connect-Activity-Tracker-mag.html (Last accessed: 01/09/2015)

[11] http://www.samsung.com/global/microsite/gear/gearlive_design.html (Last accessed: 01/09/2015)

[12] http://content.samsung.com/us/contents/aboutn/sHealthIntro.do (Last accessed: 01/09/2015)

[13] https://www.moves-app.com/ (Last accessed: 01/09/2015)

[14] https://www.endomondo.com/ (Last accessed: 01/09/2015)

[15] https://play.google.com/store/apps/details?id=com.google.android.maps.mytracks (Last accessed: 01/09/2015)

The overall testing comprised of two main parts:

- Controlled environment test – a short test at the beginning of each experiment comprising of two simple walking and running exercises at the fixed distance and pace. The purpose of this test was to estimate the average step length while walking and running, therefore only accelerometer device was used as a reference. Some of the commercial devices required such step length data (see Table 2.) in order to track distance more accurately. It was also useful to determine the behavior of the devices in relatively short physical activity episodes. This test was accomplished in the hall of the KTU Santaka Valley building, which is 80 m long (see Figure 7). After this test, all required data was calculated and synchronized with the devices.
- Uncontrolled environment test – the main test where the participant was able to choose his own walking pace and some parts of the route. All equipment, described earlier, was used. Data was recorded after each part. This test was divided into 4 parts:
  - 1000 m long casual walking exercise where the participant was able to choose his own walking pace. The default route for the exercise was predefined (see Figure 7). It was designed to represent common walking activities in daily life.
  - 200 m long running exercise – short exercise of running 100 m forward and back without stopping, at a slow pace (close to jogging). This was carried out in order to find out how well each device works under running conditions.
  - 200 m long slow walking exercise – walking 100 m forward and back without stopping, at a very slow pace. This was carried out in order to find out how well each device works under non-standard walking conditions.
  - 5 floors stair climbing exercise was carried out mainly in order to find out how well energy estimation works in each device. There can be no distance estimation comparison, because the GPS sensor does not work inside the building.

Figure 7. Controlled environment testing site (left) and the uncontrolled environment testing track (right)

Table 2. Personal data required before the test					
Device	Birth date	Height	Weight	Step length	Running step length
Flex	✓	✓	✓	✓	✓
One	✓	✓	✓	✓	✓
iHealth	✓	✓	✓	–	–
Vifit	–	✓	✓	✓	–
Gear	–	–	–	–	–
Shealth	–	✓	✓	–	–
Moves	–	–	–	–	–
Tracks	–	–	✓	–	–
Endo	✓	✓	✓	–	–

The whole protocol can be described briefly:

1. Controlled environment 160 walking test (80 m forward and back with pause).
2. Controlled environment 160 running test (80 m forward and back with pause).
3. Uncontrolled environment 1000 m walking test (round track, no pause).
4. Uncontrolled environment 200 m running test (100 m forward and back, no pause).
5. Uncontrolled environment 200 m slow walking test (100 m forward and back, no pause).
6. Uncontrolled environment 5 floors climbing test (5 floors up and down, pause on the top).

Overall, 4 subjects participated in the experiments: 3 males and 1 female. The results were processed calculating relative error for each measurement. In order to summarize the results, the mean value and the standard deviation of the relative errors were calculated. However, due to the small number of participants, we decided to additionally use the non-parametric Mann-Whitney U test[16] statistic method. It is the null hypothesis test, where the null hypothesis is that datasets from a tested device and the reference are the same. The p value shows probability of the null hypothesis.

The results were divided in two categories:

- simple walking activities (including 1st, 3rd and 5th exercises);
- less frequent activities (including 2nd, 4th and 6th exercises).

In order to rank the physical activity devices and mobile apps, the following criteria were used:

1. The mean error is the most significant.
2. The SD of error is less significant than the accuracy.
3. The p value from the non-parametric test is the least significant.
4. Overall, the first category (simple walking activities) is more important than the second one (less frequent activities).

If the performance of the device (or the mobile app) is selected as the best in two or more criteria, the device is considered superior.

[16] Mann-Whitney U test. Online: http://en.wikipedia.org/wiki/Mann%E2%80%93Whitney_U_test (Last accessed: 01/09/2015)

2.2.3. Results of testing and comparison

Summarized results from the physical activity sensors testing are presented in the tables bellow. Table 3 – Table 5 fall into the first category (simple walking activities) and Table 6 – Table 8 fall into the second category (less frequent activities). Bold values depict the best result in each line. These best results were chosen individually for both – devices and apps.

Table 3. Results from controlled environment 160 m walking test.								
		Devices					Apps	
		Flex	One	iHealth	Vifit	Gear	Shealth	Moves
Error in steps	Mean	15,3%	**1,0%**	5,5%	48,5%	22,8%	**2,6%**	17,4%
	SD	16,8%	**0,6%**	7,3%	34,1%	32,4%	**2,1%**	12,0%
p value		0,206	**0,802**	0,397	0,206	0,206	**0,857**	0,198

Table 4. Results from uncontrolled environment 1000 m walking test.										
		Devices					Apps			
		Flex	One	iHealth	Vifit	Gear	Shealth	Moves	Tracks	Endo
Error in steps	Mean	-12,7%	**-0,8%**	-5,7%	-16,0%	-2,0%	-0,5%	**-0,4%**	N/A	N/A
	SD	11,2%	**1,1%**	4,8%	6,5%	3,9%	**1,6%**	9,1%	N/A	N/A
p value		0,056	**0,579**	0,222	0,032	0,548	0,310	**0,548**	N/A	N/A
Error in distance	Mean	-17,3%	**-5,8%**	-48,1%	-20,1%	N/A	10,0%	N/A	1,5%	**0,5%**
	SD	6,8%	4,5%	**2,4%**	4,2%	N/A	21,5%	N/A	3,2%	**0,8%**
p value		0,008	**0,016**	0,008	0,008	N/A	**0,841**	N/A	0,333	0,516
Error in energy	Mean	27,4%	**24,2%**	36,2%	-38,6%	N/A	-8,3%	N/A	**7,0%**	-9,3%
	SD	41,9%	17,2%	17,7%	**10,3%**	N/A	14,3%	N/A	30,8%	**10,9%**
p value		**0,151**	0,056	0,008	0,008	N/A	0,151	N/A	0,690	**0,802**

Table 5. Results from uncontrolled environment 200 m slow walking test.								
		Devices					Apps	
		Flex	One	iHealth	Vifit	Gear	Shealth	Moves
Error in steps	Mean	-17,4%	-7,4%	-17,5%	-24,0%	**-1,2%**	**1,1%**	-26,1%
	SD	21,2%	**6,5%**	19,8%	15,8%	8,7%	**10,5%**	26,5%
p value		0,200	0,486	0,486	0,114	**0,886**	**1,000**	0,114
Error in distance	Mean	**-3,4%**	13,6%	-39,9%	-9,4%	N/A	**11,0%**	N/A
	SD	**12,5%**	16,4%	19,2%	15,3%	N/A	**36,6%**	N/A
p value		**1,000**	0,143	0,029	0,343	N/A	**1,000**	N/A
Error in energy	Mean	65,6%	55,6%	61,4%	**-34,7%**	N/A	**-20,1%**	N/A
	SD	20,9%	26,2%	36,8%	**14,7%**	N/A	**15,8%**	N/A
p value		0,029	0,029	**0,114**	0,086	N/A	**0,343**	N/A

The Fitbit One is superior sensor among the physical devices in the simple walking activities category. It shows the best performance for all observables in controlled environment walking test, as well as in the uncontrolled environment test; it shows however a slightly lower performance (although not the worst) in slow walking test. On the contrary, there is no clear winner on the mobile apps side. Endomondo sports tracker showed the best

performance in long walking test, while Samsung S Health showed the best performance in short tests. Moves showed the best performance in counting steps during the long walk experiment. On the other hand, Samsung S Health is platform dependent (Samsung S4 and S5 only), while Moves does not output energy expenditure and Endomondo Sport Tracker use only GPS (which is not suitable for indoor monitoring).

Table 6. Results from controlled environment 160 m running test.								
		Devices					Apps	
		Flex	One	iHealth	Vifit	Gear	Shealth	Moves
Error in steps	Mean	-15,8%	-14,6%	**-7,7%**	-16,9%	-2,7%	**0,4%**	-76,5%
	SD	9,1%	**5,9%**	12,6%	19,2%	2,2%	**10,0%**	29,2%
p value		0,029	0,029	**0,457**	0,257	0,629	**1,000**	0,029

Table 7. Results from uncontrolled environment 200 m running test.								
		Devices					Apps	
		Flex	One	iHealth	Vifit	Gear	Shealth	Moves
Error in steps	Mean	-15,6%	-11,2%	-10,9%	-16,3%	**-1,8%**	**18,7%**	-84,4%
	SD	14,6%	7,0%	11,7%	17,2%	**2,1%**	37,5%	**4,6%**
p value		0,086	0,229	0,143	0,343	**0,857**	0,486	**1,000**
Error in distance	Mean	-44,9%	**-26,9%**	-56,8%	-45,8%	N/A	**8,0%**	N/A
	SD	**5,0%**	26,3%	22,9%	16,9%	N/A	**20,0%**	N/A
p value		0,029	**0,314**	0,029	0,029	N/A	**1,000**	N/A
Error in energy	Mean	59,4%	61,7%	66,2%	**-31,5%**	N/A	**58,0%**	N/A
	SD	**4,8%**	18,9%	21,7%	15,4%	N/A	**15,7%**	N/A
p value		0,029	0,029	0,029	**0,057**	N/A	**0,029**	N/A

Table 8. Results from uncontrolled environment stairs climbing test.								
		Devices					Apps	
		Flex	One	iHealth	Vifit	Gear	Shealth	Moves
Error in steps	Mean	-6,9%	0,7%	-1,3%	-19,4%	**0,6%**	**6,2%**	-22,9%
	SD	11,2%	**5,1%**	9,0%	11,2%	7,0%	**9,0%**	13,6%
p value		0,343	0,457	0,371	0,057	**0,486**	**0,886**	0,029
Error in energy	Mean	26,4%	27,2%	**17,3%**	-51,5%	N/A	**-31,8%**	N/A
	SD	16,4%	20,3%	11,4%	**3,2%**	N/A	**16,1%**	N/A
p value		0,057	**0,086**	0,057	0,029	N/A	**0,029**	N/A

Results from the less frequent activities testing experiments are inconclusive. Each device is superior in different test for the different observables. Such outcome should be expected as these devices probably are designed to be used in simple walking activities, which occur most of the time in one's daily life. On the mobile apps side, the Samsung S Health seems to perform better than the Moves app, but the problems stated earlier arise as well.

2.2.4. Conclusion

Fitbit One is clearly superior device for the physical activity monitoring in simple walking activities. While there is no other such device in the other category, the Fitbit One is proposed as the most appropriate device. Its

splash- and sweat-proof case, clear design, user-friendly mobile app and relatively low price only confirm this proposal. On the other hand, high error rates of energy estimation and limitations due to less frequent activities should be kept in mind.

We should also conclude that there is no superior app for the physical activity monitoring. While each app shows some advantages under specific conditions, their disadvantages are more important. The most important disadvantage is clear – mobile phone should be always carried by the person in order for the app to work precisely.

2.3. Sensors for blood glucose measurement

2.3.1. Usability and functionality investigation

Two personal glucometer devices were acquired for investigation: iHealth BG5[17], Medisana Meditouch 2[18]. Since we did not have any possibility to test the accuracy of these devices, this chapter includes only the usability and functionality investigation.

iHealth glucometer is wireless and synchronizes via iHealth Gluco-Smart[19] app. However, this app is unavailable in Europe at the moment. The device itself has on-board display which is very bright and not comfortable. The iHealth glucometer is quite expensive (price about 70 EUR) and works only with original iHealth strips.

The Medisana glucometer needs an USB connection and personal computer (PC) software in order to synchronize the data from the device to the cloud. However, the device has a 480 memory slots that enable to perform this synchronization only once in a while. Meditouch 2 has large and clear display, is relatively cheap (about 22 EUR) and seems to work with any kind of test strips.

2.3.2. Conclusion

The fact that iHealth Gluco-Smart app seems to be unavailable in Europe rules out the possibility to choose this device. Furthermore, the only disadvantage of Medisana Meditouch 2 against iHealth glucometer is the wired connection and PC software, but the on-board memory softens this problem. In overall, we propose to use Medisana Meditouch 2 glucometer for blood glucose monitoring.

2.4. Sensors for cardiovascular state monitoring

2.4.1. Selected sensors for investigation

Based on previous investigation in Task 2.3, the following devices for blood pressure monitoring have been preselected for investigation:

- Medisana BU575 Connect[20] (entitled as Medisana)
- iHealth BP5[21] (entitled as iHealth)

---

17 http://www.ihealthlabs.com/glucometer (Last accessed: 01/21/2015)

18 http://www.medisana.com/en/Health-control/Blood-glucose-monitor/MediTouch-2-mg-dL-Blood-glucose-monitor-incl-starter-set.html (Last accessed: 01/21/2015)

19 https://play.google.com/store/apps/details?id=jiuan.androidBg.start

20 http://www.medisana.com/en/Health-control/Blood-pressure-monitor/Upper-arm-blood-pressure-monitor-with-Bluetooth-BU-575-connect.html (Last accessed: 01/21/2015)

21 http://www.ihealthlabs.com/blood-pressure-monitors/wireless-blood-pressure-monitor/ (Last accessed: 01/21/2015)

– Withings Blood Pressure Monitor[22] (entitled as Withings)

Also, eMotion Faros 180°[23] ECG recording device have been selected for the simple testing, since there is no suitable investigation methodology and this device has no worthy competitors.

2.4.2. Testing and evaluation methodology

All providers of selected ambulatory blood pressure devices declare the same pressure measurement accuracy ±3 mm Hg[24,25,26] which seems suitable for ambulatory monitoring. However, resent debates raised some concerns about the accuracy of new "smart" (smartphones and App based) blood pressure monitors[27]. Thus we decided to test the selected devices.

There are 3 recognized protocols specifically designed for validation of blood pressure devices: 1) the British Hypertension Society (BHS) protocol[28], 2) the Association for the Advancement of Medical Instrumentation / International Standards Organization (AAMI/ISO) protocol[29], 3) the International Protocol published by the European Society of Hypertension (ESH)[30]. For example, AAMI standard says that the mean difference between different blood pressure measurement methods must be less than ±5 mmHg and the SD (standard deviation) must be less than ±8 mmHg with 85% of the measurements in the 20-250 mmHg range. Accuracy better than ±10 mmHg must be achieved with 95% of the measurements. All three standards require to perform validation of blood pressure measurement devices on human subjects against auscultatory method (standard mercury sphygmomanometer) with 2 human observers. ESH protocol requires 33 subjects, other two standards – 85 subjects. Due to many restrictions on subjects' population composition: age, gender, arm circumference etc. these device validation studies are complex, time consuming and expensive.

Less time consuming and cheaper BP monitoring device testing method is based on application of specialized patient simulators (Figure 8 (a), (b)). Patient simulators are devices used for testing and calibration of clinical patient monitors and they are able to simulate various vital signs: electrocardiogram, non-invasive blood pressure, invasive blood pressure, oxygen saturation, patient respiration, patient temperature etc. Both patient simulators (shown in Figure 8 (a), (b)) are able to simulate human blood pressure changes for both systolic and diastolic measures induced oscillometric vibrations in the whole dynamic range 20 -240 mmHg. The simulators are embedded in pneumatic circuit between BP monitor and cuff.

---

22 http://www.withings.com/us/blood-pressure-monitor.html (Last accessed: 01/21/2015)

23 http://www.megaemg.com/products/faros/ (Last accessed: 01/21/2015)

24 iHealth BP5 Technical Specs, http://www.ihealthlabs.com/blood-pressure-monitors/wireless-blood-pressure-monitor/ (Last accessed: 01/21/2015)

25 Medisana BU 575 connect, Manual, http://www.medisana.com/out/pictures/media/manual/51296bu575connectwestv1_4webam20140303.pdf (Last accessed: 01/21/2015)

26 Withings blood pressure monitor Tech specs, http://www.withings.com/us/blood-pressure-monitor-tech.html (Last accessed: 01/21/2015)

27 Inaccuracy plagues mobile blood pressure devices http://www.ehospitalistnews.com/index.php?id=2050&type=98&tx_ttnews[tt_news]=286065&cHash=da03e20e36 (Last accessed: 01/21/2015)

28 O'Brien E, Petrie J, Littler WA, et al. The British Hypertension Society Protocol for the evaluation of blood pressure measuring devices. J Hypertens. 1993;11 Suppl 2:S43–S62.

29 Association for the Advancement of Medical Instrumentation. American National Standard: non-invasive sphygmomanometers – part 2: clinical validation of automated measurement type; ANSI/AAMI/ISO. 2009;81060–81062.

30 O'Brien E, Atkins N, Stergiou G, et al. Working Group on Blood Pressure Monitoring of the European Society of Hypertension. European Society of Hypertension International Protocol Revision 2010 for the validation of blood pressure measuring devices in adults. Blood Press Monit. 2010;15:23–38.

a) b) c

Figure 8 AccuSim-BP Handheld NIBP Simulator (a), Fluke Prosim 8 (b), and measurement setup (c)

Patient simulators have advantages and disadvantages against living subjects based validation of BP measuring devices. One important advantage of this method is possibility to perform comparison of different BP monitors in equal conditions and to minimize influence of various physiological effects. It is known that systolic and diastolic blood pressure values of a person are varying. These variations are due to different origins including respiration which causes 3–6 mmHg variation in the SBP while in normal respiration and 15–20 mmHg when breathing heavily[31]. Because oscillometric measurement methods determine the instantaneous SBP/DBP values, this results in a low reproducibility. In addition, the patient simulator method minimizes comparison subjectivity. Aforementioned reasons motivated to employ specialized BP patient simulator "AccuSim-BP Handheld NIBP Simulator" (Datrend Systems Inc., Canada) for comparisons of 3 selected "smart" BP monitors. Two popular automatic ("classical") BP monitors were included into the study as well.

2.4.3. Results of testing and comparison

We tested 3 "smart" and 2 "classical" devices. Accuracy and precision in terms of mean difference and SD of tested blood pressure sensors are presented in Table 9. It can be observed that all devices fulfill accuracy requirements of BPM validation protocols (mean difference <10 mmHg). The negative signs in front of mean differences point out to underestimation of BP measurements.

Table 9. Testing results of smart blood pressure monitors with AccuSim-BP NIBP simulator

Device	Error in Systolic BP, mmHg		Diastolic BP, mmHg	
	Mean	SD	Mean	SD
Medisana	-1.1	2.8	-0.1	1.2
iHealth	-6.6	2.7	1.9	1.5
Withings	-4.9	1.6	N/A	N/A
LogicoDigit	1.0	4.0	6.0	4.0
Microlife	4.0	1.9	5.0	2.5

Due to technical problems testing of diastolic BP in Withings BPM case was unsuccessful. Therefore we rely on independent validation results[32], which show that mean difference is 0.4 mmHg and SD is ±4.2 mmHg in diastolic BP measurements.

[31] M. Ramsey, III, "Blood pressure monitoring: Automated oscillometric devices"J. Clin. Monit. Comput., vol. 7, no. 1, pp. 56–67, Jan. 1991.

[32] Topouchian J, Agnoletti D, Blacher J, Youssef A, Chahine MN, Ibanez I, Assemani N, Asmar R. Validation of four devices: Omron M6 Comfort, Omron HEM-7420, Withings BP-800, and Polygreen KP-7670 for home blood pressure measurement according to the European Society of Hypertension International Protocol. Vasc Health Risk Manag. 2014 Jan 16;10:33-44.

Figure 9 and Figure 10 show graphical representation of testing results for SBP and DBP values in terms of XY diagrams (measured parameter against the reference) and Bland – Altman plots (the difference against the average of measured and reference values).

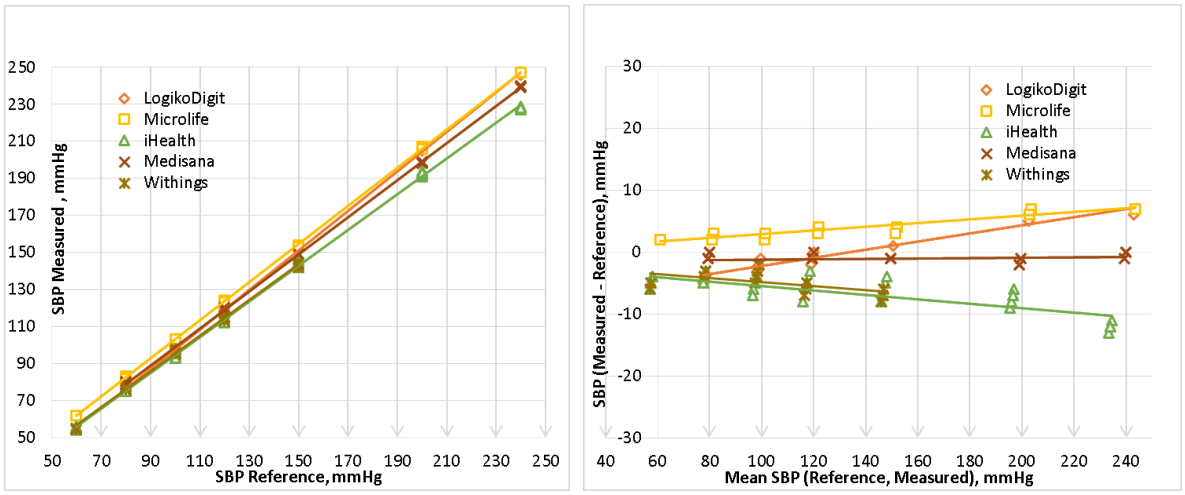

a) b)

Figure 9 Testing results for SBP values: XY diagram (a), Bland - Altman diagram (b)

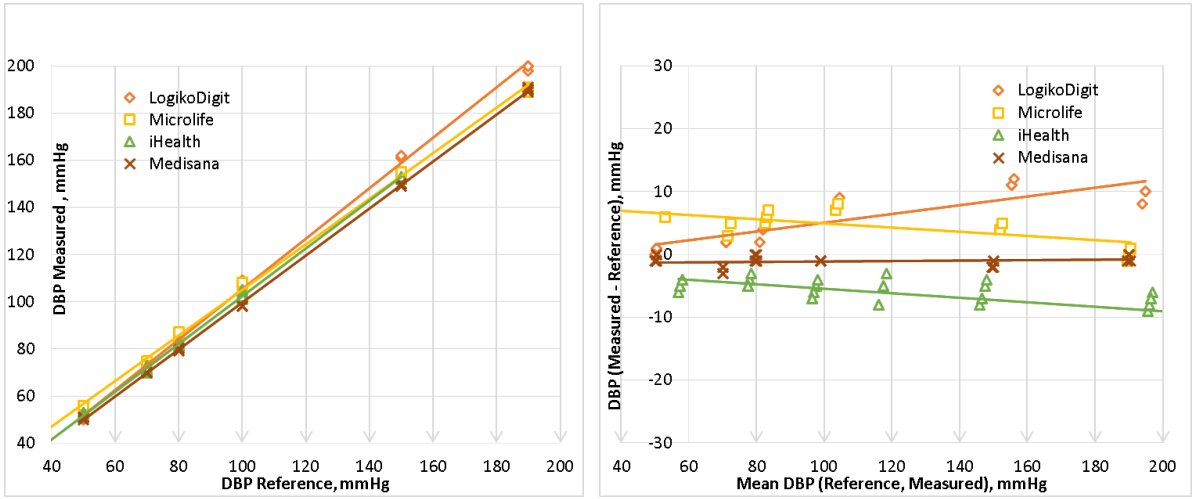

a) b)

Figure 10. Testing results for DBP values: XY diagram (a), Bland - Altman diagram (b)

2.4.4. Conclusion

Medisana blood pressure monitor (BPM) has a number of advantages:

- it is the most accurate;
- it measures blood pressure while inflating the cuff, therefore the discomfort is lower and the measurement is shorter;
- has on board display;
- powered by rechargeable battery, which lasts for a few months;
- has memory of up to 180 measurements;

- also works as an alarm clock, therefore promotes to keep it on a nightstand and measure daily blood pressure in the morning, as the alarm goes off;
- it is relatively cheap (about 100 Euro).

However, there are two main disadvantages:

- it does not allow to enter data manually;
- the synchronization is slow (about 1 min. 30s, while the measurement itself only 30s) and does not work 100% of the time.

We propose that problems with Medisana synchronization could be alleviated by using its internal memory. If some problems occur, the synchronization phase could be skipped for that day and resumed manually the next day.

On the other hand, Withings blood pressure monitor is operated more easily, the app and synchronization works all the time. However, it has no rechargeable batteries, no memory, no display, the accuracy is lower and the price is higher (130 EUR), than Medisana BPM.

iHealth BPM is similar to the Withings BPM in terms of functionality and control with the advantage of measuring blood pressure while inflating the cuff (shorter and more comfortable measurement process). However, it is the least accurate among tested devices.

Therefore, Medisana BU-575 is preferred BPM since it has the number of operating related advantages and is the most accurate. If the ease of operation is especially important, Withings BPM could be chosen.

3. Investigation of possibilities to develop sensors and algorithms for cardiorenal patient monitoring

The results from testing and evaluating the 3rd party sensors showed that they are not well suited for the project purposes: some of them lack of functionality, some of them are difficult to use, while the remaining are both of limited functionality and difficult to use. Therefore, it is desirable to develop three custom hardware and software modules. The first proposed hardware module is a wristwatch type device suitable for long-term monitoring of physiological parameters (i.e., cardiovascular). The second proposed hardware module is a weight scale system for intermittent monitoring of weight, hydration and cardiovascular parameters. The last one is a software module with an algorithm for atrial fibrillation detection in ECG signals. The description of these three modules are presented in more detail in the following chapters.

3.1. An algorithm and software module for ECG based arrhythmia detection

3.1.1. Motivation

Atrial fibrillation (AF) is cardiac arrhythmia, which affects 3% of the general population older than 20 years. AF is a progressive disease associated with detrimental effects on hemodynamics, increased risk of stroke and heart failure[33]. Various studies show that renal diseases and AF frequently coexist and complicate treatment of both conditions[34,35].

[33] Kirchhof P, Benussi S, Kotecha D, et al. 2016 ESC Guidelines for the management of atrial fibrillation developed in collaboration with EACTS. *European Heart J*, 2016.

[34] Reinecke H, Brand E, Mesters R. Dilemmas in the management of atrial fibrillation in chronic kidney disease. *J Am Soc Nephrol*. 20; 2009:705-711.

[35] Piccini JP, Stevens SR, Chang Y., et al. Renal dysfunction as a predictor of stroke and systemic embolism in patients with nonvalvular atrial fibrillation. *Circulation*, 127; 2013:224–232.

Kidney disease is usually found in 10–15% of patients with AF. AF coexistence with chronic kidney disease was reported to be associated with a 67 % higher rate of progression to end-stage renal disease[36]. It has been argued that renal dysfunction in AF patients further increases the risk of stroke and systemic embolism, therefore should be worthy to be included into the scheme of stroke risk stratification. However, there is no clear principle on the management of such patients, since oral anticoagulation therapy (i.e. using warfarin) increases the risk of major bleeding of up to 10-times in this group[37]. Gastrointestinal (58 %) and intracranial (5 %) bleeding were documented as the most frequently occurring major bleeding events in patients with renal dysfunction. Hence, treatment against the formation of blood clots in these patients is a complicated problem, requiring careful assessment of the risk-benefit ratio.

In today's clinical practice, a qualitative approach to confirm AF presence (yes or no AF) is preferred which usually relies on analysis of ECG recorded during rest or 24-hour Holter monitoring. While standard techniques are suitable for reliable detection of permanent or persistent AF, nevertheless, they are associated with high chances of missing paroxysmal AF episodes that usually appear at the beginning of arrhythmia development[38]. In order to detect paroxysmal AF episodes, novel patient-friendly diagnostic utilities for long-term ambulatory ECG monitoring have been proposed[39]. Moreover, extended AF monitoring enables the possibility of changing the prevailing concept of qualitative AF assessment to quantitative (the amount of AF) approach.

Standard time domain parameters applied for analysis of heart rate variability, i.e., standard deviation of RR intervals or root mean square differences of successive intervals can be used for AF analysis as well. However, more specific parameters, such as AF burden and AF density, are preferred for quantitative evaluation of paroxysmal AF[38]. AF burden is expressed as a proportion of time a patient is in AF, and therefore does not provide information about temporal AF behavior. The purpose of AF density is to evaluate temporal distribution of paroxysmal AF episodes which can be useful for assessing AF recurrence patters, i.e., relating paroxysmal AF episodes to arrhythmia provoking events. Temporal AF pattern of AF recurrence may be of interest for drugs management and evaluation of thromboembolism risk. Furthermore, such information can be beneficial for understanding the specific factors resulting in evolving AF burden and AF density for cardio-renal patients.

3.1.2. Commercial ECG recorder and the algorithm for arrhythmia detection

We propose a low cost solution for paroxysmal AF detection and parametrization (Figure 11). The solution combines a commercial low cost single lead ECG recorder eMotion Faros 180 (Mega Electronics, Finland) and a software module with the state-of-the-art algorithm for AF detection included[40]. The algorithm was extensively tested on publically available and internationally accepted ECG databases (Physionet MIT-BIH Atrial Fibrillation, MIT-BIH Arrhythmia, Long-Term AF database, etc.) containing annotated AF episodes. The results showed that the proposed low-complexity algorithm outperformed the most advanced AF detectors in terms of AF detection performance (sensitivity of 97.1%, specificity of 98.3%) and complexity (only 8 multiplications, 2 divisions and 45 additions per RR interval). The ECG recorder is user friendly: weights 13 g, battery lasts for 3 days. The ECG signal is recorded to open source EDF file format[41].

---

[36] Bansal N, Fan D, Hsu CY, et al. Go. Incident atrial fibrillation and risk of end-stage renal disease in adults with chronic kidney disease. *Circulation*. 2013, 127(5), 569-574.

[37] Jun M, James MT, Manns BJ, et al. The association between kidney function and major bleeding in older adults with atrial fibrillation starting warfarin treatment: population based observational study. *BMJ*. 2015, 350:h246.

[38] Charitos EI, Stierle U, Ziegler PD, et al. A comprehensive evaluation of rhythm monitoring strategies for the detection of atrial fibrillation recurrence: insights from 647 continuously monitored patients and implications for monitoring after therapeutic interventions. *Circulation* 126; 2012:806 – 814.

[39] Turakhia MP, Hoang DD, Zimetbaum P, et al. Diagnostic utility of a novel leadless arrhythmia monitoring device. *Am J Cardiol* 112; 2013:520–524.

[40] Petrenas A, Marozas V, Sornmo L. Low-complexity detection of atrial fibrillation in continuous long-term monitoring. *Comp Biol Med*. 2015, 65, 184-191.

[41] European Data Format specifications, http://www.edfplus.info/specs/edf.html

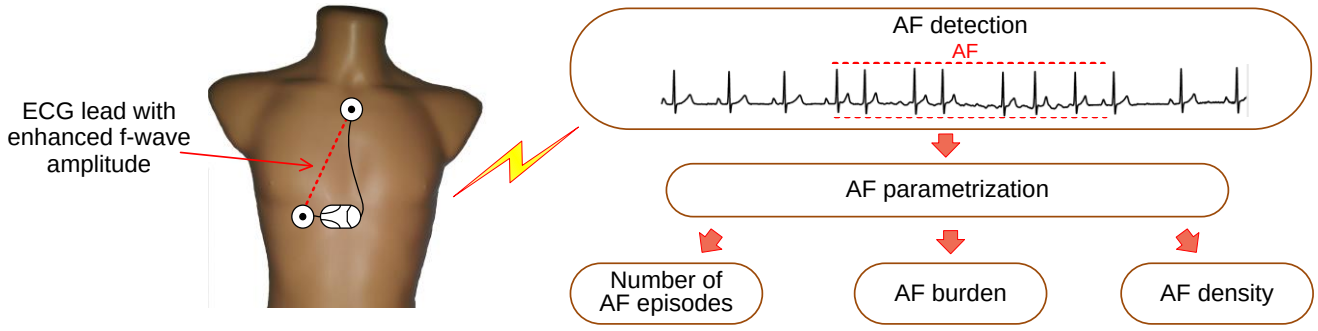

Figure 11. Implementation concept of PAF arrhythmia detection and parametrization

3.1.3. MATLAB GUI for paroxysmal atrial fibrillation detection and parametrization

The signal processing algorithms and GUI for AF detection and parametrization was implemented in Matlab (Mathworks Inc., Natick, USA) programming environment. With the presented GUI (Figure 12), the parameters for both characterization of hearth rhythm and AF are provided. In addition to analysis of heart activity, the user can analyze instantaneous physical activity, which is synchronously recorded with the ECG signal, and thus can provide additional information on AF behavior during increased physical activity.

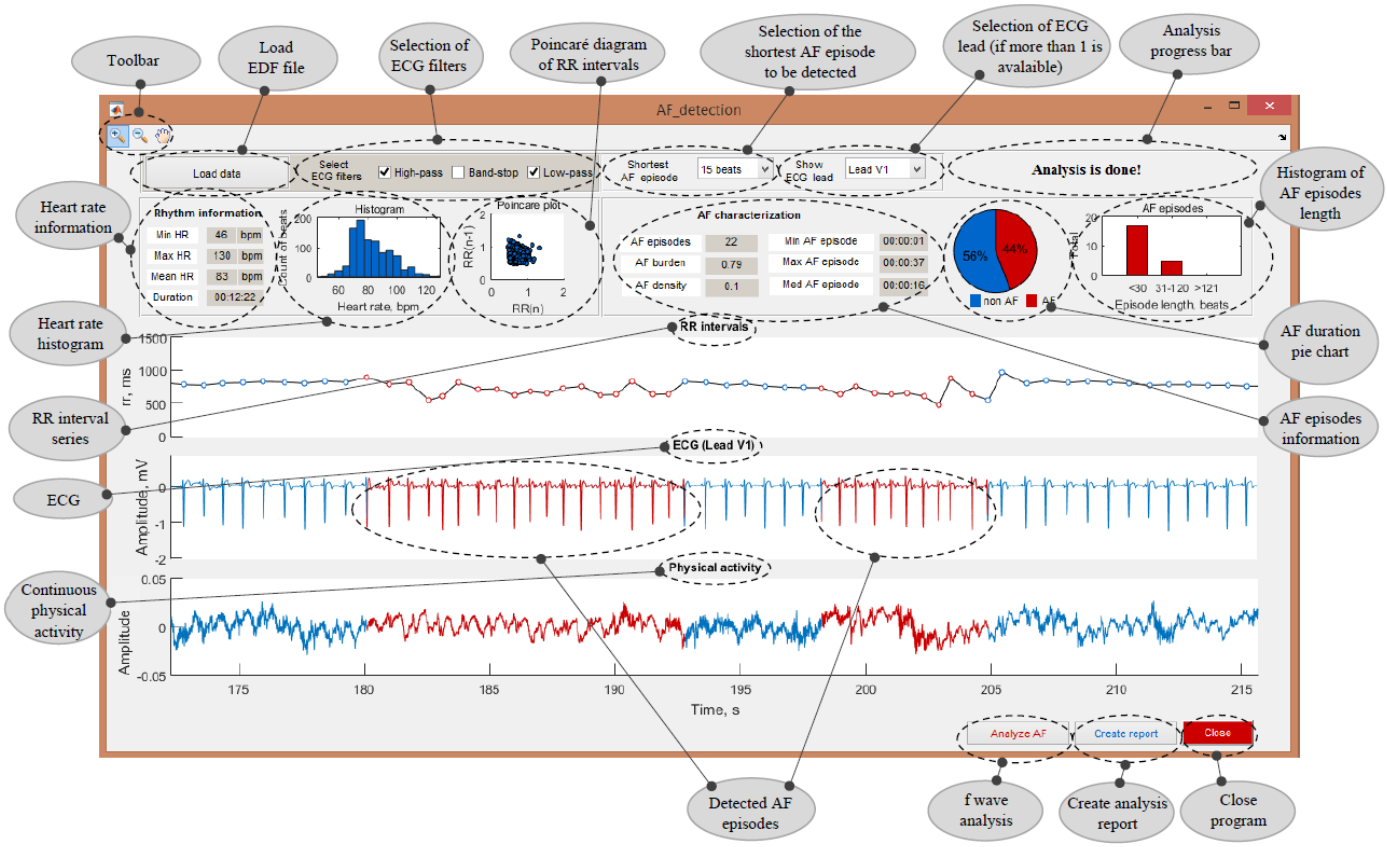

Figure 12. The main GUI window for paroxysmal AF arrhythmia detection and parametrization

The parameters that describe paroxysmal AF are as follows:

- the total number of paroxysmal AF episodes during recording time;
- AF burden;
- AF density.

Both AF burden and AF density take values between 0 and 1. In case of AF burden, 0 indicates that no AF is observed, whereas 1 denotes that the patient was in AF throughout the entire monitoring period (Figure 12). In case of AF density, values closer to 0 indicate that AF is uniformly spread during monitoring period, whereas values closer to 1 stand for a high aggregation of AF episodes. The AF density equal to 1 is obtained when a single AF episode is observed (independently of AF episode length).

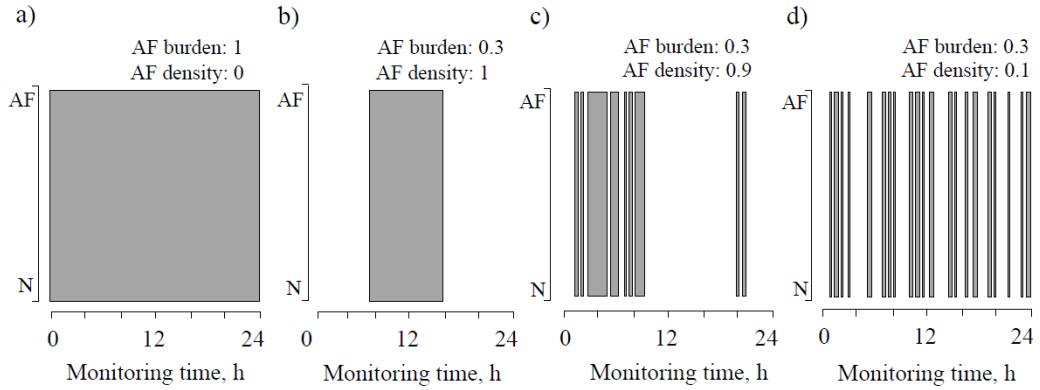

Figure 3. Examples of different cases of temporal distribution of AF episodes: a) AF during the entire monitoring period, b) a single paroxysmal AF episode, c) highly aggregated paroxysmal AF, d) paroxysmal AF is spread throughout the entire monitoring time

It is desirable not only to detect all episodes of paroxysmal AF, but also to provide quantitative information on fibrillatory activity (i.e., f-wave frequency) during each AF episode. Long-term monitoring of fibrillatory activity would allow to better evaluate temporal AF behavior and provide signal analysis based parameters that could provide additional information on the efficiency of different treatment strategies. In order to analyze fibrillatory activity, f-waves have to be extracted by using some QRST cancellation technique. An additional window of the developed GUI is dedicated to fibrillatory activity extraction and AF parametrization (Figure 12).

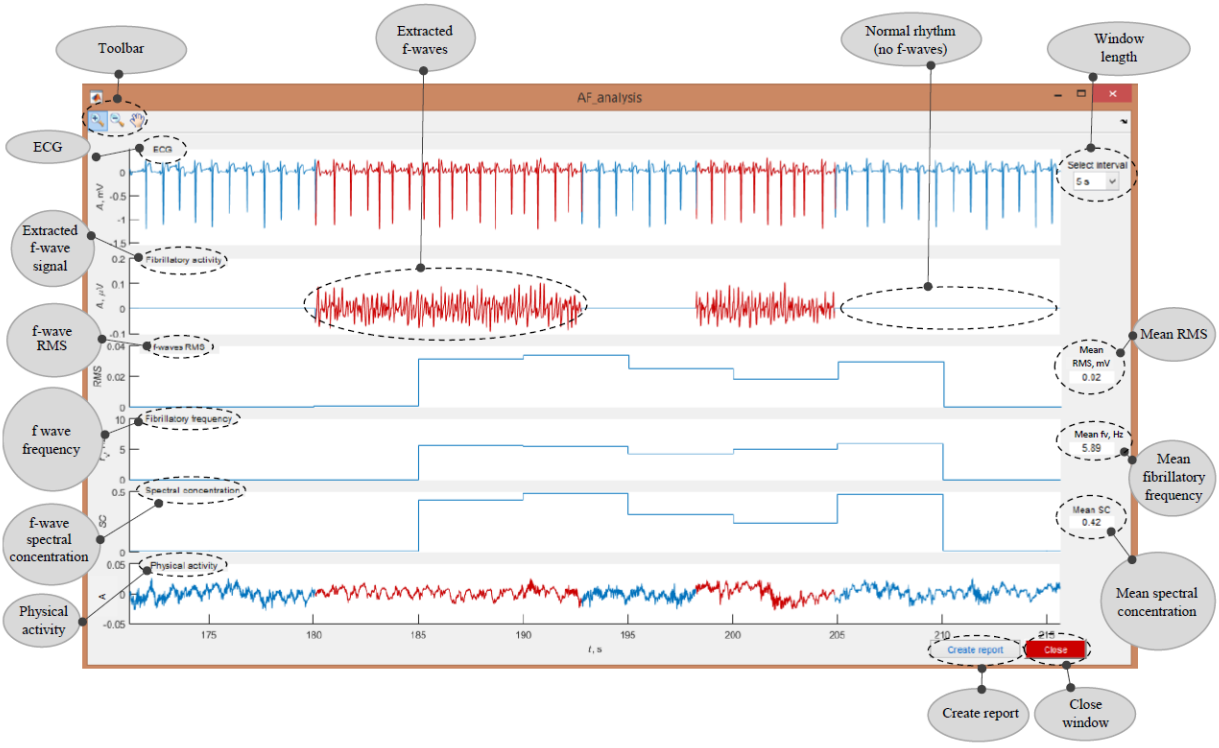

Figure 4. An additional GUI window for analysis of fibrillatory activity (f-waves)

With the additional window of the GUI the following information is provided:

- Extracted atrial fibrillatory activity during each paroxysmal AF episode;
- Instantaneous f-wave RMS level;
- Instantaneous f-wave frequency;
- Instantaneous f-wave spectral concentration;
- Instantaneous physical activity.

3.1.4. Implementation in CARRE Life style and ECG aggregator

The AF detection algorithm presented in the previous subsection was also used in CARRE ECG aggregator. The ECG aggregator was integrated into the CARRE Life-style aggregator. The ECG aggregator accepts .EDF file format used by the eMotion Faros ECG recorders. When Faros device is connected to the personal computer via USB port, the directory containing the recorded ECG .EDF files is automatically opened and the user is able to select the file of interest. The manual file selection is possible as well and is performed browsing via tray menu (Figure 13). After ECG file is selected, ECG aggregator analyses the signal: performs preprocessing in order to filter out noise, detects RR intervals, analyzes and performs parametrization of rhythm. The rhythm parameters include: the time at which AF episode begins, the duration of the AF episode and an average heart rate in AF episode. The analysis of ECG is followed by uploading parameters of the detected AF episode to the private RDF repository and generation of the report in .PDF format (Figure 14), which could be then viewed by clicking button in the CARRE Life-style and ECG aggregator tray menu.

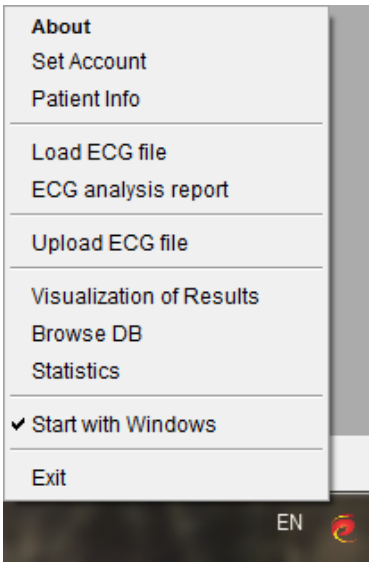

Figure 13. Tray menu of the CARRE Life-style and ECG aggregator

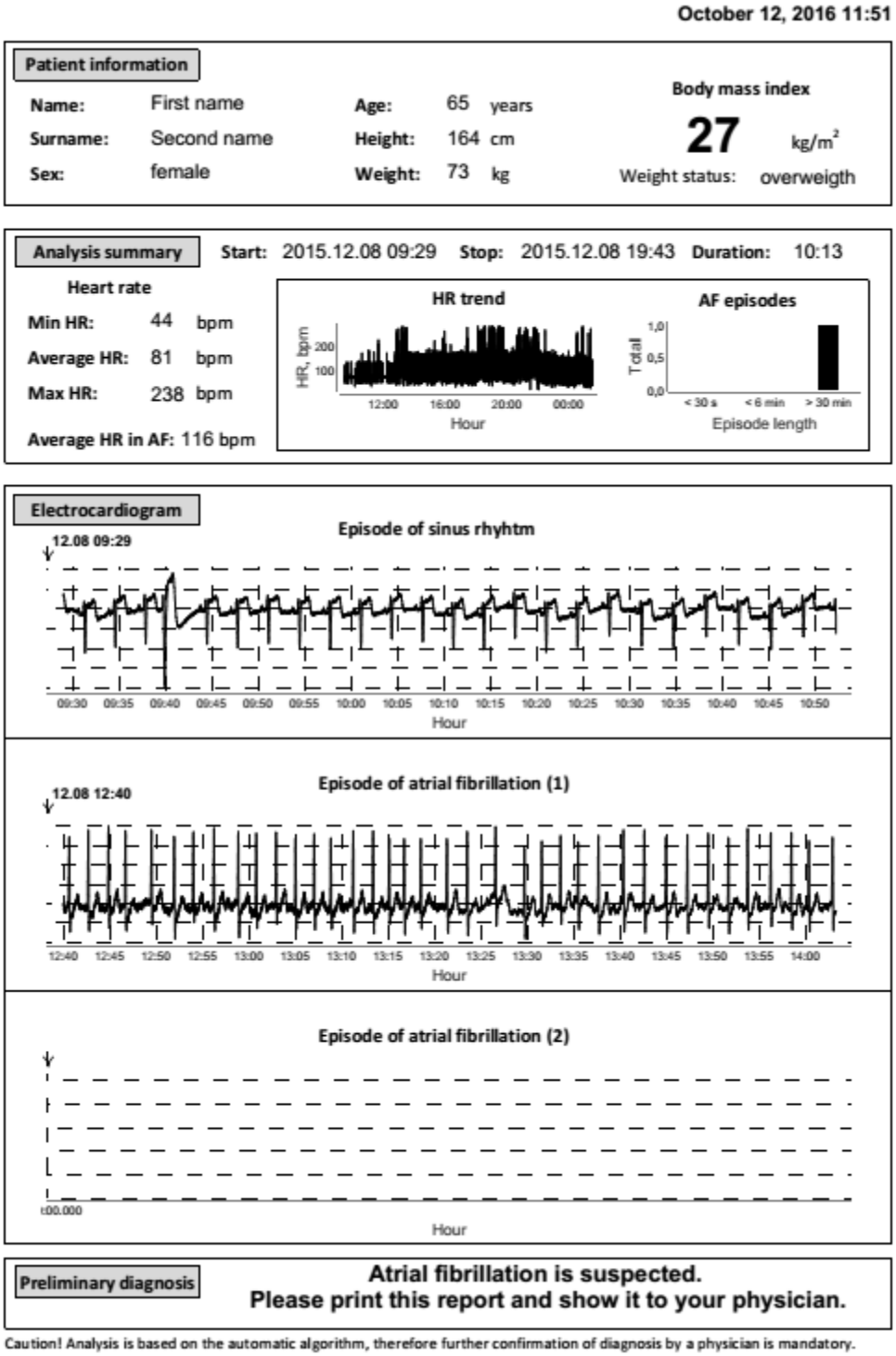

Figure 14. The ECG analysis report, generated by CARRE Life-style and ECG aggregator

3.2. Wrist worn device for continuous health parameters monitoring

3.2.1. Motivation

Wrist worn device is the longest known wearable device. It is considered completely unobtrusive and could be accepted by patients for continuous monitoring. Existing commercial smart wrist worn devices already try to measure some health related parameters (heart rate, steps, or burned calories). However, we anticipate that more specific observables, such as arrhythmias (ventricular premature beats, atrial fibrillation), pulse rate variability, or sleep apnea, could be also monitored. These information channels could open new information channels to the health condition of a patient with cardiorenal syndrome. The list of observables, which could be monitored using some specific wristwatch type device is presented in Table 10.

Table 10. Personal data required before the test

Observable	Method
Apnea – hypopnea index (AHI)	SpO2, inertial measurements
Heart rate	PPG
Breathing rate	PPG
Metabolic equivalent (MET)	PPG, GSR, inertial measurements
Physical exercise	PPG, GSR, inertial measurements
Premature ventricular contraction (PVC)	PPG
Atrial fibrillation (AF)	PPG

As already mentioned, physical activity related parameters (energy consumption – MET, physical exercise) and heart rate are monitored by already commercially available smartwatches. Even though they may not be very accurate at the moment, there are interesting future plans from big and experienced companies. Some new greatly improved trackers are already available on the market e.g. Fitbit Surge[42], Jawbone UP3[43]. We expect that sooner or later these new generation physical activity trackers will solve most of the previous tracker problems. Therefore, we do not propose to include the monitoring of these lifestyle related observables in the new sensor development.

On the other hand, the monitoring of such health related observables as AHI and arrhythmias are not that well-developed for independent home care applications. There are only few cases known for arrhythmia[44] (e.g. PVC[45], AF[46]) detection in simple and unobtrusive way. While some systems are commercially available for sleep apnea monitoring at home (Pacific Medico Sleep diagnostic device[47], Braebon Medibyte[48]), they could be hardly identified as unobtrusive. Therefore, we propose to conduct/continue the research in these two fields in order to develop new sensors. However, it is crucial to understand that these proposed problems are entirely a matter of the scientific research with no assured results or solutions. There is a possibility to provide such sensors for some of the subjects in the pilot phase, but definitely not for all of them.

---

42 https://www.fitbit.com/surge

43 http://jawbone.com/store/buy/up3

44 T. Suzuki, K. I. Kameyama, and T. Tamura, “Development of the irregular pulse detection method in daily life using wearable photoplethysmographic sensor”, 31st Ann. Int. Conf. IEEE EMBS, pp. 6080–6083, 2009.

45 E. Gil, P. Laguna, S. Member, and J. P. Mart, “Heart Rate Turbulence Analysis Based on”, IEEE Trans. Biomed. Eng., vol. 60, no. 11, pp. 3149–3155, 2013.

46 J. Lee and B. Reyes, “Atrial fibrillation detection using an Iphone 4S”, IEEE Trans. Biomed. Eng., vol. 60, no. 1, pp. 203–206, 2013.

47 Pacific Medico Co. Ltd., Respiratory Care Product http://www.pacific-medico.com/english/division_2.html

48 Braebon – Medibyte http://www.braebon.com/products/medibyte/

3.2.2. Requirements and concept of implementation

The main idea of CARRE wristwatch is to improve personal data observables monitoring in 3 ways:

- to provide higher quality data (raw signals) for signal processing units;
- to address several kinds of observables with one device (multi-parametric sensing);
- to improve convenience (e.g. comparing to Holter monitors).

The technical and functional specification of CARRE wrist worn device and explanation is presented in Table 11. It must be noted that unobtrusiveness and convenience are the most important factors.

Table 11. Wrist worn device technical and functional requirements

Requirement	Details
Green LED PPG channel	As our previous research shows[49], it is highly suitable for PPG in the wrist area. This PPG signal should be used for AF and PVC detection.
Red LED PPG channel	Suitable for SpO2 measurement.
IR LED PPG channel	
3-axis accelerometer	Suitable for inertial measurements.
3-axis gyroscope	
Altimeter	
At least 24 hours operating time	–
Wireless communication for control	For minimum unobtrusiveness. Bluetooth protocol preferred due to smartphone compatibility.
Micro SD memory card for primary stage	Minimum 4 GB.
SpO2 measurement	–
Real-time PVC detection	Possible research output. Based on algorithms developed by KTU.
Real-time AF detection	
Sleep apnea detection	
Minimalistic user interface	For maximum unobtrusiveness and user-friendly maintenance.
High comfort	

General concept of the device is presented in Figure 15. It can be divided into three layers. The hardware layer is the simplest one. In measurements layer, there are some risks and uncertainties:

- PPG waveform often suffer from movement artifacts, which disturb further measurements;
- the accuracy of SpO2 value might depend on different LED characteristics, temperature, etc.;
- there is no clear approach of quantitative measurements of the movement.

The algorithmic layer seems to be the most challenging. The development of algorithms heavily depends on available input data and possibility to test under clinical conditions.

The dashed line indicate the part reserved for future developments.

[49] V. Vizbara, A. Sološenko, D. Stankevičius, and V. Marozas, “Comparison of green, blue and infrared light in wrist and forehead photoplethysmography”, in Biomedical Engineering 2014, 2013, pp. 78–81.

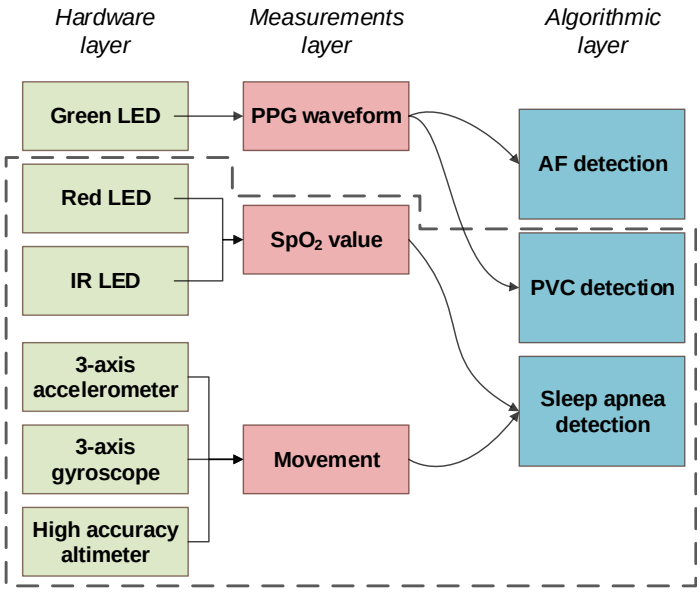

Figure 15. Concept of the CARRE wrist worn system

CARRE wrist worn device integration into CARRE scheme could not be specifically described yet. It should be implemented under some “Custom API”, or via “CARRE consortium cloud”. The latter ones will be described in Chapter 4 of this document.

3.2.3. Hardware

The hardware of the device consists of three subsystems: sensors, power management, and main controller (see Figure 16). Power is managed using a specific battery charger and two 3.3 V LDO regulators. One of which is dedicated for micro SD memory card and the other is dedicated for the rest of the system. Main microcontroller is nRF51822 from Nordic Semiconductor. It contains ARM Cortex-M0 core and radio with Bluetooth Low Energy capability. All sensors and the LCD are enabled via the same SPI interface. Inertial measurement sensors consist of two-in-one accelerometer and gyroscope LSM330DLC and additional high resolution (up to 10 cm) altimeter MS5611-01BA03. Temperature and humidity are measured using two-in-one digital sensor HIH6131. Photoplethysmography signals are obtained using analog front-end AFE4490. GSR sensing was accomplished using external analog to digital converter AD7192 with specific analog signal conditioning circuit.

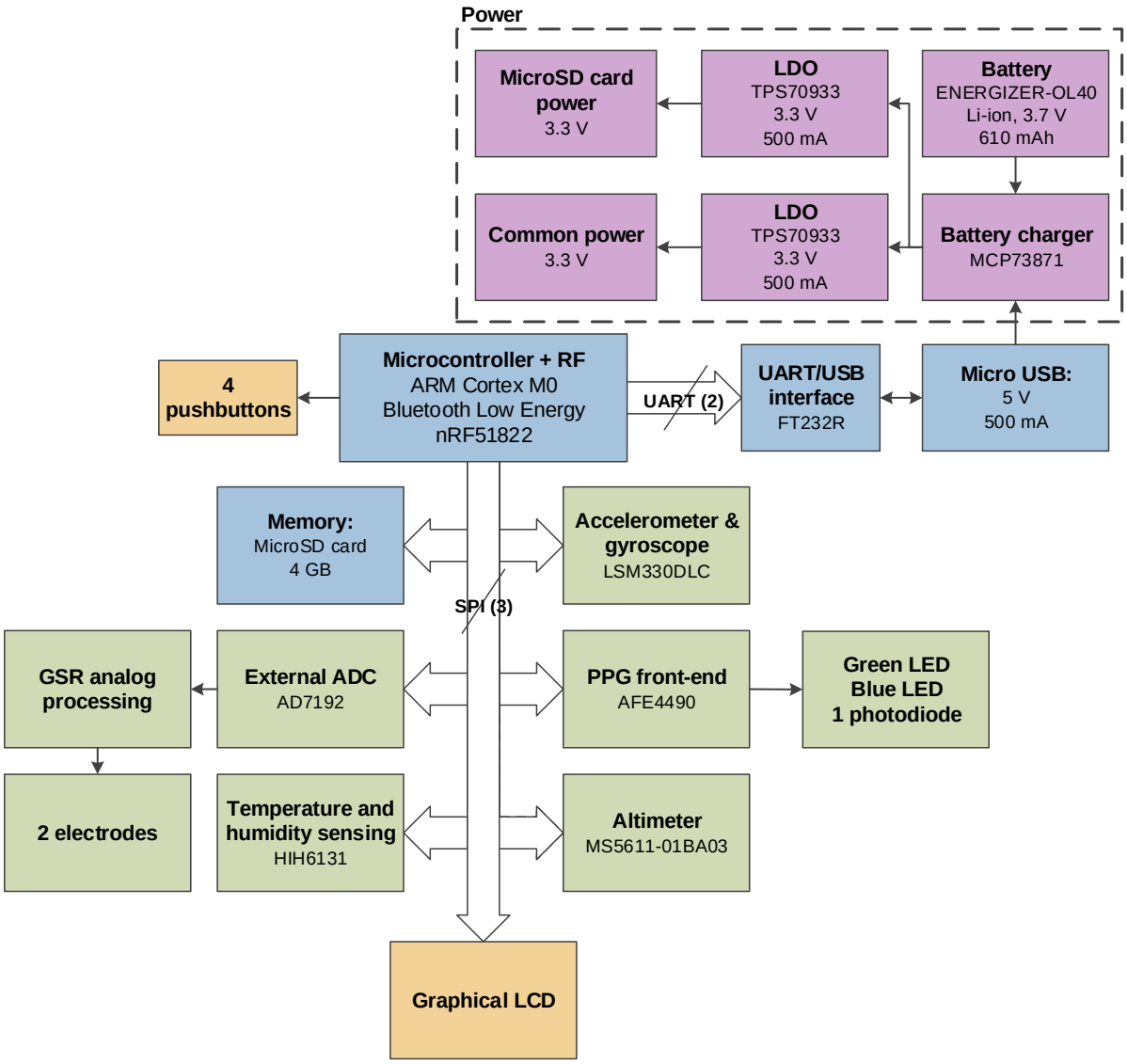

Figure 16. Block diagram of the CARRE wrist worn device device

The parameters of the sensors are summarized in Table 12.

Table 12. Parameters of the sensors of the wrist-worn device

Sensor	Parameter	Value	Units	Note
PPG	Chip name	AFE4490	-	
	Power consumption	<2.3	mW	At supply voltage of 3 V
	Green LED wavelength	520-525	nm	
	Blue LED wavelength	465-470	nm	
	Sampling frequency	500	Hz	
	Signal resolution	22	bits	
IMU	Chip name	LSM330DLC		
	Acceleration range	16	g	

	Angular velocity range	2000	deg/s	
	Sampling frequency	50	Hz	
	Signal resolution	16	bits	
Altimeter	Chip name	MS5611-01BA03		
	Measurement resolution	10	cm	
	Signal resolution	24	bits	
	Average supply current	<1	uA	
Temperature & humidity	Chip name	HIH6131		
	ADC chip name	AD7682		
	Resolution	14	bits	
	Sampling frequency			
	ADC type	SAR		

The mechanical 3D drawings of the enclosure of the device are presented in Figure 17 and Figure 18. The enclosure was designed using Solidworks software and manufactured by 3D printing from the ABS plastic. The device is attached to the wrist via elastic textile strap. Pictures of the assembled device are presented in Figure 19.

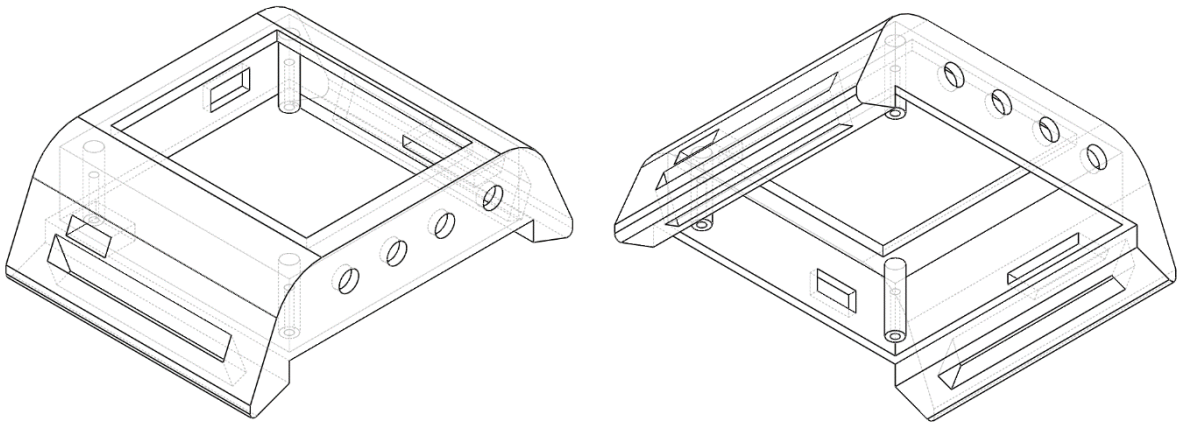

Figure 17. Drawings of the enclosure of the wrist-worn device (top)

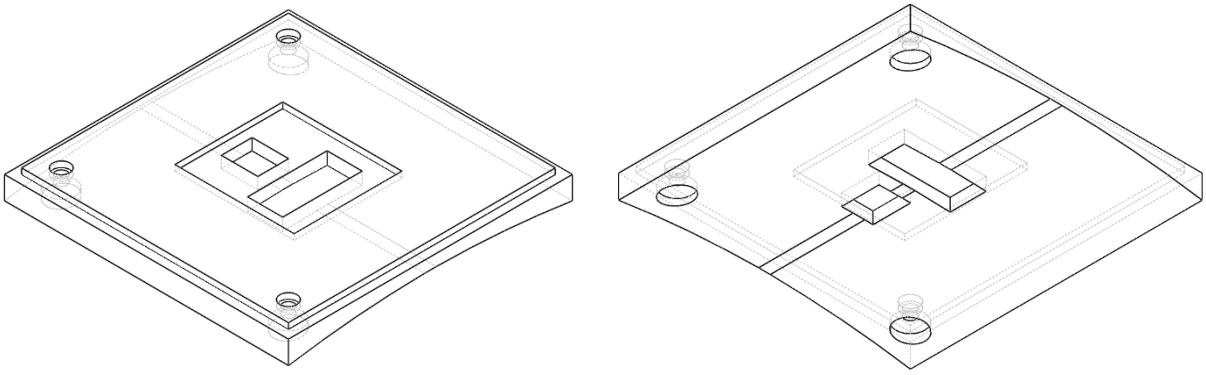

Figure 18. Drawings of the enclosure of the wrist-worn device (bottom)

Figure 19. Wrist worn device front (left) and back (right)

3.2.4. Performance evaluation of hardware

The device was tested in terms of quality of the signals and relative error of the measured parameter, where applicable. Figure 20 shows an example of the PPG signal recorded on the wrist. Since the PPG waveform can be identified clearly and no high-frequency noise is present in the signal, we can state that the quality of the signal is sufficient and the PPG sensors is working correctly.

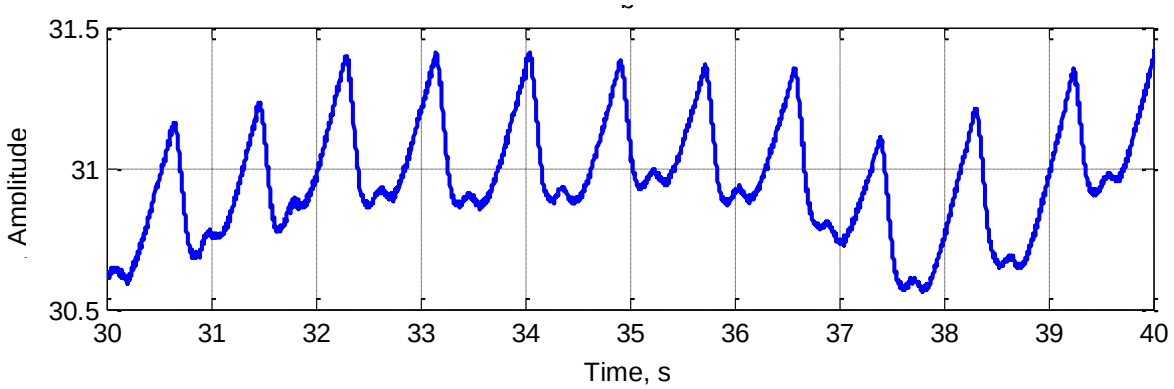

Figure 20. Example of recorded PPG signal

While evaluating the accuracy of HIH6131 sensor temperature measurement, the reference temperature was measured with BIOPAC TSD202B – thermistor probe, dedicated for skin surface temperature measurements with 0.2 °C accuracy. Both sensors were attached to the skin as near to each other as possible. Temperature signals were sampled at 2 Hz. Later, 5 seconds length episodes were extracted from those recordings, the average temperature and error were calculated in the episode. Table 13 shows quantitative results from these temperature measurements. The results indicate that there is a high absolute error resulting in relative error of around 1.5 % in the range of human skin temperature. The absolute error could possibly be eliminated during calibration and the relative error would drop down.

Table 13. Evaluation of temperature measurements

Test No.	Reference temperature value, °C	Measured temperature value, °C	Absolute error, °C	Relative error, %
1	33,85	34,34±0,005	0,49	1,43
2	33,89	34,34±0,016	0,50	1,47
3	33,92	34,46±0,010	0,54	1,59
4	33,96	34,48±0,005	0,52	1,53
5	34,04	34,57±0,009	0,54	1,58

The resistance of three different value resistors was measured and compared to FLUKE 199C LCR meter (0.6 % accuracy) in order to evaluate the GSR sensor. Intermittent measurement was accomplished 30 times for each resistance value and averaged. Table 14 presents the evaluation results from GSR measurements. As it can be seen, relative error does not exceed 1 % in the range of typical resistance of human skin (66 kΩ – 10 MΩ), but outside this range error it tends to increase.

Table 14. Evaluation of skin resistance measurements

Test No.	Reference resistance value, Ω	Measured resistance value, Ω	Absolute error, Ω	Relative error, %
1	47900	47413±31	487	1,02
2	149900	149453±37	447	0,30
3	1400000	1399205±216	795	0,06

3.2.5. Algorithm for PPG based AF detection

In the preprocessing stage, a low-pass filter with cut-off frequency f_c is used to suppress high frequency noise. Then, an adaptive filter based on least mean squares (LMS) is used to remove the baseline wander from the PPG signal. Parameters of the filter consist of one adaptive coefficient ω_1 and the adaptation step μ. The resulting PPG signal without the baseline wander $p_a(n)$ branches into two routes. In one way, the $p_a(n)$ is further passed on to the peak detector. The first step in peak detection is slope sum function (SSF) with window length N. The output of the SSF $s(n)$ is compared with threshold T. The threshold T is updated based on a median $a_m(m)$ of the amplitude $a(m)$ of the last five peaks found. For each peak found the index $i(m)$ is noted and peak-to-peak interval $\Delta i(m)$ is calculated. Finally, the AF detector, takes place for decision making. This detector was originally used for analysis of RR intervals obtained from the ECG. The last block in the diagram is for signal quality evaluation. The preprocessed PPG $p_a(n)$ is passed as the input to this block. The low-quality-signal detector is characterized by three parameters: W - the window length, σ - smoothing factor, t_q - threshold to produce binary output. The output of this detector has two states: “High” for the high-quality signal “Low” for the low-quality signal. The signal quality meter controls the output switch of the entire algorithm. It connects the final output $O(m)$ to either the output of the AF detector or to the state “None”, if the quality of the signal is not sufficient. It should be noted that there are three different sampling indexes: n - representing the nth sample in the PPG, m - representing the mth peak-to-peak interval, and k - representing the kth sample of the low-quality-signal detector.

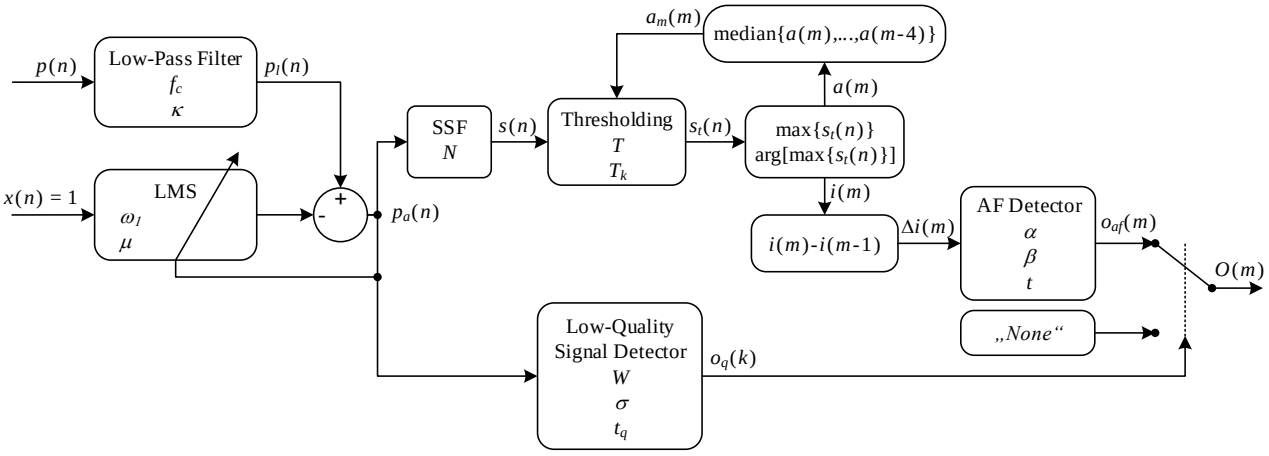

Figure 21. Structure of the algorithm for PPG based AF detection

3.2.6. Performance evaluation of PPG based AF detection algorithm

The performance of the algorithm was evaluated in terms of sensitivity, specificity, total ROC and area under ROC at different SNR levels. Figure 22 displays the ROC curves at different SNR levels. The ROC curve for the SNR level of 20 dB is close to that of the ideal performance of a diagnostic test, while the ROC curve for the SNR level of 0 dB is very close to that of random guessing.

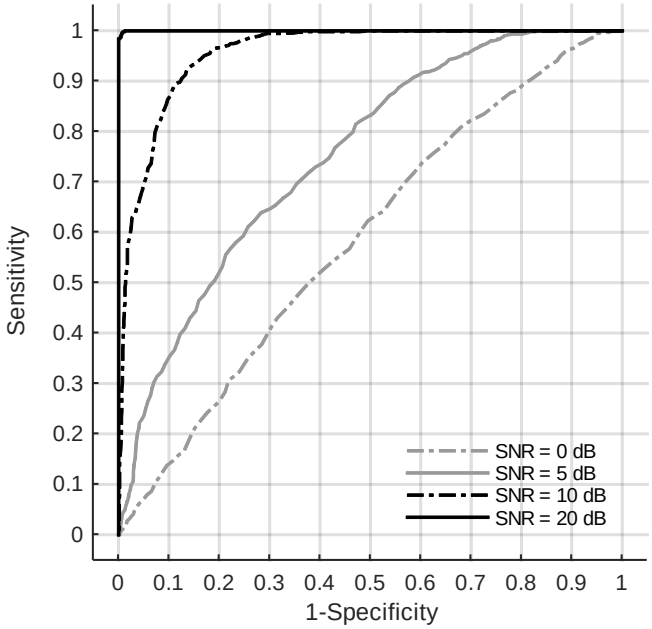

Figure 22. ROC curves at different SNR levels

Figure 23 shows the area under the ROC curves for different SNR levels. The area holds close to linear relationship for SNR levels between 0 dB and 12 dB, and then saturates to 0.99. The overall results indicate that the proposed algorithm requires high-quality signals with at least 13 dB of SNR. With such data, the algorithm performs adequately.

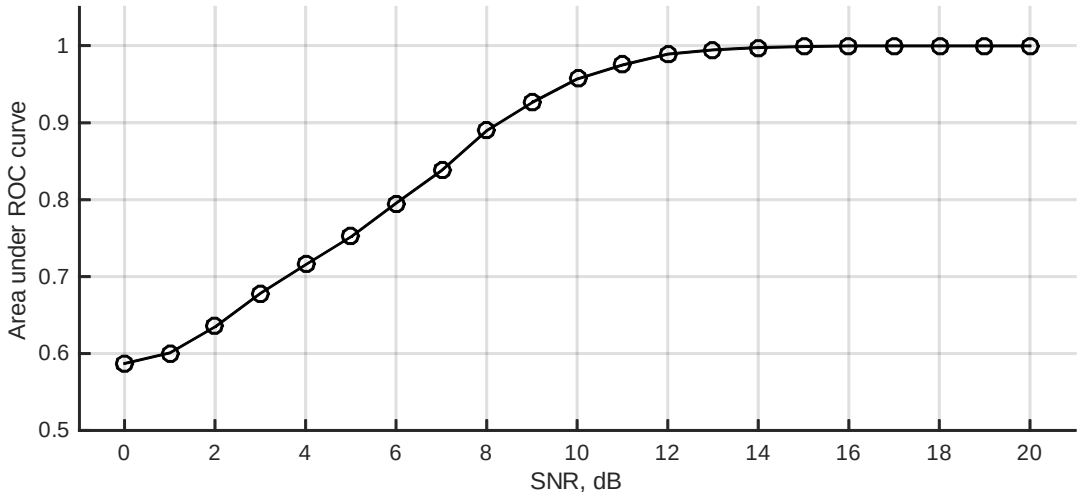

Figure 23. Area under ROC as a function of SNR

3.2.7. Continuation of the development and exploitation

CARRE results are exploited in the next version of the prototype of the wrist worn device, which is under development in the scope of another project by KTU "Automatic algorithms for atrial fibrillation risk prediction after acute myocardial infarction", funded by Research Council of Lithuania, 2015-2017.

The structure of the new version has been altered when compared to the previous version (see Figure 24). The main microcontroller is the system-on-chip solution nRF52832, which comes with ARM Cortex-M4 core and Bluetooth Low Energy 4.0. The power supply subsystem consists of four separate linear voltage regulators each providing supply voltage for the separate subsystem. The micro type of universal serial bus (USB) connector is used to charge, read the data from micro-SD memory card, and as a connector for the electrocardiography electrodes. The specialized USB signal switch ADG772 and the multiplexer TS3A27518E are used to switch between recording and USB-connection modes. All recorded data is buffered in FRAM and then transferred to the micro-SD memory card. The sensors include the electrocardiography and photoplethysmography front-ends from Texas Instruments, isolated analog to digital converter (ADC) ADE7913 together with an analog circuit for galvanic skin response (GSR) measurements, and a 3-axis accelerometer. Small, 96 pixels wide and height, 1.3-inch LCD is used for indication.

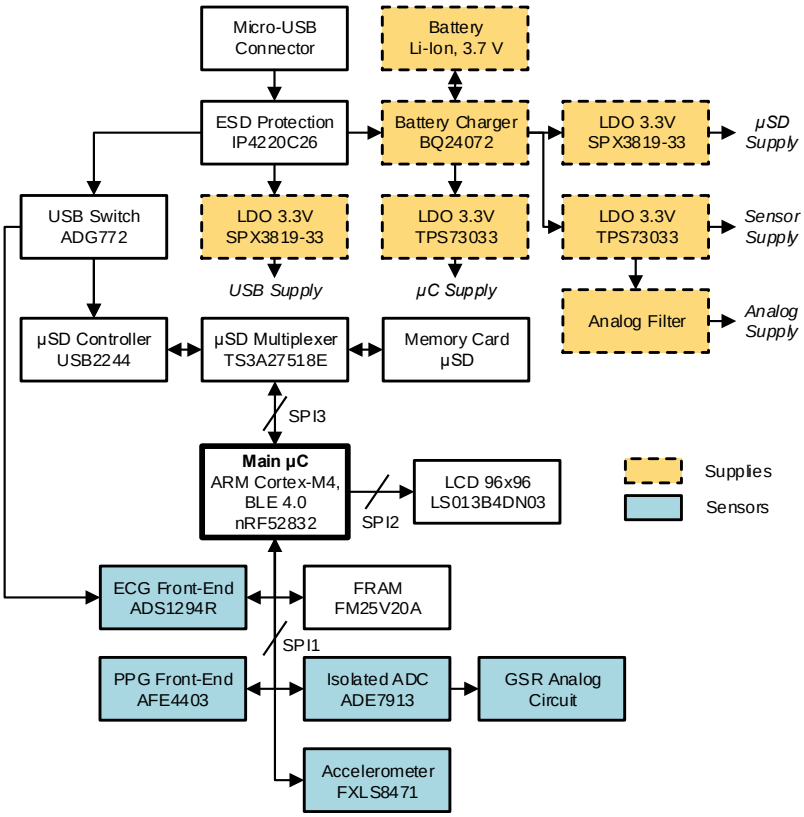

Figure 24. Block diagram of the prototype of the wearable device new iteration

The new version of the wrist worn device was implemented and tested on 18 patients (9 with AF) at Kulautuva Rehabilitation Hospital of Kaunas Clinics, Lithuania[50]. Figure 25 shows the developed device attached on the subject. The study revealed that nearly two thirds of monitoring time photoplethysmography signal was of satisfactory quality allowing detection of AF with 92.8% sensitivity and 91.9% specificity. This observation allows to anticipate that the wrist-worn device has potential to be applied for, e.g., long-term mass screening of target population[51].

[50] Study approval by Kaunas Region Biomedical Research Ethics Committee (No. BE-2-20)

[51] Steinhubl, S. R., Mehta, R. R., Ebner, G. S., Ballesteros, M. M., Waalen, J., Steinberg, G., Jr., P. V. C., Felicione, E., Carter, C. T., Edmonds, S., Honcz, J. P., Miralles, G. D., Talantov, D., Sarich, T. C., and Topol, E. J. (2016). Rationale and design of a homebased trial using wearable sensors to detect asymptomatic atrial fibrillation in a targeted population: The mHealth Screening To Prevent Strokes (mSToPS) trial. American Heart Journal, 175:77 – 85.

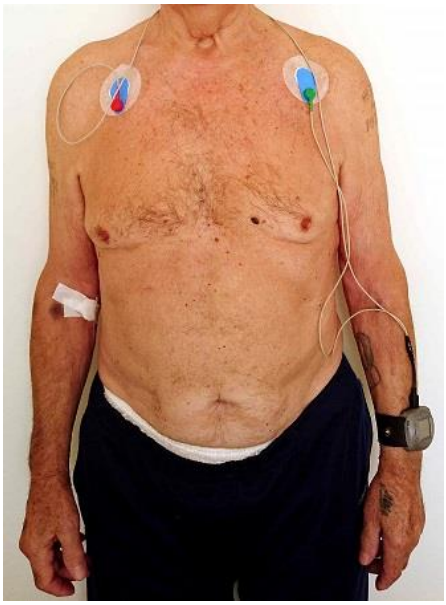

Figure 25. Wrist-worn device for acquiring PPG data.
The ECG electrodes serve for the purpose to obtain reference signal.

3.3. Multiparametric weight scales for intermittent (periodic) monitoring of health parameters

3.3.1. Motivation

Bioimpedance registration and analysis allows to estimate human body composition, in particular, the volume of body fluids, and plays a significant role in cardiorenal syndrome management[52]. Detection of overhydration in patients with heart failure or renal dysfunction can improve blood pressure control, also may be useful in guiding pharmacologic therapies for restoring such patients to a optivolemic state. At-home monitoring of bioimpedance and other relevant physiologic parameters, analysis of trends of these parameters may help to detect early onset of heart failure or renal dysfunction worsening and to prompt early intervention i.e. weeks before urgent hospitalization.

Very important aspect of monitoring heart failure or renal dysfunction related parameters is easy-to-use and operator-less method of data registration. These requirements can be fulfilled by body composition scales where bioimpedance is measured between the subject's feet (lower extremities impedance) and arms (thorax impedance).

The investigation of 3rd party body composition scales showed, that none of them are particularly well suited for project tasks. While errors in the measurement of weight acceptable, the errors in body fluids estimation parameters: total body water (TBW), intracellular body water (ICW) and extracellular (ECW) are unknown. Furthermore, we propose that other observables, related to cardiovascular system (such as heart rate, short term heart rate variability parameters, arrhythmia detection, intracellular and extracellular body water, pulse arrival time (PAT)[53]) could be monitored via body scale, too.

---

[52] Nadia Aspromonte, Dinna N. Cruz, Claudio Ronco, Roberto Valle, Role of Bioimpedance Vectorial Analysis in Cardio-Renal Syndromes, Seminars in Nephrology, Volume 32, Issue 1, January 2012, Pages 93-99.

[53] Paliakaitė, Birutė; Daukantas, Saulius; Sakalauskas, Andrius; Marozas, Vaidotas. Estimation of pulse arrival time using impedance plethysmogram from body composition scales // 2015 IEEE Sensors Applications Symposium (SAS), April 13-15, 2015, Zadar, Croatia: proceedings. Piscataway, NJ: IEEE, 2015, ISBN 9781479961160. p. 69-72.

3.3.2. Requirements and concept of implementation

After the analysis of scientific literature, we noticed that there are three methods available for body composition monitoring. Most of the customer grade bioimpedance measurement devices use traditional bioelectrical impedance analysis (BIA) method, which is accurate enough for assessment of healthy individuals, but is inadequate for body composition estimation in unhealthy conditions. More sophisticated methods, such as bioelectrical impedance spectroscopy (BIS) or bioelectrical impedance vector analysis (BIVA) would be more suitable for body composition monitoring in sick individuals. However, the latter two methods are not employed by low-cost commercial devices. On the other hand, these different methods are not so different on the hardware level.

CARRE Multiparametric weight scale is to improve personal data observables monitoring in 3 ways:

- to provide raw signals for signal processing units;
- to address several kinds of observables with one device (multi-parametric sensing);
- to simplify measurement procedure and eliminate additional operator (e.g., compare to tonometers for pulse wave velocity measurement).

The technical and functional specification of CARRE Multiparametric weight scale and explanation is presented in Table 15. It must be noted that unobtrusiveness and convenience are the most important factors.

Table 15. Multiparametric weight scale technical and functional requirements

Requirement	Details
Weight measurement range 40-150kg, measurement error 0.1kg	
4 stimulus & 4 sensing electrodes for feet & palms	Tetrapolar configuration of electrodes is superior to bipolar because it eliminates the source of error originating in additional impedances caused by skin, wires, and electrodes.
Bioimpedance parameters (modulus and phase) for 4 frequencies (8, 16, 32, 64 kHz) and for all combinations of 4 stimulus and 4 sensing electrodes.	
Body composition measurement current 970 μA	The highest value according to standard?
Impedance dynamic range 0 - 3 kΩ	
Electrocardiogram signals for 3 leads: a) right arm – left arm (standard lead I), b) right arm – left leg (standard lead II), c) left arm - left leg (standard lead III)	
Electrocardiogram signal sampling rate 500Hz, amplitude resolution 24bits	Recommended sampling rate in heart rate variability analysis is 500Hz (reference?)
Synchronization error between bioimpedance and electrocardiogram signals less than 2ms	This requirement originates because of the need to estimate pulse arrival parameter.
Micro SD memory card for local data storage & configuration	Minimum 4 GB.
WiFi wireless communication for data communication	WiFi is selected for minimum unobtrusiveness (no need to switch on a smartphone and start a dedicated app software), automatic data file transmission for analysis in the computing server, receiving of the analysis results.
Rechargeable battery	
Atrial fibrillation arrhythmia detection	Possible research output. Based on algorithms developed by KTU.
Estimation of ultrashort time heart rate variability (HRV) parameters during normal and paced breathing conditions	
Bioimpedance waveform recording	
Pulse arrival time estimation	

General concept of the system is presented in Figure 26 represents the concept of the multiparametric weight scale monitoring system. The Omron BF508 weight scale[54] enclosure was used for prototyping as it consists of two parts with 8 electrodes in total – feet plate and handlebar. Two key components are Texas Instruments Inc. integrated front-ends ADS1294 and AFE4300. The AFE4300 contains complete analog and digital frontend for body composition scales and weight measurement. It allows employing the BIS and BIVA methods for body composition monitoring and simplifies the overall design of the weight scale system. It is also compatible with other sensors, e.g. electrocardiography and respiration rate measurement subsystems. Therefore, we find this integrated circuit as well suited for high end scale measurement system for the project needs. The ADS1294 is dedicated for obtaining 3 channel (Einthoven leads) ECG, including right leg drive circuitry. This hardware allows performing weight and body composition as well as ECG measurements. Further on, on integrated algorithmic level, some specific observables, e.g. heart rate or respiration rate are estimated.

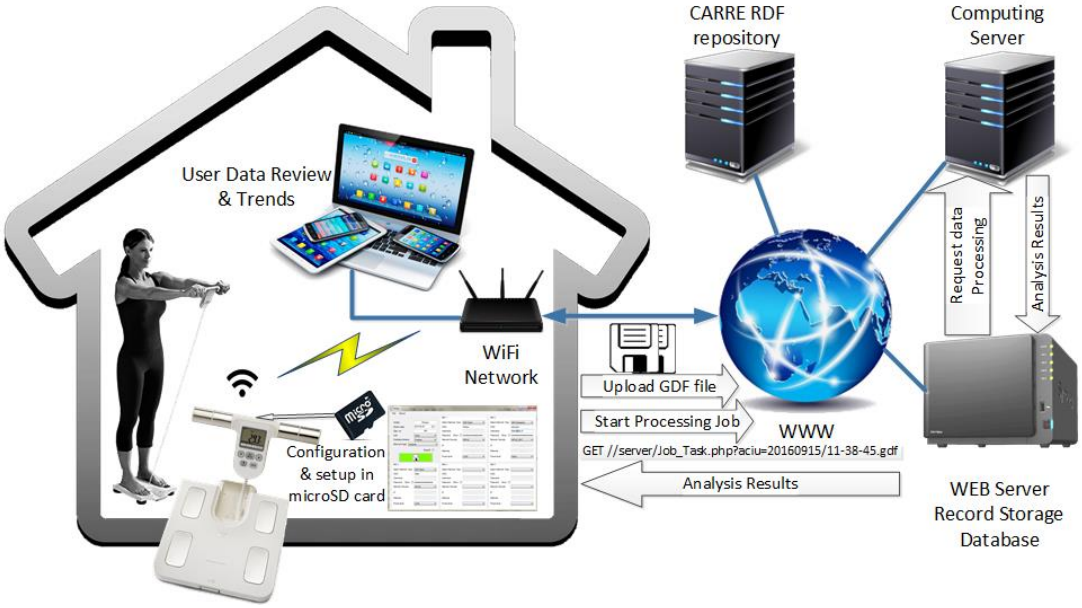

Figure 26. Architecture and system block diagram

The raw data is registered to multichannel, standard data file for biosignals – general data format (.GDF). The .GDF files are stored locally on micro-SD memory card. Configuration setup, required to operate the scale, is also stored in the same micro-SD card. LCD provides instant feedback for the patient.

In addition to measurement process, the device has Wi-Fi transceiver to send automatically just recorded GDF files to the remote record storage server and receive the analysis results. Recorded data analysis and estimation of parameters is done online, on the computing server, which has greater computational power and data aggregation capabilities. Small subset of estimated parameters is delivered back to the user while detail analysis of acquired data can be performed by software application “CARRE Multiparametric Scales Data Analyzer”.

3.3.3. Hardware implementation

The block diagram of hardware is shown in Figure 27. Three different microprocessors take care about tasks and ongoing processes in the scales. The main processor is Cortex-M3, LPC1765 (NXP Semiconductors). It was chosen due to the large number of general purpose inputs/outputs and speed. It’s task is to gather data from all on board sensors and write them to the micro-SD card. Additional tasks are to display information in the graphical LCD screen with resolution of 320 x 240 pixels and keyboard input control. There is a sound codec connected by I2S and I2C communication channels for the audible guidance and information then the

[54] http://www.omron-healthcare.com/eu/en/our-products/weight-management/bf508 (Last accessed 2015-01-27)

measurement starts and stops. Real time clock is implemented as a separate module in order to have time stamps on demand. ESP8266 module is used for WiFi communication. It's firmware is written separately for the file access from the micro-SD card, transfer to the server and to retrieve the results.

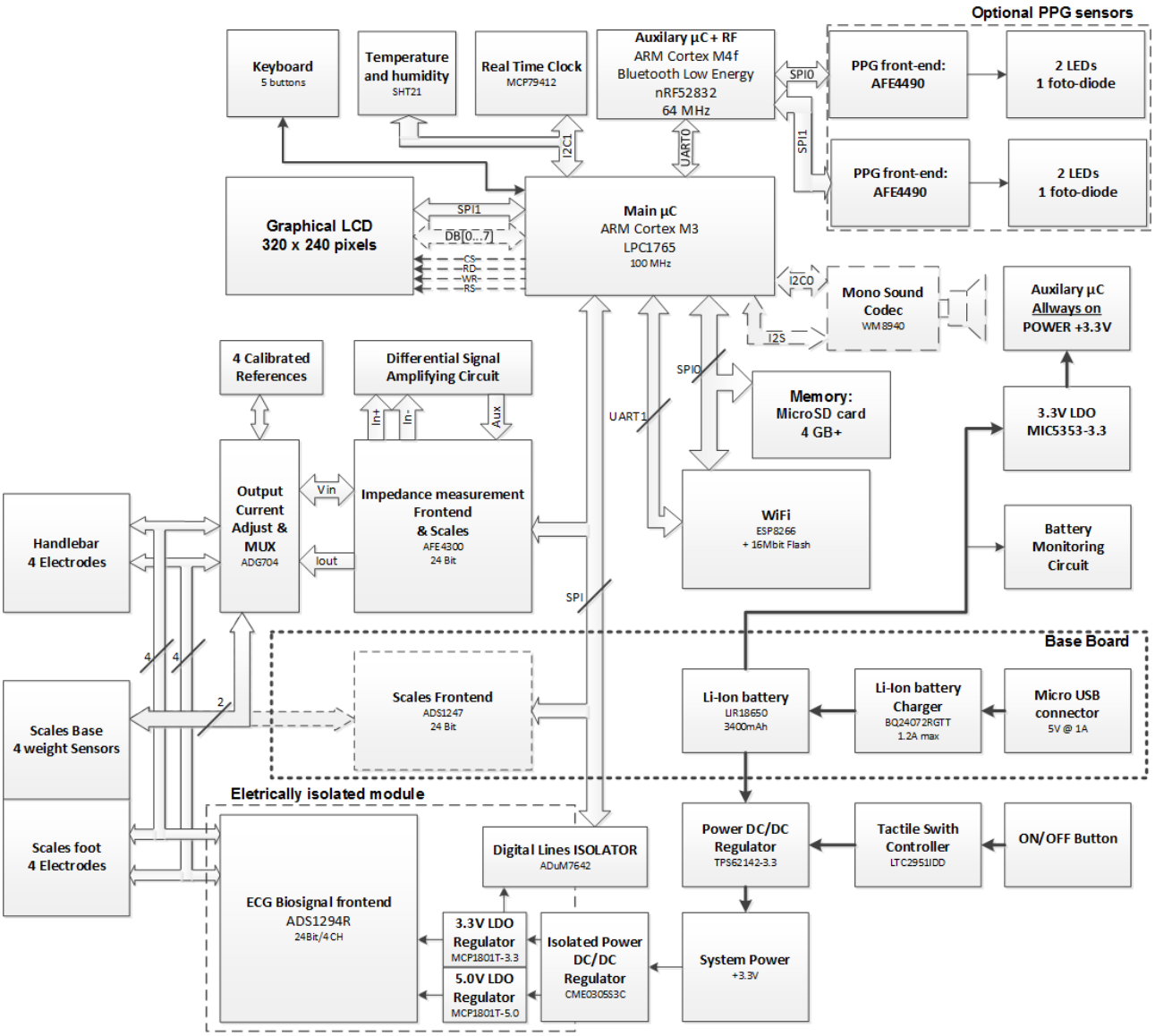

Figure 27. Block diagram of CARRE multiparametric weight scales hardware

Three ECG signals are acquired by the biosignal frontend ADS1294R (Texas Instruments Inc.). It is configured to register 3 ECG leads. Signals are sampled at 500Hz with 24 bits resolution. Weight and bioimpedance signals are measured by weight scales and impedance measurement frontend AFE4300 (Texas Instruments Inc.). External circuit was developed for the AFE4300 in order to increase injected current magnitude and pulsatile impedance changes arising from blood pulsations.

Ambient temperature and humidity is registered by SHT21 sensor, connected to the main processor unit by the I2C bus.

Auxiliary MCU, nRF52832 (Nordic Semiconductor) combines ARM Cortex-M4f processor with multipurpose radio and can be used for communication by proprietary protocols or by Bluetooth Low Energy (V4.0 and up) in central or device roles. Central role allows to receive data from other devices, such as wrist worn device and transfer the data via WiFi channel to the server. This microprocessor unit is always powered on; energy consumption depends on the given task. This processor monitors battery level, sends alarm if battery level is low and the secondary functions is to read optional photoplethysmogram (PPG) signals from AFE4490 sensors

mounted in handlebar (future developments). PPG signals from red and infrared channels can be used, e.g. for estimation of SpO2 values. The sensing modalities and main electronics components are summarized in Table 16. Assembled printed circuit board is shown in Figure 28.

Table 16. Sensing modalities and main electronics components

Sensor	Parameter	Value	Units	Note
PPG	Chip name	AFE4490	-	Optional
	Power consumption	<2.3	mW	At supply voltage of 3 V
	Green LED wavelength	940	nm	
	Blue LED wavelength	650	nm	
	Sampling frequency	100	Hz	SF: 62.5 – 5000 Hz
	Signal resolution	22	bits	
ECG and Impedance 1ch	Chip name	ADS1294R		
	Input referred noise	4	µV (rms)	
	Signal resolution	24	bits	
	Sampling frequency	500	Hz	SF:250 – 32000 Hz
Weight & Impedance	Chip name	AFE4300		
	Excitation frequency	1-100	kHz	
	Signal resolution	16	bits	
	Sampling rate	860	Hz	SF: 8 – 860 Hz
Temperature & humidity	Chip name	SHT21		
	Humidity resolution	12	bits	
	Accuracy(humidity)	±2	% RH	
	Temperature resolution	14	bits	
	Accuracy(temperature)	±0.3	ºC	
	Sampling frequency	2	Hz	SF: up to 2Hz

Figure 28. Top and bottom of printed circuit board of CARRE Multiparametric weight scale with modifications. (Note: version 1.0 hardware is presented. Currently, version 2.0 is being developed)

CARRE Multiparametric weight scale implementation is shown in Figure 29:

a) b) c)

Figure 29. CARRE Multiparametric weight scale implementation: weight scale (a), display (b), usage (c)

3.3.4. Hardware calibration and testing

Weight measurement. Weight measurement was calibrated by observing raw output mode (ADC units in the range 0- 65535) after placing known weight on the scales base. The calibration results are shown in Table 17.

Table 17. Scales weight calibration data							
Weight placed on the scales, Kg	**24.2**	**29.6**	**54.2**	**65.9**	**80.1**	**100.1**	**120**
ADC Value Registered By Scales	**1280**	**3200**	**13184**	**18048**	**24256**	**33152**	**41792**

Matlab Data fitting toolbox (Matlab Inc.) was employed to find the best fitting polynomial function and its coefficients (Figure 30).

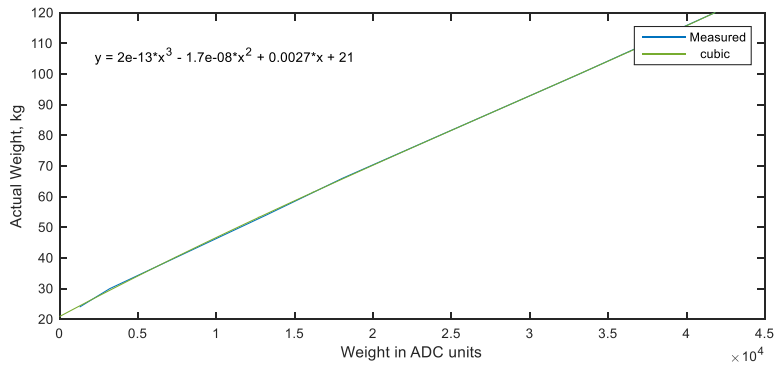

Figure 30. Calibration of weight measurement function

The resulting error in weight measurement is shown in Figure 31.

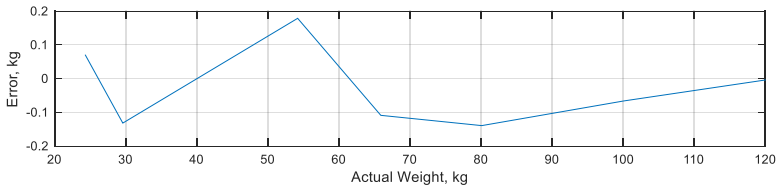

Figure 31. Error in weight measurement of the scales

Impedance measurement. Human body segmental impedances are measured by AFE4300 front end. It has two modes of operation. The first method is a Full Wave Rectifier (FWR) mode and the second method is the IQ mode. FWR mode is used to compute the magnitude of the impedance using a single frequency. This mode is also referred to as Single Frequency Bio-Impedance Analysis (SF-BIA). IQ mode is used to compute both the magnitude and the phase using, at most, five frequencies. This mode is also referred to as bioelectrical spectroscopy (BIS). External reference resistors with known values are used for calibration of bioimpedance measurement function. Calibration takes place before each bioimpedance measurement.

Impedance measurement flowchart is displayed in Figure 32.

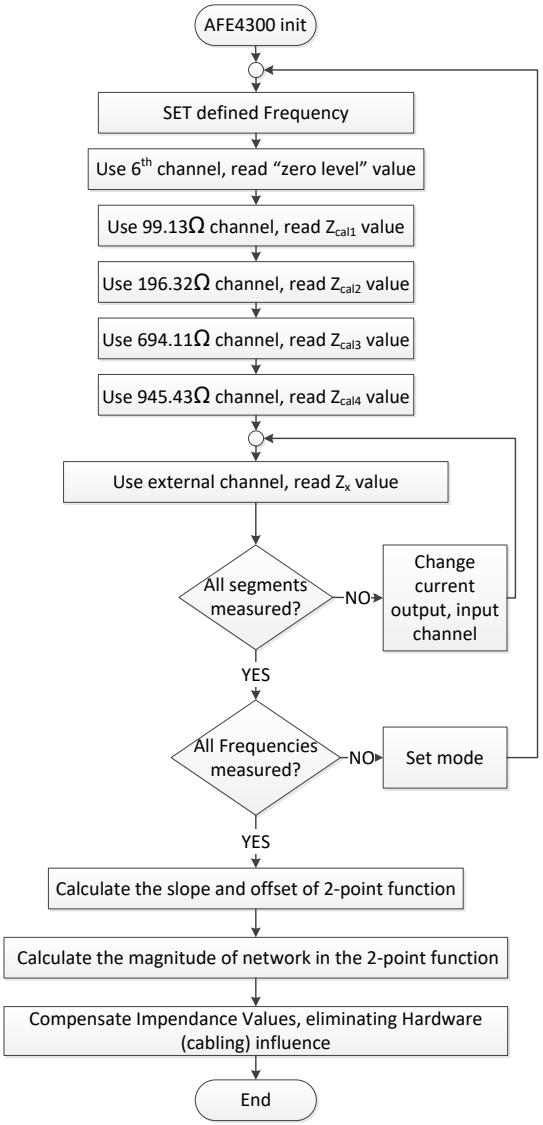

Figure 32. AFE4300 impedance calibration and measurement flowchart

The array of 4 calibration resistors (99.13Ω, 196.32Ω, 694.11Ω, 945.43Ω) is connected directly to the AFE4300. The 6th input channel is connected to ground and is used to measure zero level value (bias). Sensing electrodes are connected by cable and feet electrodes are the most affected with stray capacitances.

Electrical circuit that simulates a body segment and serves as a test circuit for bioimpedance spectroscopy measurements is shown in Figure 33:

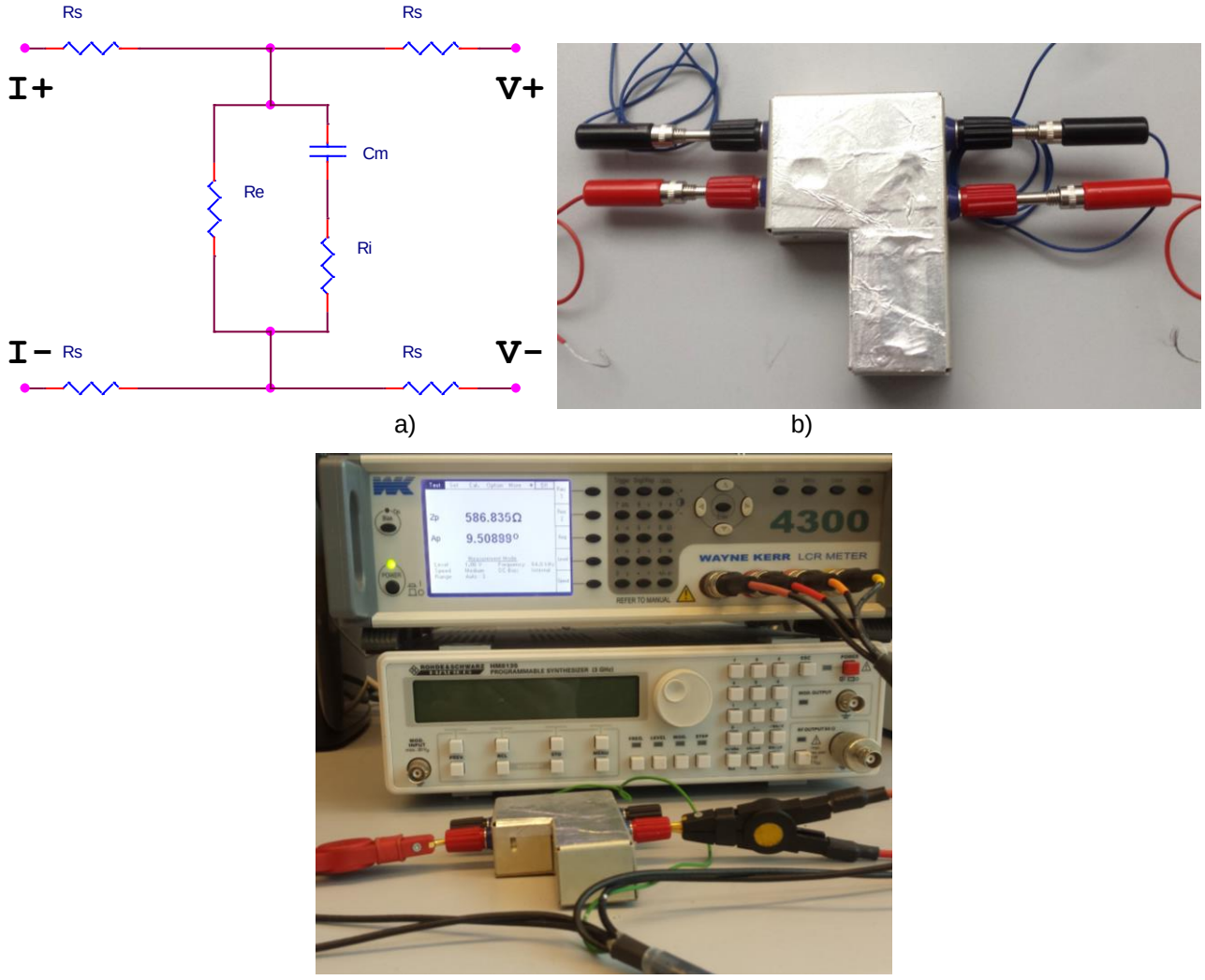

Figure 33. Body segment simulating electrical circuit (a), body segment dummy model mounted in shielded case (b), impedance and phase measurement setup (c)

Body segment simulating model values are presented in Table 18.

Table 18. Body segment simulating model values

Re	Ri	Cm	Rs
592 Ω	1188 Ω	1.704 nF	52.7 Ω

Measurements for dummy model was taken with Wayne Kerr RCL 4300 series meter. Results are provided in Table 19.

Table 19. Dummy model measurement results					Cm, Ri not connected	
Frequency, kHz	|Z|, Ω	Phase, °	Resistance, Ω	Reactance, Ω	|Z|, Ω	Phase, °
8	693.663	2.4741	693.016	29.943	697.727	0.01067
16	682.731	4.6932	680.442	55.859	697.737	0.01097
32	649.097	7.8410	643.028	88.553	697.749	0.01953
64	586.835	9.5088	578.772	96.945	697.752	0.03593
125	533.410	7.5749	528.755	70.316	697.807	0.07202
255	509.134	4.4093	507.627	39.143	698.059	0.15189
510	502.427	2.3792	501.994	20.856	698.512	0.29870

The results for electrical circuit that simulates a body segment and serves as a test circuit for bioimpedance spectroscopy analysis measurements is shown in Figure 34:

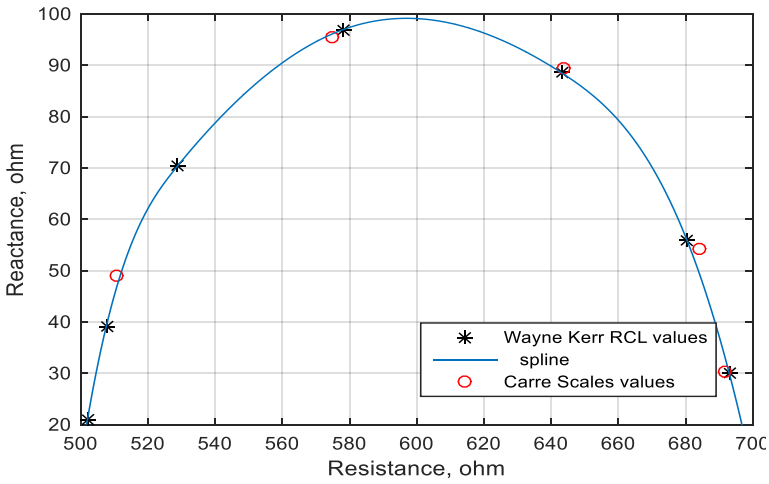

Figure 34. Bioimpedance spectroscopy analysis results – measured with Wayne Kerr RCL Meter (*) and CARRE multiparametric scales (o)

Test of electrocardiogram acquisition. Electrocardiogram recording test was performed by using ProSim 8 Vital Signs Patient Simulator (Fluke, Netherlands) and a real subject volunteer. A reference ECG recording system Biopac MP36 (Biopac Inc., USA) was used in later case.

Figure 35 compares morphology of ECG signal (lead II: right arm – left leg) generated with Vital Signs Patient Simulator and acquired with commercial ECG recorder and CARRE weight scales. No significant differences in acquired signal morphologies can be observed.

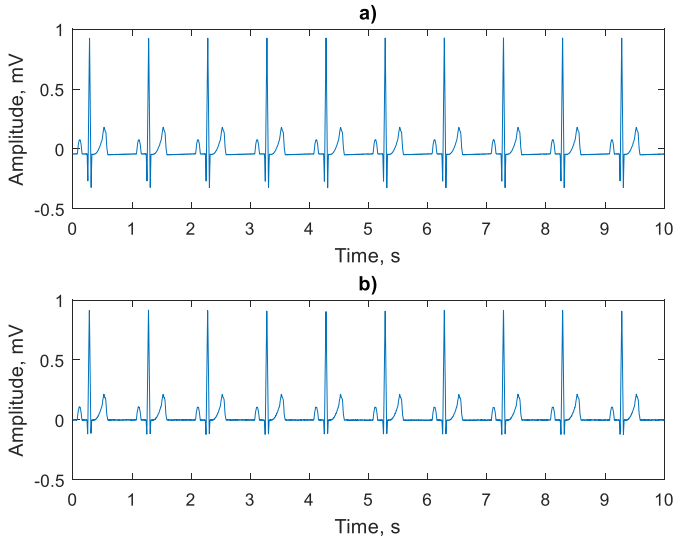

Figure 35. ECG recordings from Vital Signs Patient Simulator accomplished with: reference recording system Biopac MP35 and (a) and CARRE weight scales (b)

Figure 36 compares morphology of ECG recordings (lead II: right arm – left leg) from real subject volunteer. In order to observe raw signal quality, both recordings are shown unprocessed. The ECG acquired with CARRE weight scale is noisier and has significant baseline drift, however, heart rhythm related information (R waves) is largely preserved. This signal quality is sufficient to estimate RR intervals, run short time heart rate variability analysis, and detect arrhythmia (atrial fibrillation).

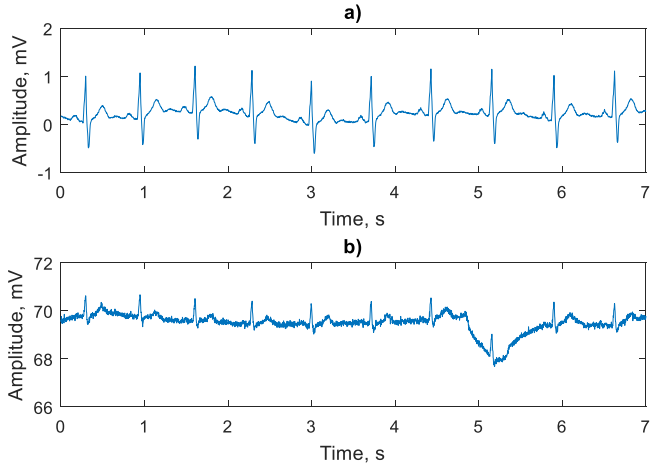

Figure 36. ECG recordings from real subject volunteer accomplished with: reference recording system Biopac MP35 and (a) and CARRE weight scales (b)

3.3.5. Software

Firmware. Flow diagram of operations performed by firmware is presented in Figure 37. Some subroutines such as keyboard I/O are used several times, but many functions cannot be reused, including specific sequences of initialization of sensor IC's due to their bugs on a wafer level. All firmware is written in C programming language.

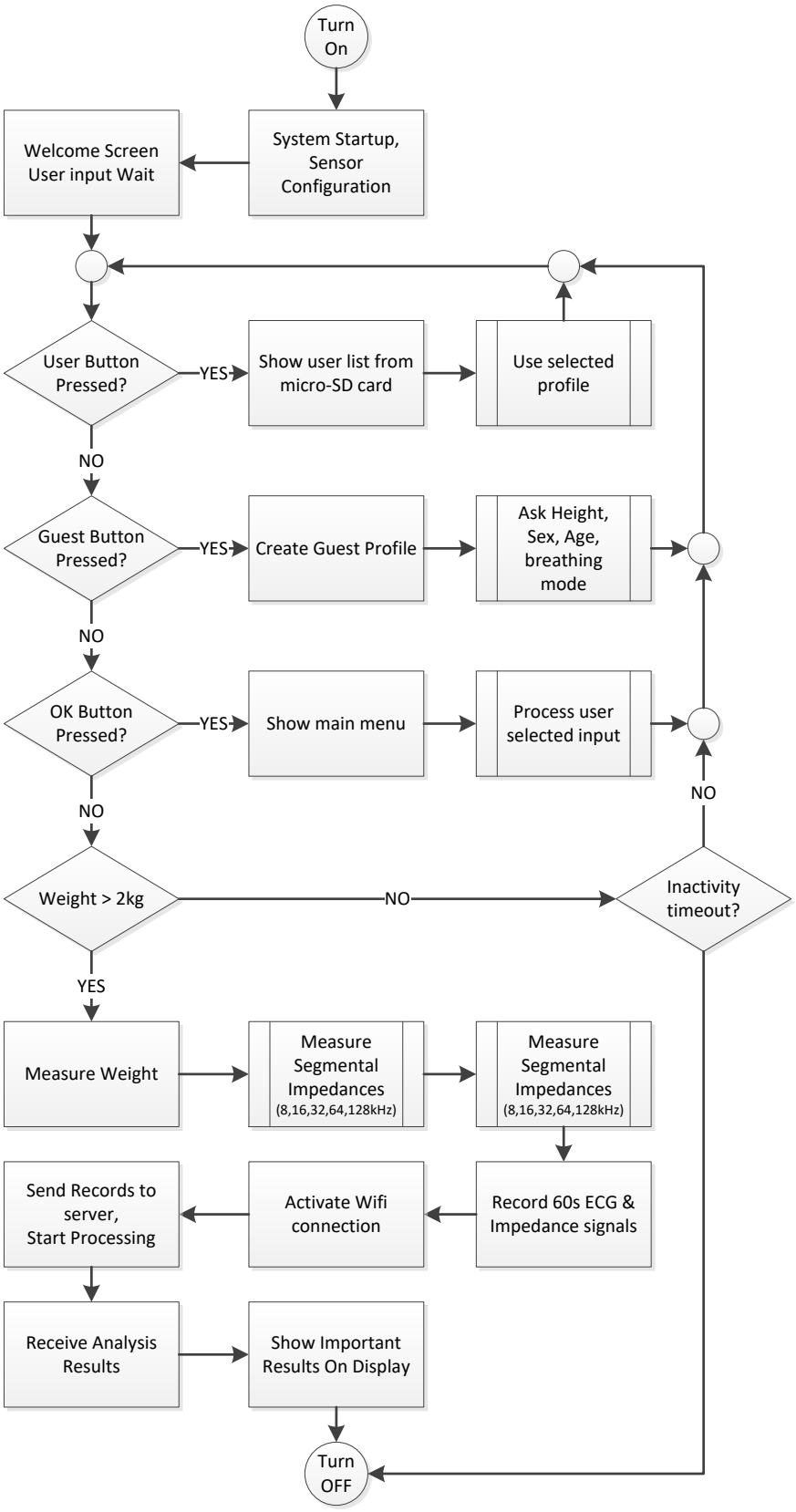

Figure 37. Flowchart diagram of firmware

Computer software. In order to process and analyze recorded files, the Matlab application with graphical user interface (CARRE Multiparametric Scales Data Analyzer) was developed. The application has the following functionality:

- Signal selection, processing, and preview;
- Estimation of pulse arrival time and pulse wave velocity representing the features of the arterial stiffness;
- Estimation of heart rate variability parameters representing the cardiovascular functional status;
- Estimation of body composition parameters;
- Atrial fibrillation arrhythmia detection.

Figure 38 presents the main window of the application where all acquired signals can be observed and visually evaluated. There is possibility to disable all digital filters to evaluate the quality of raw signals.

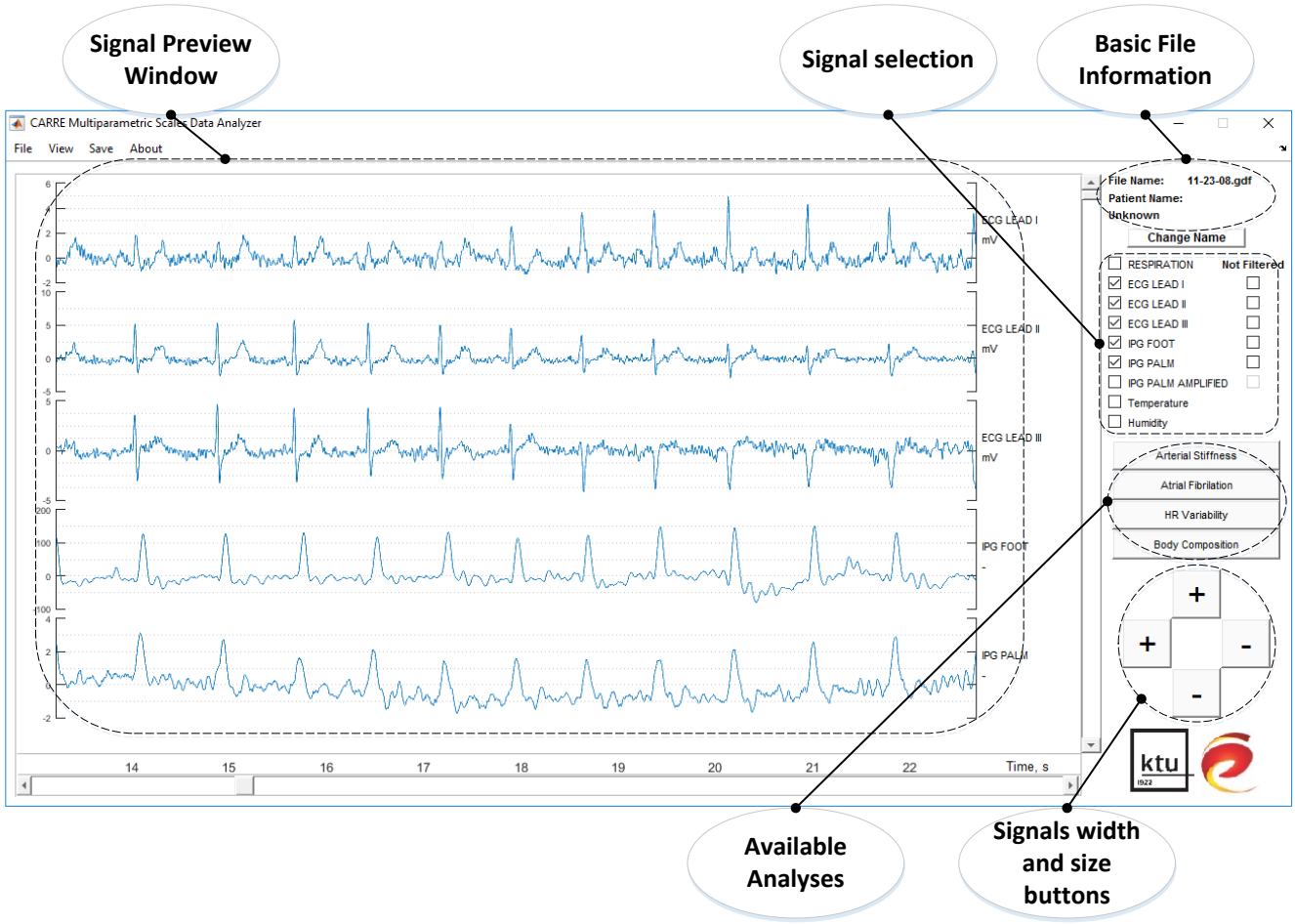

Figure 38. The main GUI window for signal preview, analysis selection

The buttons in Available analyses open other windows where dfferent kind of analyses and signal processing results are presented. “Arterial Stiffness” button opens “Arterial Stiffness Analysis” window which provides information extracted from synchronously recorded electrocardiogram and bioimpedance waveform from feet electrodes (Figure 39). The main parameter estimated from above mentioned signals is pulse arrival time (PAT). PAT is known to be associated with arterial stiffening – stiffening decreases PAT. The algorithm for

PAT estimation from electrocardiogram and bioimpedance signals is presented in our article[55]. The parameter PAT can be useful in long term monitoring of trends. However, there are no established normality distributions for this parameter as a function of age. Pulse wave velocity (PWV) is considered as a gold standard for arterial stiffness assessment. PWV can be estimated using PAT by subtracting left ventricular pre-ejection period (PEP) and knowing the traveled distance of blood volume wave. The normality values of PWV according to the subject age are established and available in the literature[56].

One minute long signals are used for PAT estimation in our application. The signals are recorded either in normal or paced (with period of 10s) breathing conditions. Respiration modulates heart rate and PAT as well. Therefore PAT median is calculated and is used for presentation in normality range (Figure 39).

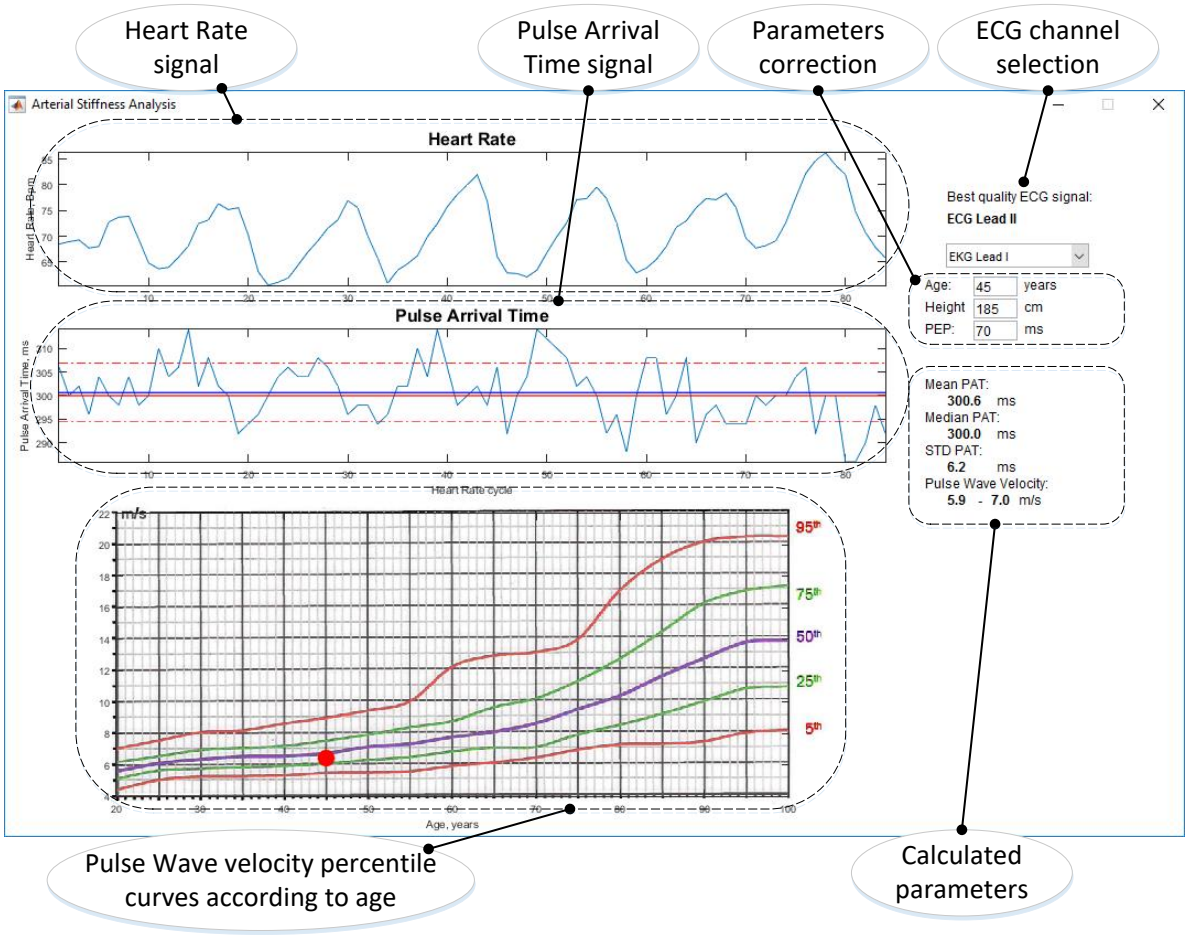

Figure 39. GUI window for arterial stiffness analysis

[55] B. Paliakaite, S. Daukantas, V. Marozas, Assessment of pulse arrival time for arterial stiffness monitoring on body composition scales, Computers in Biology and Medicine, available online April 22, 2016, http://dx.doi.org/10.1016/j.compbiomed.2016.04.012

[56] Determinants of pulse wave velocity in healthy people and in the presence of cardiovascular risk factors: 'establishing normal and reference values' The Reference Values for Arterial Stiffness' Collaboration European Heart Journal Oct 2010, 31 (19) 2338-2350; DOI: 10.1093/eurheartj/ehq165.

"Atrial fibrillation" button opens "Atrial Fibrillation Detection" window which shows ECG and arrhythmia related information. At this moment one arrhythmia - AF (the most popular) is considered. An original, published algorithm is employed for AF detection[57].

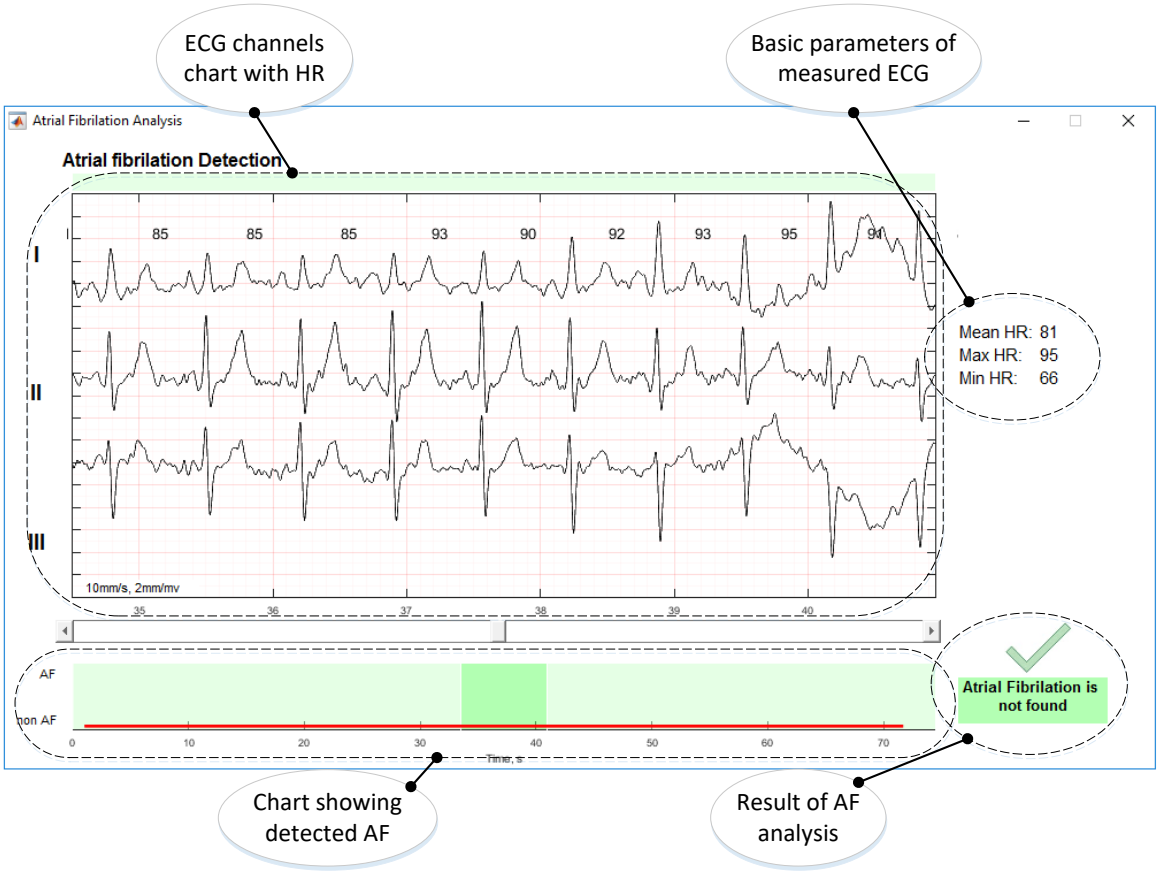

Figure 40. GUI window for Arterial fibrillation analysis

[57] A. Petrėnas, V. Marozas, L. Sornmo, Low-complexity detection of atrial fibrillation in continuous long-term monitoring, Computers in Biology and Medicine, vol. 65, 184-191, 2015.

"HR variability" button opens a new window with heart rate variability analysis results. Heart rate variability quantifies beat-to-beat fluctuations in heart rate and is considered an index of autonomic nervous system balance. Reduced heart rate variability has been associated with increased risk of coronary disease, cardiac mortality, and all-cause mortality. Recent research shows that even (ultra-) short recordings (multiples of 10s) can be used to obtain accurate heart rate variability parameters in time domain[58]. CARRE scales acquires 60s long electrocardiogram signal during each recording session. If the device is used periodically (e.g., every morning) trends of heart rate variability parameters can be evaluated.

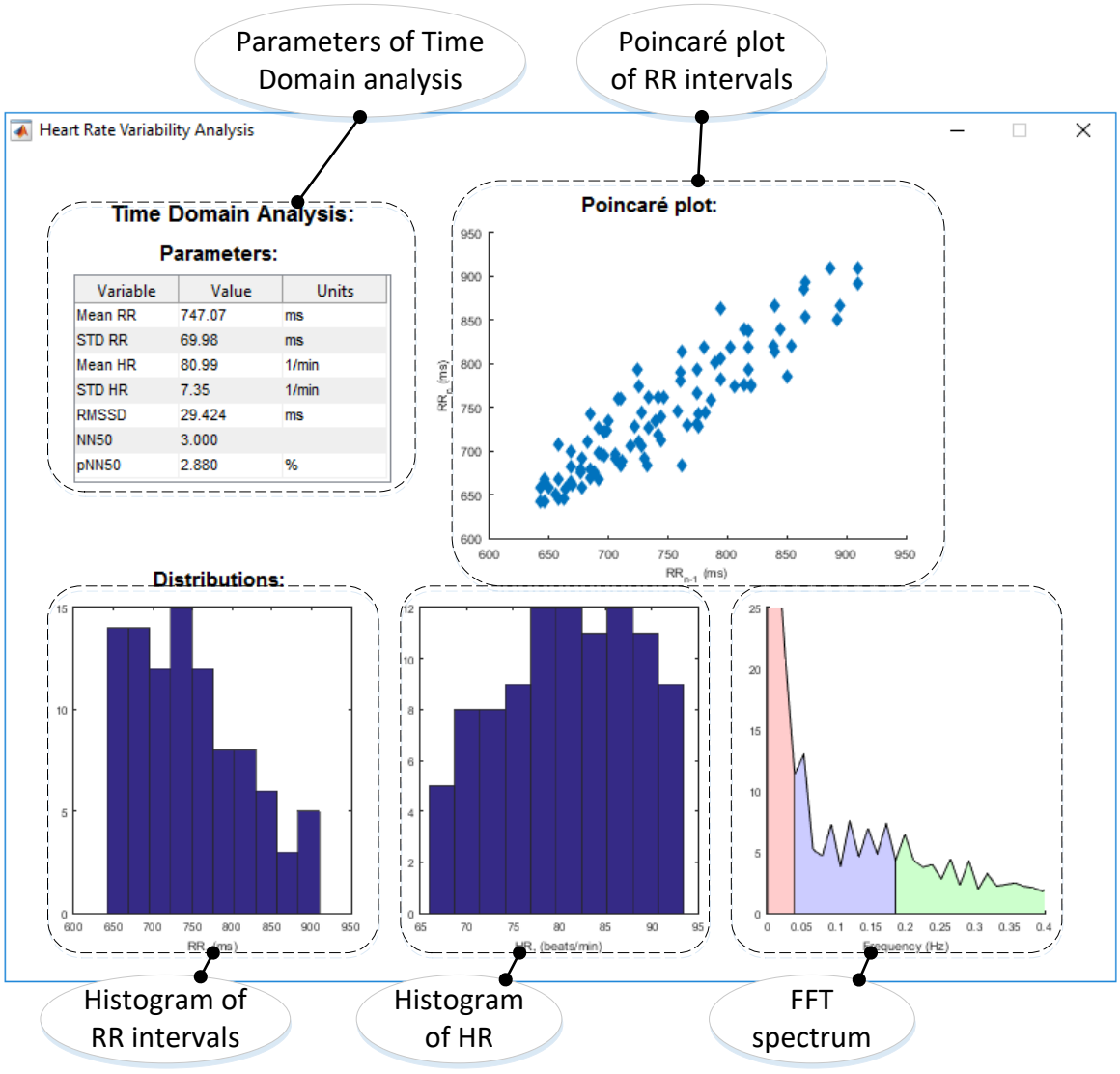

Figure 41. GUI window for heart rate variability analysis

[58] M. L. Munoz, A. Van Roon, H. Riese, C. Thio, E. Oostenbroek, I. Westrik, E. J. C. De Geus, R. Gansevoort, J. Lefrandt, I. M. Nolte, and H. Snieder, "Validity of (Ultra-)Short recordings for heart rate variability measurements," PLoS One, vol. 10, no. 9, pp. 1–15, 2015.

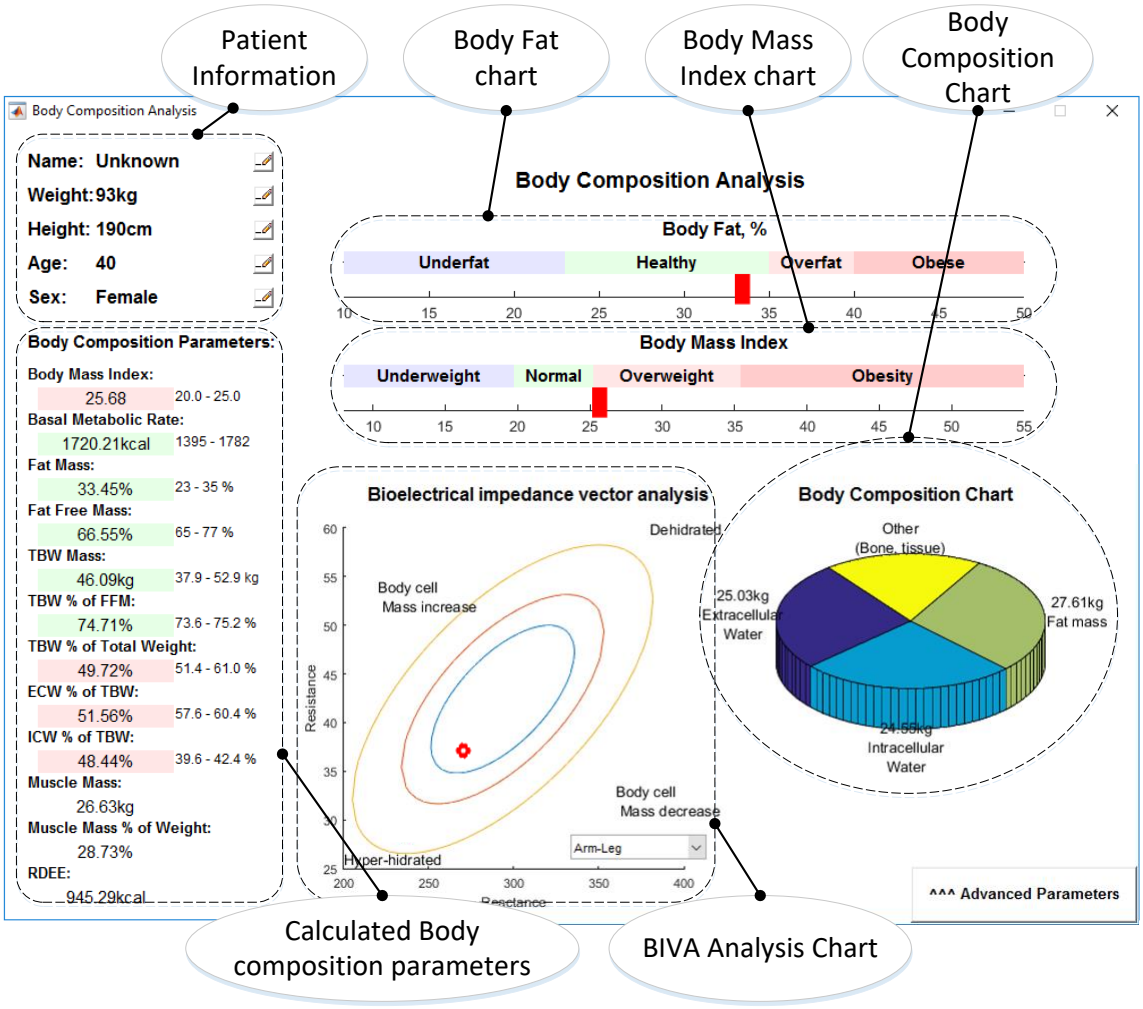

Figure 42. GUI window for Body Composition analysis

After each analysis, a report file in pdf format can be created. In addition, software is also capable of saving main analysis parameters (PWV, BMI, HRV) as trends in a separate (subject specific) file. Parameter changes over time can be later be reviewed. This information shows user information about long term improvements or worsening of health.

3.3.6. Analysis of medical regulatory requirements

The analysis of medical device regulatory requirements for the developed sensors was conducted in order to prove compliance of the developed sensors to requirements in testing phase and to provide interested parties with such information if the mass production will be carried out in the future. The EU medical device regulatory requirements will be briefly covered in this analysis.

Developers of medical devices for the EU market should register their product and through the registration process obtain CE marking. According to 93/42/EEC[59], medical device is “any instrument, apparatus, appliance, software, material or other article, whether used alone or in combination, including the software intended by its manufacturer to be used specifically for diagnostic and/or therapeutic purposes and necessary for its proper application, intended by the manufacturer to be used for human beings for the purpose of:

[59] COUNCIL DIRECTIVE 93/42/EEC http://eur-lex.europa.eu/LexUriServ/LexUriServ.do?uri=CONSLEG:1993L0042:20071011:en:PDF

diagnosis, prevention, monitoring, treatment or alleviation of disease, <…>". The classification of the device to the medical device category strictly depends on the manufacturers declaration of the purpose for which the device is intended to be used. Developed devices prototypes fall under the description of "medical device" as the main purpose of using them is monitoring, prevention and (if accepted by further clinical trials) diagnosis. Manufacturer can decide and describe the intended purpose of the device not for diagnostic monitoring but for the use in home only for self-control of healthiness by the patient himself. In this case, device can be declared to be non-medical device and do not fall under 93/42/EEC regulation.

Medical devices manufacturers should follow the procedures according to 93/42/EEC as it is shown in Figure 43.

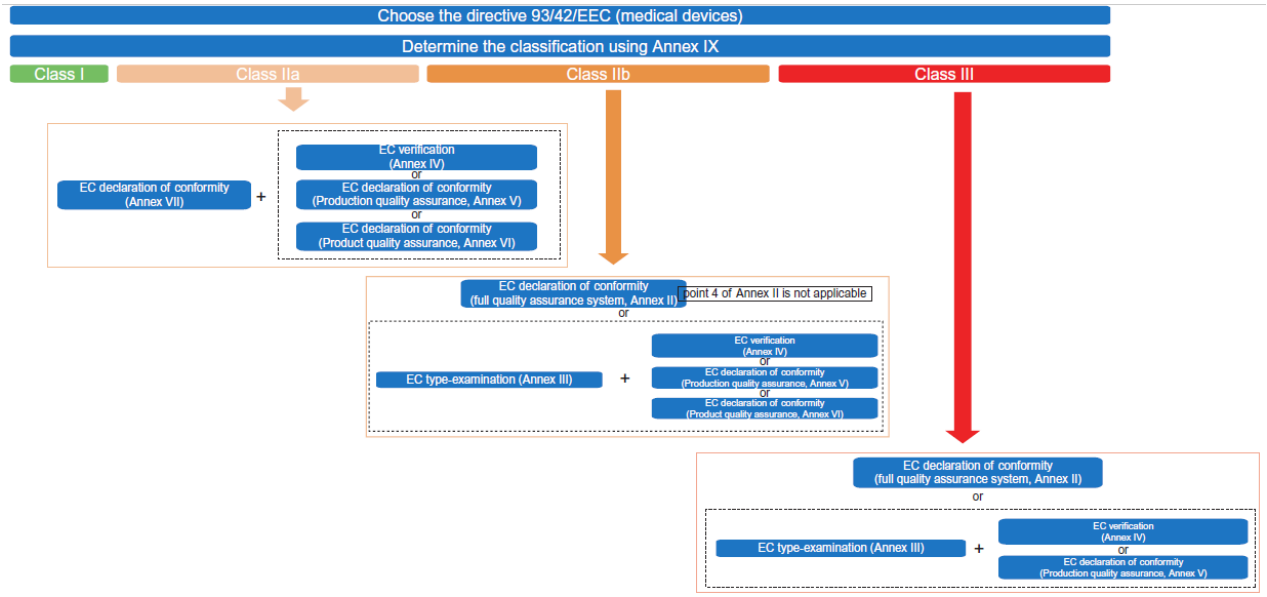

Figure 43. The procedure for medical device manufacturers who intend to obtain the CE marking to market their products in the EU[60]

The summary of the developed devices with the main parameters and comments regarding regulatory requirements is presented in Table 20.

Table 20. Summary of developed sensors and main components of them for the analysis of medical device regulatory requirements

Developed sensors	**Hardware**	**Software**	**Main points regarding regulatory requirements**
ECG based arrhythmia detection	eMotion Faros 180 (*Mega Electronics, Finland*), Class IIa medical device[61]. Measures: • one lead ECG • movement (accelerometer)	Software for paroxysmal atrial fibrillation detection and parameterization (prototype in Matlab)	Hardware used already is certified Class IIa medical device. The software must be validated according to the state of the art taking into account the principles of development lifecycle, risk management, validation and verification.

60 S. Ramakrishna, L. Tian, Ch. Wang, S. Liao and W. Eong Teo Medical Devices. Regulations, Standards and Practices. Elsevier, 2015. ISBN: 978-0-08-100291-9

61 http://www.megaemg.com/products/faros/

Wrist worn device for continuous health parameters monitoring	Developed by KTU Measures: • PPG (three channels: green, red, IR • Movements (accelerometer, gyroscope, altimeter) • Temperature and humidity	Software for atrial fibrillation detection using PPG signal (prototype in Matlab)	Hardware has physical contact with the skin; do not have galvanic contact; there is transmission of energy in optical and IR range of EM waves; battery operated. The software must be validated according to the state of the art taking into account the principles of development lifecycle, risk management, validation and verification.
Multiparametric weight scales for intermittent (periodic) monitoring of health parameters	Developed by KTU Measures: • PPG (three channels: green, red, IR • Movements (accelerometer, gyroscope, altimeter) • Weight • ECG • Bioimpedance • Temperature and humidity	Software for estimation of pulse arrival time, pulse wave velocity; heart rate variability; body composition parameters; atrial fibrillation arrhythmia detection (prototype in Matlab)	Hardware has physical contact with the skin; there is galvanic contact; the current is transmitted through body for the bioimpedance measurement; there is transmission of energy in optical and IR range of EM waves battery operated. The software must be validated according to the state of the art taking into account the principles of development lifecycle, risk management, validation and verification.

Classification of the devices into classes is provided in accordance with Annex IX of the 93/42/EEC.

ECG based arrhythmia detection device is classified as Class IIa device as the hardware part of the device already is Class IIa device and also software is an *active medical device* and is "intended to allow <…> or monitoring of vital physiological processes <…>"[62]. The wristwatch and the multiparametric scales fall into this category also, so all devices can be classified as Class IIa medical devices.

For Class IIa medical devices in order to affix the CE marking should be followed the procedure relating to the EC declaration of conformity set out in Annex VII, coupled with either procedures described in Annex IV, V or VI of 93/42/EEC. As the developed prototypes are not the final products, here we will analyse only the most important key aspects of regulatory requirements for medical devices.

Medical device safety is the most important factor for any regulatory body and this requirement is written as a first requirement in Annex I of 93/42/EEC. Safety and risk arising using the product is not limited to medical device regulations but are required by other related regulations also, especially for electronic devices. In addition, devices with a measuring function should provide sufficient accuracy. Further, we briefly analyse the key safety and accuracy aspects of the developed devices.

The safety of the medical device is defined by the product risk assessment. Most manufacturers typically use ISO 14971 for the formalization of a system of risk management. Not going into detail risk analysis as the medical device regulations typically require risk assessment and control beyond product design, the safety of the devices is essential question. As the devices are electronic and are in contact with the human, the electrical safety is the main factor. The electrical safety should be considered during the electrical circuit design stage of the device and is regulated by the IEC 60601 "Medical electrical equipment".

[62] Annex IX, Rule 10 of the 93/42/EEC

Medical electronic equipment with respect to electrical contact with patient is classified to type B, BF or CF applied parts. The developed devices belongs to type BF applied part (the definition is: electrically connected to Patient but not directly to heart; electrically isolated from external electrical sources).

Among the developed devices, the multiparametric weight scales must be mostly considered to be checked by the safety rules as this device have galvanic contact with the skin and is injecting current through the body. The allowable values for the injected into patient currents are defined in IEC 60601-1 Table 3 and are the following for a type BF applied parts: 10 μA (d.c.) and 100 μA (a.c., r.m.s) for normal conditions and 50 μA (d.c.) and 500 μA (a.c., r.m.s.) for single fault conditions. The alternating currents are estimated with frequency weighted model (see Figure 12 in IEC 60601-1) and are limited to 10 mA r.m.s. in normal and single fault conditions. Recalculating maximum allowable currents using frequency-weighted model, the frequency dependant current limit graph can be plotted (see Figure 44). From the plot we can see, if the frequency of the injected current is 50 kHz, the r.m.s. value of the current should not exceed 5,18 mA. However, it should be considered, what in single fault condition, if the excitation frequency due fault decreases to less than 1 kHz, circuit should limit the current below 500 μA r.m.s.

The core of the body composition scales for the bioimpedance measurement are AFE4300[63] (for body composition channel) and ADS1294R[64] (for pulse transition time) front ends. ADS1294R front end is designed (see Annex 3 of this document) according to recommendations of technical documentation and meets IEC60601-1, IEC60601-2-27, and IEC60601-2-51 standards as is declared in his technical documentation. The AFE4300 front end then used according to technical specification injects current into body not bigger than 450 μA (RMS value) and also conforms the electrical safety standards.

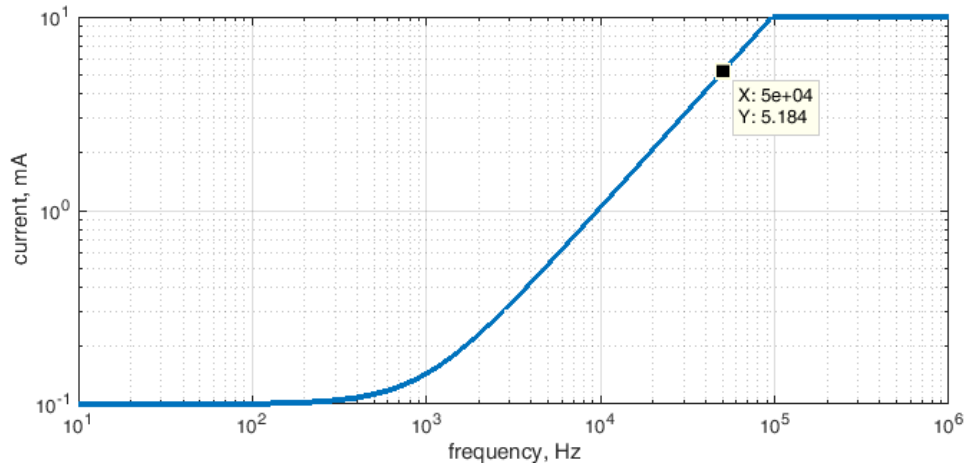

Figure 44. Frequency-maximum allowable current plot according IEC 60601-1 with respect to frequency-weighted model

The Non-automatic weighing instruments (NAWI)[65] directive defines the level of accuracy required by a weighing scale by giving it a Class. This directive applies to medical scales if they are used for "determination of mass in the practice of medicine for weighing patients for the purposes of monitoring, diagnosis and medical treatment". Medical scales for human body weighing are classified as Class III scales. If scales are used in, for example, fitness centres, they do not have to conform to the NAWI regulations – as long as the weighing is only for reference and is not used for any purpose mentioned above.

Verification interval *e* for the developed scale is 100 g, minimal capacity is 20 kg (i.e. 200**e*), maximal capacity is 150 kg (i.e. 1500**e*). According to directive, this applies to Class III scale device (200**e*…10000**e*). Accuracy of the scales is defined by *maximum permissible error (MPE)*, that in this case have two intervals (according directive: 0≤m≤500e and 500e<m≤2000e): 20-50 kg and 50-150 kg. For the first interval, 20-50 kg MPE should be 0,5**e*=50 g, and for the second interval MPE should be 1**e*=100 g. The weight measurement results (Figure

63 http://www.ti.com/lit/ds/symlink/afe4300.pdf

64 http://www.ti.com/lit/ds/symlink/ads1294r.pdf

65 Directive 2014/31/EU on the harmonisation of the laws of the Member States relating to the making available on the market of non-automatic weighing instruments http://eur-lex.europa.eu/legal-content/EN/TXT/?uri=CELEX:32014L0031&locale=en

31) shows that developed scale do not confirm NAWI Class III requirements and should be improved if marketing as Class III scale device is foreseen. In addition, eccentricity, discrimination and repeatability tests should be performed for full assessment as NAWI Class III device. These issues can be done and fulfilled preparing device for mass production.

Another part of the devices is the software and the 93/42/EEC explicitly mentions “software”’ in its definition of medical device. The developed devices uses software prototypes developed in scientific programing environment (Matlab) and include algorithms for the signal acquisition, processing and parameterization. These algorithms are the core of software and the device as a whole. Going into mass production of the devices, the implementation of the developed algorithms should be done according to the medical device regulation procedures. The form of the software can be stand-alone software or mobile application. The latter case is spreading into the usability in real life. The requirements for the app to be registered as medical device strictly depends on that the software does and the risk to the patient this software can carry. So, the classification depends on the manufacturer and on the responsibility what he can accept.

The basic requirements for the software as medical device are described in IEC 60601-1, “Medical electrical equipment - Part 1: General requirements for basic safety and essential performance”. The standard IEC 62304 “Medical device software - Software life cycle processes” covers both software as a component of a medical device and standalone software. The software algorithms of the developed devices in some cases can be implemented separately in stand-alone software, not depending on the hardware (ECG based arrhythmia detection device is an example of this case). IEC 82304 “A dedicated health software system standard” is in development[66] expanding IEC 62304 and providing a product safety standard for health software products what are software only products.

3.3.7. Towards new standards and security – modification of GDF data file standard

General Data Format (GDF) v2.51 for biomedical signals was chosen for our records. It has high flexibility by adapting multiple types of signals, multiple sampling frequencies and has free form header for the user data in Tag-Length-Value format (Header3). GDF format lacks security or encoding rules in its standard.

In general, most security enabling functions can be divided into symmetric and asymmetric key (password) groups. The most widely used are symmetric key encryption algorithms, e.g. AES, blowfish or two-fish algorithms. These methods use one password for the encryption and decryption. AES 128 / 256 bit wide is most widely used standard in wireless data transfer modules (e.g. WiFi and Bluetooth). Its encryption and decryption modules exist in hardware, so it is advisable to use them in order to save power in battery-powered applications.

Asymmetric key encryption is used in various internet standards, such as Transport Layer Security (TLS), PGP, S/MIME and GPG. Key generation is difficult, time consuming task and is used to obtain “Public” key for encryption, “Private” key for decryption. Some algorithms can be used for encryption only (e.g. Diffie-Hellman key exchange), others are used to sign messages (e.g. Digital Signature Algorithm). The most often employed one is RSA algorithm which can do sign and encryption tasks. Depending on needed security, it is advisable to use key length of at least 2048 bits, and use 4096 bits or higher in high security applications.

GDF file structure in more details is explained in Table 21.

Table 21. GDF file common structure

Section	Size, bytes	Used for	Notes
Header1	256	File structure, Numer of Signals (NS) and patient description info	
Header2	NS*256	Description for every signal, scaling and filtering	
Header3	n*256	Free form Header, TLV format ([TAG(1 byte),LENGTH(2bytes),VALUE())])	n=0, 1, 2, …
Data			
	N samples from channel [1] of TYPE[1]		Type[1]

[66] IEC 82304 draft: https://www.iso.org/obp/ui/#iso:std:iec:82304:-1:dis:ed-1:v1:en

	N samples from channel [2] of TYPE[2]	Type[2]
	N samples from channel [3] of TYPE[3]	Type[3]
	…	…
	N samples from channel [NS] of TYPE[NS]	Type[NS]
Event Table	The table of events is stored after the data section. Each event is defined by the event type and position {TYP,POS}, if duration is available, then {TYP,POS,DUR,CHN}.	Variable length after DATA section

Most of file structure defining variables are in Header1, but the patient data resides here to (e.g. Patient ID, Age, Sex, Birthday etc.). Bearing that in mind it was proposed (see Table 22), that, in Header1 some reserved values can be replaced into encryption flags for the patient data (signals) and patient information (age, sex etc.).

Table 22. GDF file Header1 new information

FIXED HEADER (Header 1)	**Remark 1.x -> 2.0**	**Position Start:End [bytes]**	**Bytes**	**Type**
Version identification (GDF 2.00)	updated	0	8	char[8]
Patient identification (P-id)	smaller	8	66	char[80]
Encrypted Header1 in Header3 (Patient Information)	Proposed	74	1	uint8
Encrypted Data (encryption method, initialization vector and passphrase in Header3)	proposed	75	1	uint8
reserved	smaller	76	8	uint8
Smoking / Alcohol abuse / drug abuse /medication (see Table 2)	Added	84	1	bit[4x2]
Weight [in kg]	Added	85	1	uint8
.... Rest of header				

Patient information filled in Header1 can be encoded using asymmetric key algorithm (e.g. RSA) and placed in Header3 using TLV format. In order to maintain integrity of the file, only the vital information for file decoding is left in Header1 in next step.

If Data section of the file is to be encrypted then Encrypted Data byte in Header1 is set. Data section can be encrypted using symmetric key algorithm, e.g. AES256 in Cipher Feedback (CFB) mode. Initialization Vector (IV) and key are encoded using RSA, with different key than for the patient info and placed in Header3 using new TAG's informing that this section contains info for data decryption.

In total, at least two independent public keys are stored in device encoding data, and two private keys are required to access record data and independently patient information. Thus, researcher, or analyzing program, knowing only the key to decrypt data, does not have access to sensitive patient information.

3.3.8. Continuation of the development and exploitation

Currently, CARRE Multiparametric scale is being used as a scientific instrument for unobtrusive registration of biosignal databases. Its main strengths: multiple signals and parameters can be registred, operator-less, short registration time (~1,2 min), WiFi wireless capability for autonomous data transfer to remote server (no need for additional smartphone and App). The existing and associate CARRE partners (Lithuanian Health Science University Kaunas Clinics, Department of nephrology) will be invited for testing of the developed technology.

Fitness and self-control of health is very important applications, too. Commercial companies working in athletes' management and big data analytics expressed their interest in the technology.

Continuation of the development involves clinical validation of algorithms for: body water balance tracking, monitoring of pulse arrival time changes during guided breathing test, arrhythmia detection. Very important issue left as a future work – embedding in the device the proposed GDF file standard modification with data encryption capability (Section 3.3.7).

4. Personal sensor data aggregator architecture and implementation

4.1. Personal sensor data aggregator concept

The idea behind the personal sensor data aggregator is to collect personal sensor data from a variety of sources, such as sensor manufacturers or health data platforms, to convert those data, regardless of origin, into RDF in accordance with the schema presented in D.2.4, and to store that RDF in the CARRE semantic repository.

The aggregator needs to be easily extensible in order to support the wide range of different data providers available, and to accommodate new providers, where necessary, as they appear.

Figure 45 presents a concept of CARRE personal sensor data aggregator. The concept shows which sensor data clouds that were preselected in D.2.3 are connected to CARRE sensor data aggregator. In order to show the system scalability and to account for future developments, the concept also presents what and how other potential sensor data sources could be integrated into CARRE system. These optional connections are shown by using dashed lines. They also show that some sensor data sources can be accessed indirectly via intermediate sensor data aggregators such as HealthVault by Microsoft Inc., Google Fit by Google Inc. or Health Kit by Apple Inc.

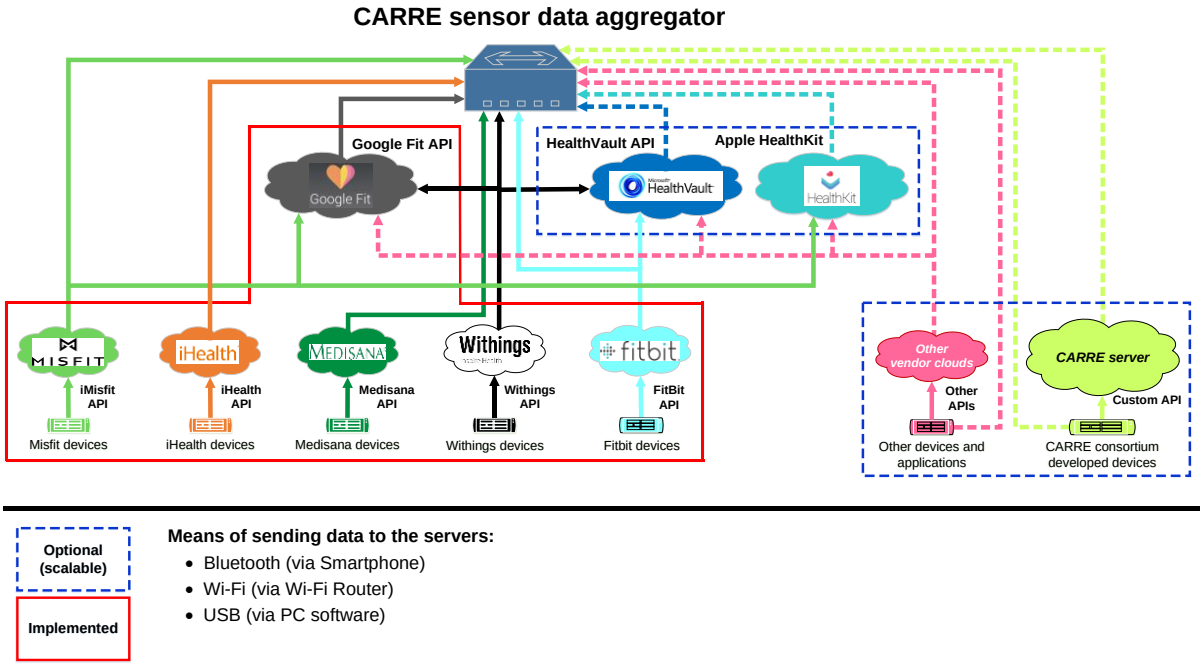

Figure 45. Personal sensor data aggregation concept

4.2. Personal sensor data aggregator design

4.2.1. Overall architecture

The personal sensor data aggregator is designed to allow easy extension with support for other devices as needed. The architecture is as shown in Figure 46.

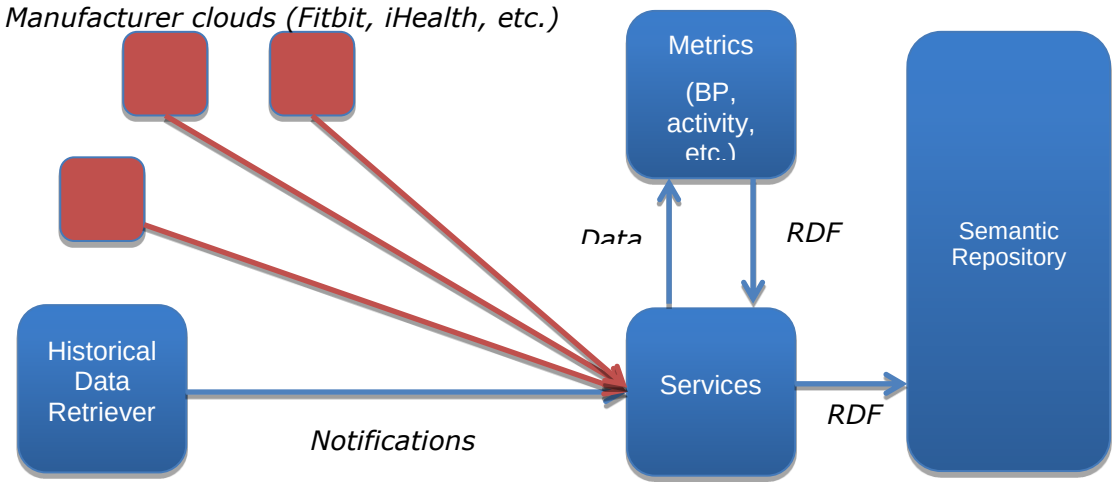

Figure 46. Personal sensor data aggregator architecture.

4.2.2. Responder design and execution flow

Almost all of the sensor providers we support implement a “notification” or “subscription” mechanism to allow any new sensor data be sent to user-approved third-party applications whenever such data is synced with the manufacturer. These all operate in a similar way: when configuring a third-party application, the URL is specified. When new data arrives for a user who has approved that application, an HTTP GET or POST request is sent to that URL with some means of identifying the user, and the timespan covered by the new data. The application can then sync with the sensor provider servers to retrieve and store the new data.

The CARRE personal sensor data aggregator plays the role of such third-party application for each of the sensor providers we cover. The responder identified in the architecture is a Web service which responds to HTTP GET or POST notifications, identifying the sensor provider who initiated the notification and the CARRE user to whom the data belongs. It invokes the relevant service corresponding to that provider, which then fetches that new data, converts it into RDF according to the schema described in Deliverable 2.4 and stores it in the CARRE semantic repository.

4.2.3. CARRE semantic repository

Each user in CARRE has a user account, and a private RDF graph on the semantic repository. The content of this graph is only accessible to that user and the CARRE system administrators. All data relating to that user is stored in the relevant private graph. User accounts and devices are managed through the CARRE Devices frontend[67], which allows a user to add a connection to a new sensor data provider. Adding a connection involves authenticating with the appropriate sensor provider servers and retrieving authentication “tokens” which can be stored securely in the user’s graph in the semantic repository. When this has been done, the responder will receive notifications from that provider for that user, and will be able to retrieve the authentication tokens in order to fetch any newly added data.

[67] https://carre.kmi.open.ac.uk/devices

4.2.4. Services

Each service, corresponding to a sensor data provider, follows the same general design. In particular, each service can:

1. Parse notifications from the relevant provider
2. Fetch appropriate authentication details for a user from the semantic repository[68]
3. Fetch data from the provider corresponding to given date ranges or data identifiers.
4. Create appropriate representations of that data for converting to RDF.
5. Store RDF data in a user's private graph in the repository.

4.2.5. Metrics

Sensor data is represented generically by the metric components. Each type of metric is a generic type of sensor data – for example, blood pressure – generic across providers, rather than a specific component corresponding to, for example "Withings blood pressure" or "iHealth blood pressure". The services are able to invoke the metric component corresponding to a data type. The blood pressure metric, for example, requires values for systolic and diastolic blood pressure. Each metric can then generate the relevant RDF containing those values, for storing in the repository. This design ensures that different sensors which measure the same underlying biomarker data have their data represented in a common way. Because of the object-oriented design, the only occasions when a specific type of Metric such as Blood Pressure needs to be referenced is when actual data is being populated by the Service. For the most part, the generic superclass Metric is sufficient, and enables a high degree of component reuse.

4.2.6. Historical data retriever

In many cases during testing, users had been wearing and using sensors for some time before the personal sensor data aggregator had been fully implemented. The historical data retriever is designed to fetch data stored by any sensor providers from *before* the date a user connected that provider to CARRE. By default, data is fetched from the start date of the CARRE project. This process only applies to users who agree explicitly to their historical data being fetched.

4.2.7. CARRE Devices

The user interface to the aggregator is provided by a website which supports the creation and management of CARRE user accounts, and allows users to make connections between their accounts and various supported sensor data providers.

4.3. Personal sensor data aggregator implementation

The responder, services and metric components are all written in Java and run on the Tomcat servlet container[69].

4.3.1. Responder implementation

The responder itself is a very thin layer which provides URLs to which each sensor provider can send notifications. For example, when new data is synced to Fitbit for a CARRE user, a notification is sent to:

---

[68] Since providers do not all use the same authentication process, this is not a generic process, and must be customized for each provider.

[69] http://tomcat.apache.org

https://carre.kmi.open.ac.uk/tomcat/responder/fitbit

whereas when data is synced to Withings, a notification arrives at:

https://carre.kmi.open.ac.uk/tomcat/responder/withings

and so on. By examining the particular URL to which the notification has been sent, the responder is able to identify which service to invoke. It passes the notification data to that service and returns an "OK" message to the sensor provider.

As stated above, nearly every sensor data provider has some form of notification mechanism. At the time of writing, the sole exception is Google Fit[70]. To handle fetching data for Google Fit, the Unix task scheduling tool, cron, is used to trigger a poll frequently.

4.3.2. Service implementation

Each service is implemented as a subclass of a generic Service class in Java, and must implement two core methods[71]:

- handleNotification
- getMetrics

The handleNotification method accepts HttpServletRequest and HttpServletResponse methods, which are passed directly from the responder and represent precisely the HTTP communication between the sensor provider and CARRE. Each service, within the handleNotification method, can extract the content of each notification. For example, a notification from Fitbit contains a JSON[72] message such as:

```
[
	{
		"collectionType":"activities",
			"date":"2014-10-01",
			"ownerId":"83CARRE",
			"ownerType":"user",
			 "subscriptionId":"carreUser3",
	}
]
```

which signifies that new activity data has arrived relating to the Fitbit user account with identifier 83CARRE, and that this data belongs to a user on the CARRE system identified by carreUser3[73]. The service therefore knows to fetch the Fitbit authentication tokens for the user identified by carreUser3, and to fetch activity data for the 1st of October 2014 from Fitbit. In particular, the service will then call getMetrics, passing date values to cover the 24 hour period of that date.

The getMetrics value accepts two date values, and returns a list of Metric objects representing the data stored for the current user with the current provider between those dates.

---

70 https://fit.google.com

71 Plus other methods related to housekeeping tasks.

72 http://www.json.org

73 The subscriptionId is simply a string unique for each user, and need not contain anything externally-identifying which could compromise privacy.

4.3.3. Metric implementation

Each Metric is implemented as a subclass of a generic Metric class in Java. Every Metric has an identifier (a string) and a date, intended to represent the date at which a measurement was taken. Each subclass of Metric must define a type (e.g., temperature).

Subclasses of Metric can vary significantly, depending on the individual type of measurement(s) represented. The Activity metric, for example, which is designed to represent the data collected by activity/fitness trackers, defines fields for steps taken, calories burned, the name of an activity (e.g., swimming) where logged, and so on. The BloodPressure metric defines fields for systolic and diastolic blood pressure values. Each particular type of Metric provides methods for getting and setting the values of each of its fields. The Service classes, when parsing data from a particular sensor provider, create instances of these Metric classes, and add values to their fields as appropriate.

The generic Metric class provides a method “toRDFString” which is passed a CARRE user identifier as a parameter. The user identifier is used to construct the base URL for the RDF representation of a Metric – an individual measurement is always given an HTTPS URL relative to the user’s own RDF graph in the repository, to ensure uniqueness and security of identifiers across users.

The actual RDF triples corresponding to a particular measurement are constructed using the Java Reflection API[74], which can inspect classes, and the names of the fields in each class. Thus the Activity metric class, for example, has a field named “steps”, and another named “sedentaryActivityDuration”. Use of the Reflection API allows the construction of RDF predicates “has_steps” and “has_sedentary_activity_duration”, respectively. By inspecting the *type* of each field, the appropriate types can be assigned to RDF literals representing the value of each field. So, for example, if “steps” is represented by a Java integer, a value for steps can be represented in RDF using the appropriate XML datatype[75] “integer”.

The benefit of using Reflection to construct RDF is that the toRDFString method needs only be defined *once*, in the generic Metric class, with no need to rewrite, customize or specialize for any particular subclass. To ensure that the fields of a specific type of Metric are assigned the appropriate RDF representations, all that is needed is to ensure that the name of the corresponding Java field matches the desired representation.

The following example shows how straightforward it is to generate the RDF representation of a blood pressure measurement:

```
BloodPressure bp = new BloodPressure(identifier);
bp.setDate(measurementDate);
bp.setSystolicBloodPressure(systolicValue);
bp.setDiastolicBloodPressure(diastolicValue);

String rdf = bp.toRDFString(carreUserName);
```

This produces a set of RDF triples similar to the following:

[74] http://docs.oracle.com/javase/7/docs/api/java/lang/reflect/package-summary.html

[75] http://www.w3.org/TR/xmlschema11-2/

```
PREFIX carreUser:<https://carre.kmi.open.ac.uk/users/CARRE_USERNAME/measurements/>

PREFIX carreSensors:<http://carre.kmi.open.ac.uk/ontology/sensors.owl#>

PREFIX carreManufacturer:<http://carre.kmi.open.ac.uk/manufacturers/>


carreUser:b3bc5 carreSensors:has_date carreUser:b3bc5_date

carreUser:b3bc5_date carreSensors:has_value "2014-05-16T13:54Z"^^xsd:datetime

carreUser:b3bc5 carreSensors:is_measured_by carreManufacturer:ihealth

carreUser:b3bc5 carreSensors:has_blood_pressure_systolic
carreUser:b3bc5_blood_pressure_systolic

carreUser:b3bc5_blood_pressure_systolic carreSensors:has_value "122"^^xsd:integer

carreUser:b3bc5 carreSensors:has_blood_pressure_diastolic
carreUser:b3bc5_blood_pressure_diastolic

carreUser:b3bc5_blood_pressure_diastolic carreSensors:has_value "88"^^xsd:integer

carreUser:b3bc5 carreSensors:has_who_b_p_level carreUser:b3bc5_who_b_p_level

carreUser:b3bc5_who_b_p_level carreSensors:has_value "4"^^xsd:integer
```

which conforms to the RDF schema for measurements given in D.2.4.

4.3.4. Historical data retriever implementation

In order to support the notification mechanisms of each sensor data provider, the aggregator is, as discussed above, able to respond to HTTP messages of various formats which each, essentially, instruct the aggregator to fetch the data corresponding to a particular user for a particular date or date range. We take advantage of this mechanism in order to retrieve the historical data for each user.

When a sensor data provider is first connected to user's account, we store the date at which the connection was made. All data created *after* that date will of course be fetched by the aggregator. We have also stored the start date of the CARRE project (1st November 2013). By making use of the Unix cron task scheduler, periodically throughout the day, a "fake" notification will be sent to the aggregator, requesting the data for that user for that sensor provider for a fixed time period, beginning at the CARRE start date. Each time the task is run, it requests data for a later period, moving forward in time until it has reached the date on which the user connected that provider. At this point, the user's graph on the semantic repository will contain all data belonging to that user from the provider in question from the beginning of CARRE to the present date (or from the date the user first started gathering sensor data, if that date is later than the beginning of CARRE).

Users who do not wish to have older data fetched have the ability to disable this feature. It is enabled by default.

4.3.5. CARRE Devices implementation

The interface to the aggregator is provided by the CARRE Devices site, hosted at

https://carre.kmi.open.ac.uk/devices

The site is built in Python. The Dashboard, with which a user is introduced on the first logging in, presents icons for all of the supported sensor data providers (Figure 47). If the user clicks or taps on any one of them, (s)he will be led through the authentication process for that provider, and asked to approve the request from the CARRE aggregator to access data from the provider. The appropriate authentication details will then be stored in the user's graph on the semantic repository, allowing the aggregator to begin fetching new data as it arrives, and triggering the historical data fetching process.

For advanced users and developers, the site also provides a SPARQL search box, for querying.

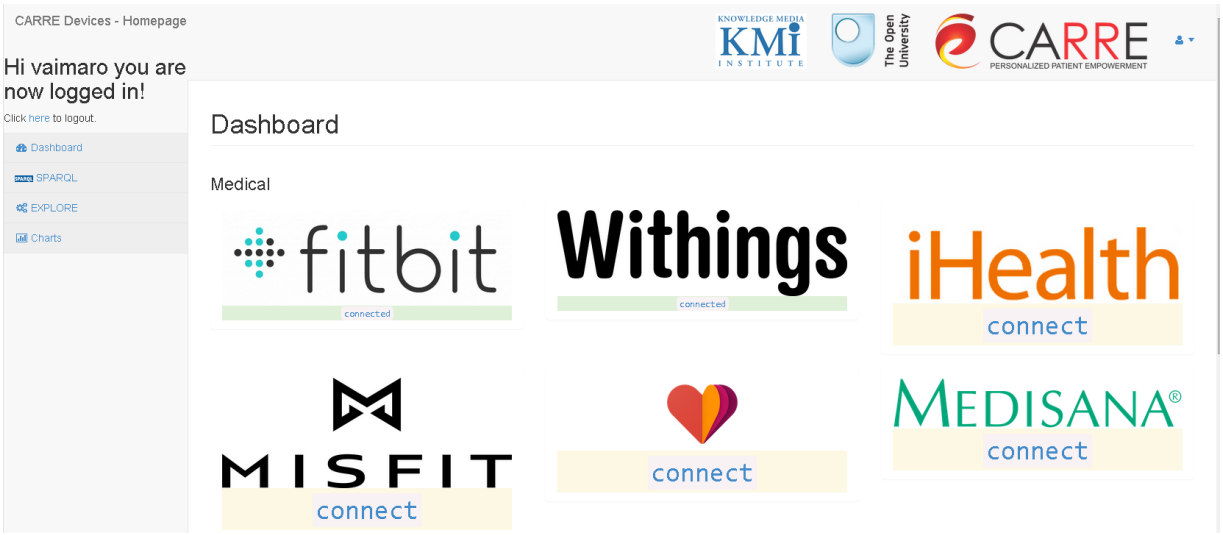

Figure 47. The CARRE Devices Dashboard

4.3.6. Sequence diagrams for authentication and personal data retrieval from 3d party sensor clouds

Figure 48 shows sequence diagram of personal data retrieval from the iHealth cloud service. iHealth uses OAuth 2.0 authentication. The first step is the creation of the application within the iHealth cloud webpage which provides the developer with access credential. In the application, the developer also sets data aggregator web addresses and monitoring URL which empowers data collection on notifications (when new user data is available). When the CARRE sensor data aggregator (the “Web Service Application” of Figure 48). After certain amount of time, the access token may expire, thus it is constantly refreshed. The sequence diagrams of other cloud services which use OAuth 2.0 authentication (e.g. Misfit, GoogleFit support both OAuth 1.0a and OAuth 2.0) are similar except of the data names.

Figure 49 shows sequence diagram of personal data retrieval from the Medisana cloud service. Medisana uses slightly modified OAuth 1.0a authentication which uses HMAC-SHA256 encryption instead of HMAC-SHA1. As in case with iHealth, the developer creates application within the Medisana cloud service page and receives the access credentials. Similarly, aggregator and notification URLs are set in the application form. After successful connection to the Medisana cloud service by aggregator web service application, personal data can be retrieved. The sequence diagrams for other vendors which support OAuth 1.0a (e.g. Withings, GoogleFit, Fitbit) authentication would be similar except the data names.

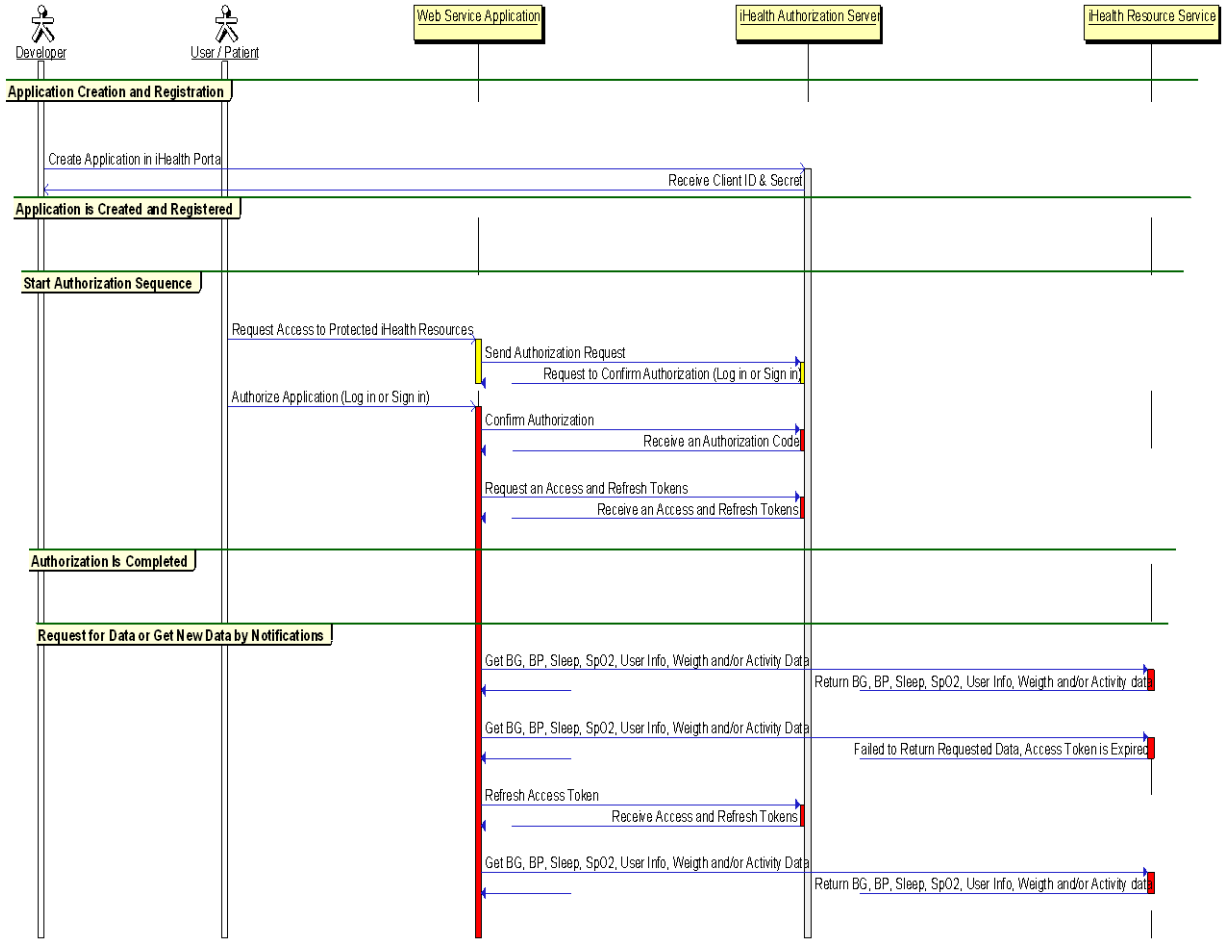

Figure 48. Sequence diagram of the iHealth personal data aggregator

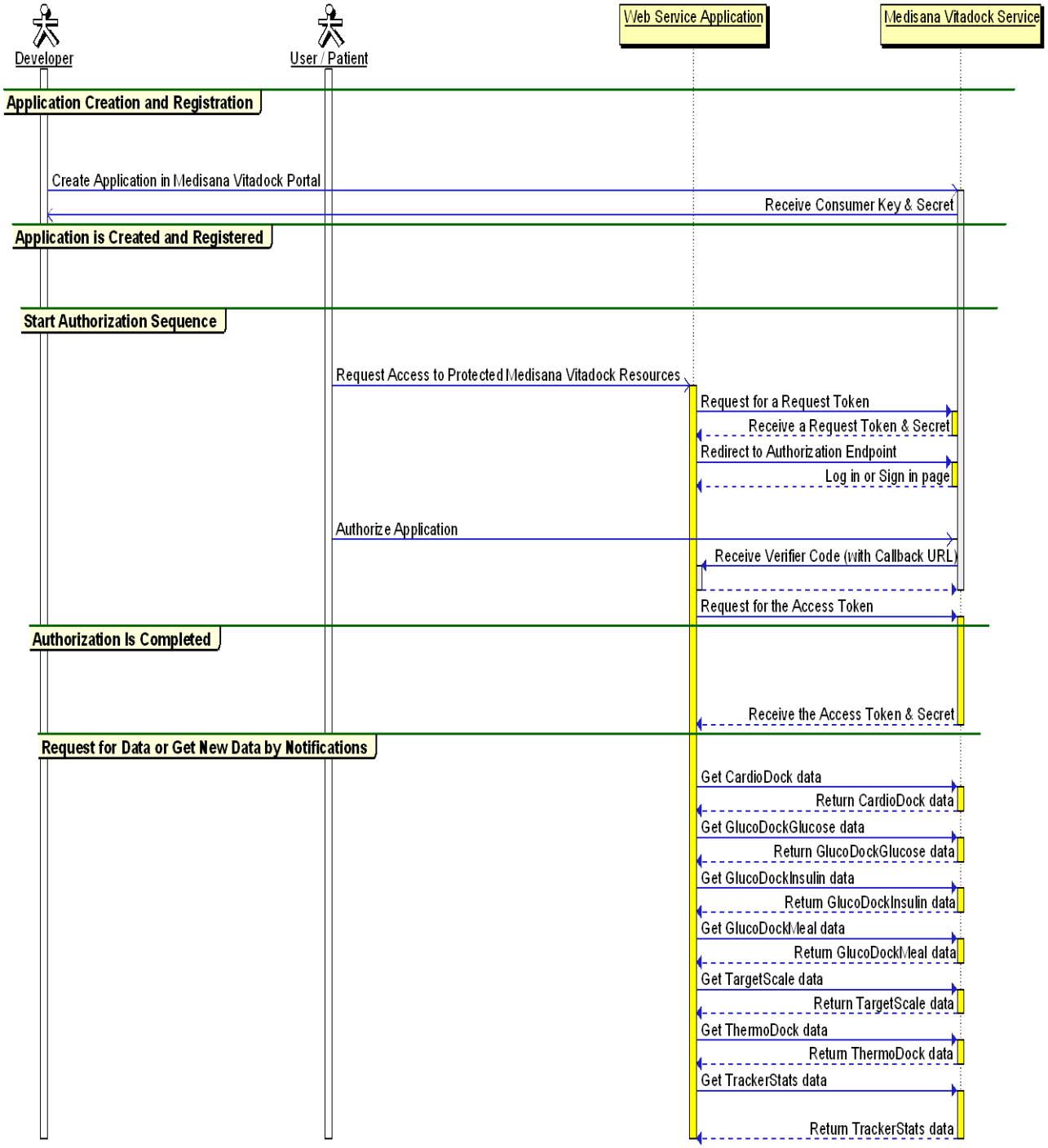

Figure 49. Sequence diagram of the Medisana personal data aggregator

4.3.7. Code metrics

Table 23 shows code metrics of Django application tripleStore that implements the backend of CARRE sensors aggregator.

Table 23. Code metrics of tripleStore	
Python code metrics	
Lines of Code	2822
Logical Lines of Code	2146
Source Lines of Code	2342
Number of Comment Lines	153
Number of Lines Representing Multi-line Strings	33
Number of Blank Lines	480

Table 24 shows code metrics of Python code which is responsible for calling the responders and fetching historical data.

Table 24. Code metrics of historicalData	
Python code metrics	
Lines of Code	277
Logical Lines of Code	190
Source Lines of Code	232
Number of Comment Lines	20
Number of Lines Representing Multi-line Strings	0
Number of Blank Lines	45

Table 25 shows code metrics[76] of Java code for sensor aggregator responders.

Table 25. Code metrics of sensor aggregator responders	
Java code metrics	
Lines of Code	7148
Method Hiding Factor	0,118
Method Inheritance Factor	0,398
Polymorphism Factor	0,167

4.4. Hardware aggregator selection

The hardware aggregator must be either an Android tablet or smartphone. It cannot be an old device in order to be compatible with sensors' apps. Bluetooth v4.0 Low Energy (BLE) compatibility is crucial, since a number of proposed sensors are provided with BLE only. Large screen is preferred having in mind the ease of use, especially for elderly patients. It is expected that the price of the device should be about 300 EUR. Further on in this chapter we will discuss tablets and smartphones separately and choose one device in each category.

[76] Calculating MOOD Metrics for Java, http://poseidon.cs.uni-magdeburg.de/oomj/index_files/MOOD%20Java%20Assumptions.doc

We propose to use both, tablets and smartphones, and enable patient to choose the device which is the most suitable for him / her.

4.4.1. Tablets

The tablet would be the most suitable device because of the screen size. Mobile internet version is preferred in case a patient does not have a Wi-Fi network at home. However, most of the BLE compatible tablets are not cheap enough. Table 26 presents the chosen tablets for comparison that are available and suitable for the project.

Table 26. Tablets for the comparison of the price

Model	Approximate price, EUR
Samsung Galaxy Tab S 8.4[77]	440-490
HTC Nexus 9[78]	570
Samsung Galaxy Tab 4 10.1[79]	310
Samsung Galaxy Tab 4 7.0[80]	200

As we can see, there are only two tablets in the expected price range. The main difference between them is the screen size. The 10.1 inch display is preferred. Therefore, the Samsung Galaxy Tab 4 10.1 LTE tablet is proposed to be used as the hardware aggregator in the project.

4.4.2. Smartphones

Smartphones, on the other hand, have their own advantages. They can be carried in the pocket all the time, thus ensuring more frequent health data updates from the sensors. Additionally, there are some smartphones with quite large displays (5-6 inch), which are sometimes even called “phablets”. The price comparison of such smartphones is presented in Table 27.

Table 27. Smartphones for the comparison of the price

Model	Approximate price, EUR
Motorola Nexus 6[81]	600
Samsung Galaxy S4[82]	300
Samsung Galaxy Note 3[83]	450
Samsung Galaxy Note 3 Neo[84]	300

In this case, again, two devices fall in the expected price range. The Galaxy Note 3 Neo is newer than Galaxy S4, has larger screen (5.5 inch vs. 5 inch). It is basically downgraded version of Galaxy Note 3. However, what is downgraded (0.2 inch smaller display, lower resolution, slightly slower processor) does not seem to affect performance required for the project and sensors’ data aggregation. Therefore, the Samsung Galaxy Note 3 Neo is proposed to be used as the hardware aggregator in the project.

[77] http://www.gsmarena.com/samsung_galaxy_tab_s_8_4_lte-6435.php (Last accessed 01/27/2015)
[78] http://www.gsmarena.com/htc_nexus_9-5823.php (Last accessed 01/27/2015)
[79] http://www.gsmarena.com/samsung_galaxy_tab_4_10_1_lte-6239.php (Last accessed 01/27/2015)
[80] http://www.gsmarena.com/samsung_galaxy_tab_4_7_0_lte-6241.php (Last accessed 01/27/2015)
[81] http://www.gsmarena.com/motorola_nexus_6-6604.php (Last accessed 01/27/2015)
[82] http://www.gsmarena.com/samsung_i9500_galaxy_s4-5125.php (Last accessed 01/27/2015)
[83] http://www.gsmarena.com/samsung_galaxy_note_3-5665.php (Last accessed 01/27/2015)
[84] http://www.gsmarena.com/samsung_galaxy_note_3_neo-5961.php (Last accessed 01/27/2015)

Annex 1
Sensor Aggregator Software

What is CARRE Sensor Data Aggregator?

The main goal of Sensor Data Aggregator is to integrate sensors data from data clouds of various manufacturers such as iHealth, Fitbit, Medisana, Misfit, Withings, Google Fit, to convert that data RDF triples and to store that RDF in the CARRE semantic repository.

The main parts of this aggregator are: the **Sensor Aggregator Responder,** the **Historical Data Retriever** and the **Triple Store**.

- The **Sensor Aggregator Responder** is a Web service which responds to HTTP GET or POST notifications, identifying the sensor provider who initiated the notification and the CARRE user to whom the data belongs. It invokes the relevant service corresponding to that provider, which then fetches that new data converts it into RDF and stores it in the CARRE semantic repository.
- The **Historical Data Retriever** is the historical data retriever designed to fetch data stored by sensor providers from before the date a user connected that provider to CARRE. By default, data is fetched from the start date of the CARRE project. This process only applies to users who agree explicitly to their historical data being fetched.
- The **Triple Store** is the Django application that implements the connection of sensors' manufacturers with CARRE's RDF repository (Virtuoso).

Download

Sensor Aggregator Responder v0.2:

- Source (687 KB): CARRE_Sensor_Aggregator_Responders_v0.2.zip (Java code)

  download from https://carre.kmi.open.ac.uk/sites/default/files/sensor-aggregator-responders-and-metrics-source%202.zip

  or from http://www.carre-project.eu/

- Source (363 KB): SCRIBE Library_v1.3.3.jar (Java binary)

  download from https://carre.kmi.open.ac.uk/sites/default/files/scribe-1.3.3W.jar

  or from http://www.carre-project.eu/

Historical Data Retriever v1.0:

- Source (4 KB): CARRE_Historical Data Retriever.zip (Python code)

  download from https://carre.kmi.open.ac.uk/sites/default/files/historicalData.zip

  or from http://www.carre-project.eu/

Triple Store v1.0:

- Source (33 KB): CARRE_Triple_Store.zip (Python code)

  download from https://carre.kmi.open.ac.uk/sites/default/files/tripleStore.zip

  or from http://www.carre-project.eu/

Sensor Data Aggregator is Open Source

CARRE Sensor Data Aggregator is Open Source and can be freely used in Open Source applications under the terms GNU General Public License (GPL).

Annex 2
Detailed drawings of printed circuit boards of CARRE wrist worn device

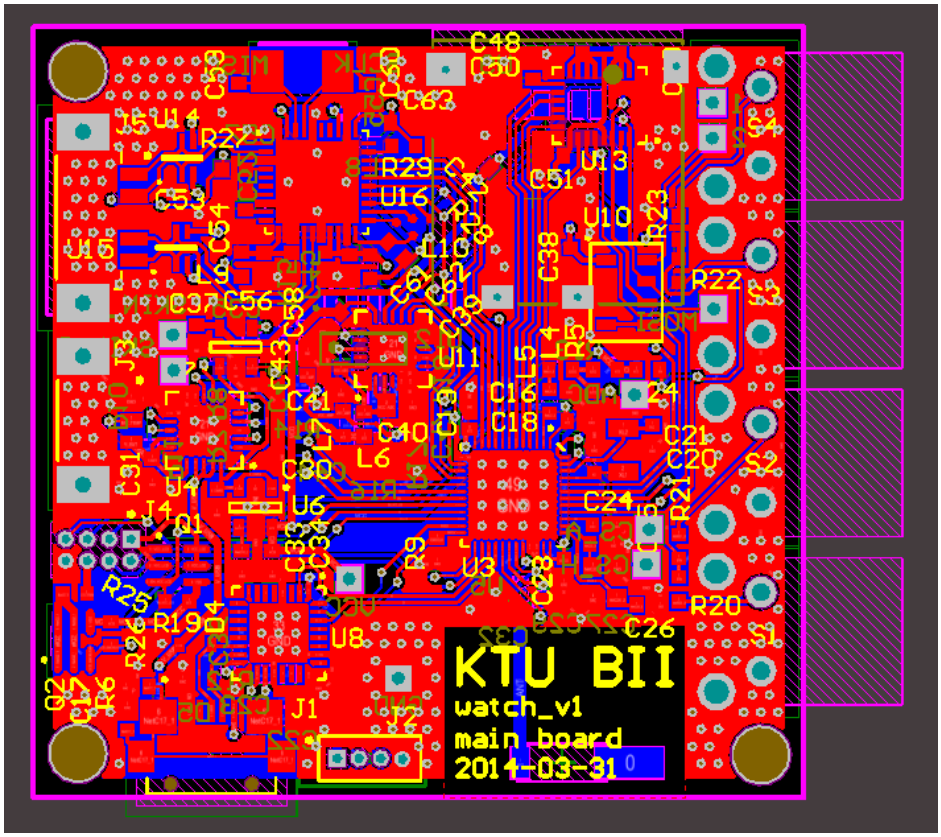

Figure 50. Top layer of the main PCB

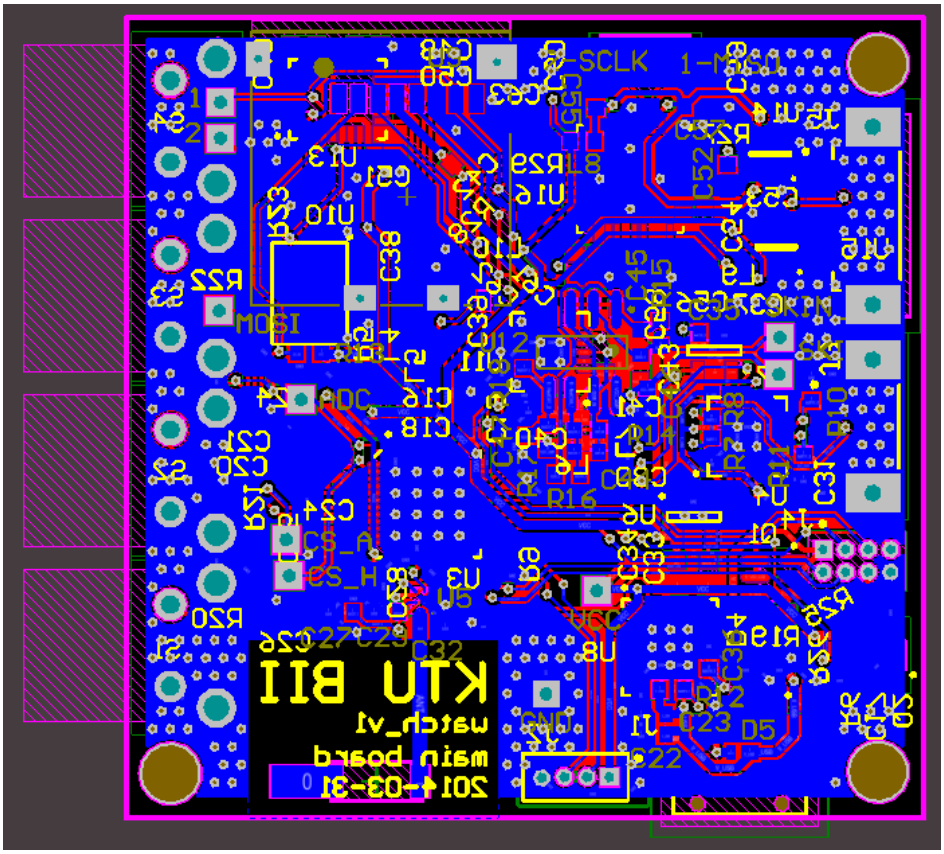

Figure 51. Bottom layer of the main PCB

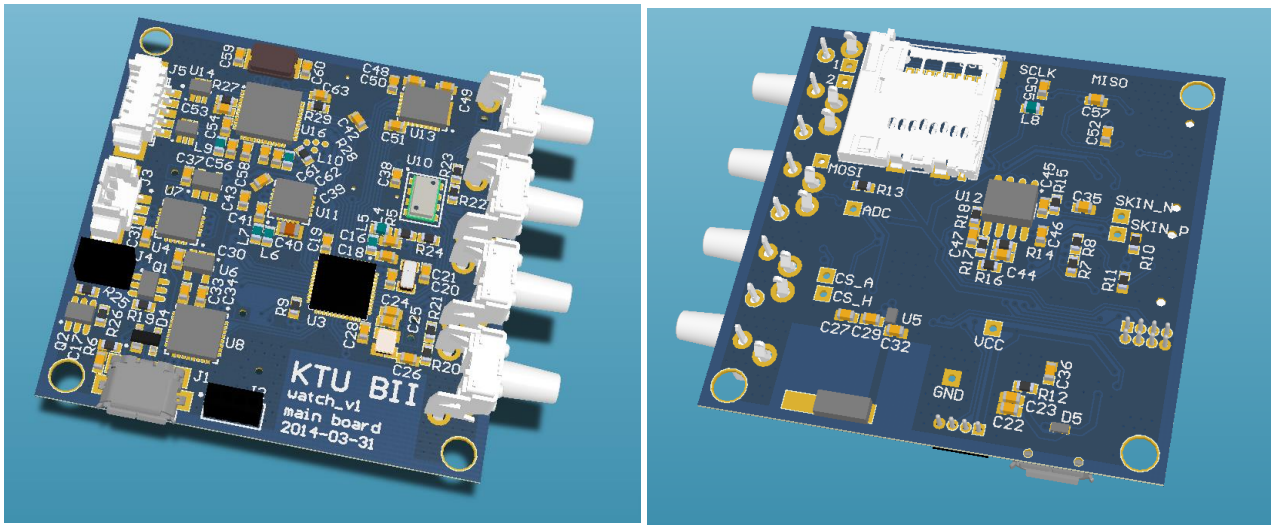

Figure 52. 3D drawings of the main PCB

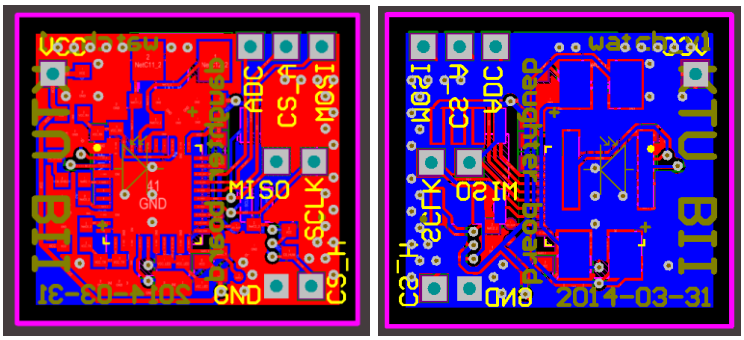

Figure 53. Top (left) and bottom (right) layer of the daughter PCB

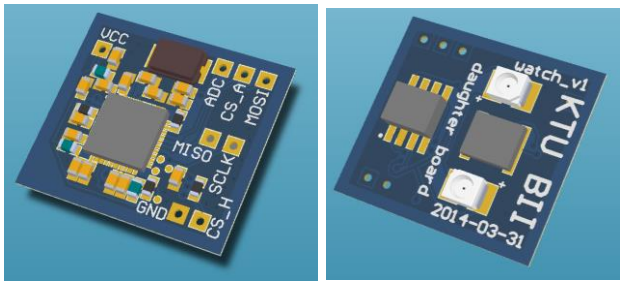

Figure 54. 3D drawings of the daughter PCB

Annex 3
Detailed drawings of printed circuit boards of CARRE multiparametric weight scale

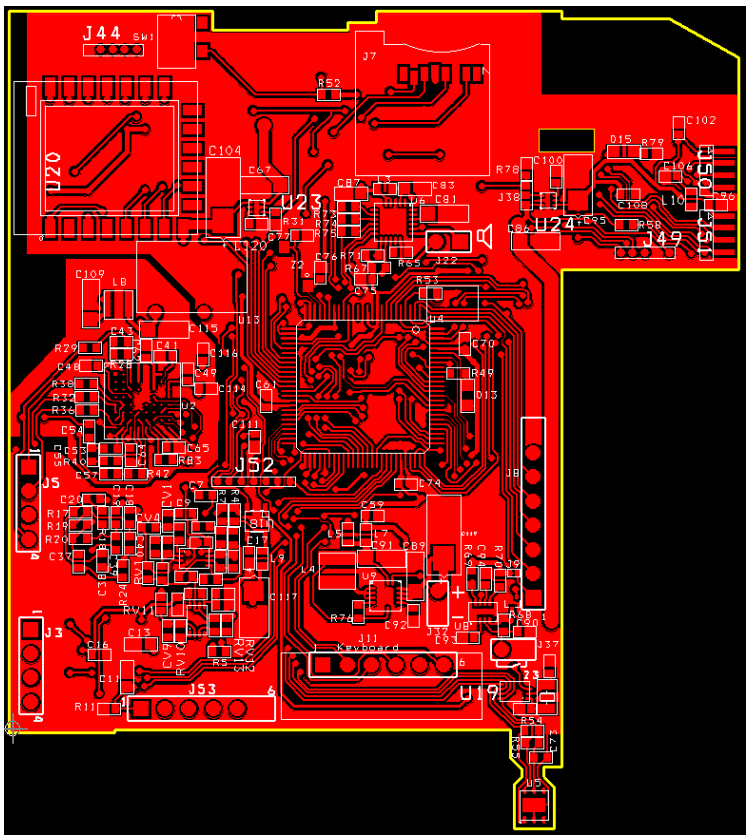

Figure 55. Top layer of the main PCB

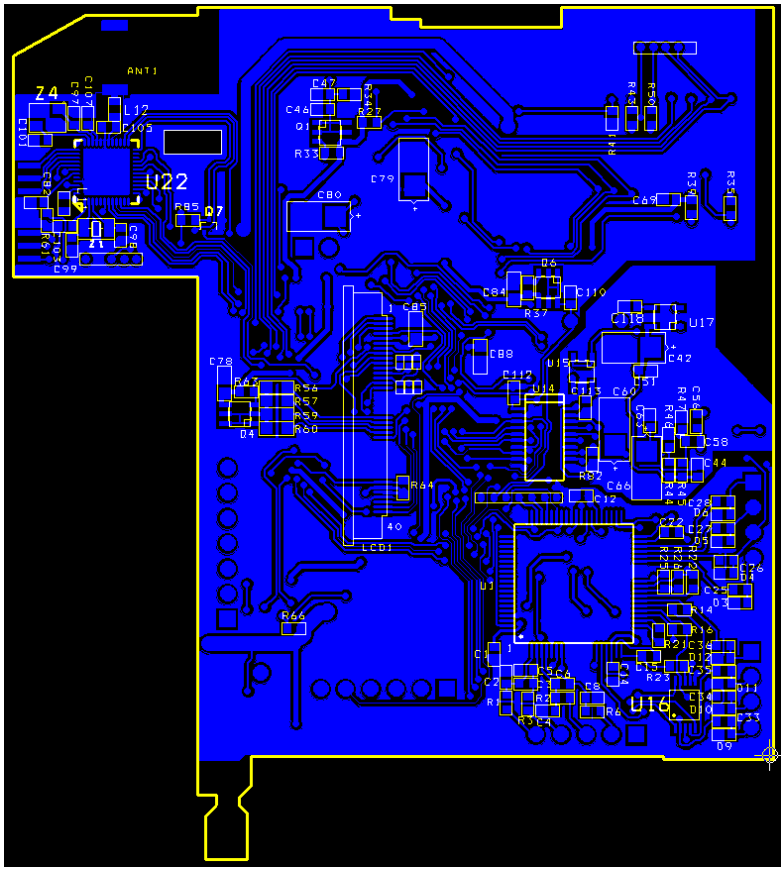

Figure 56. Bottom layer of the main PCB

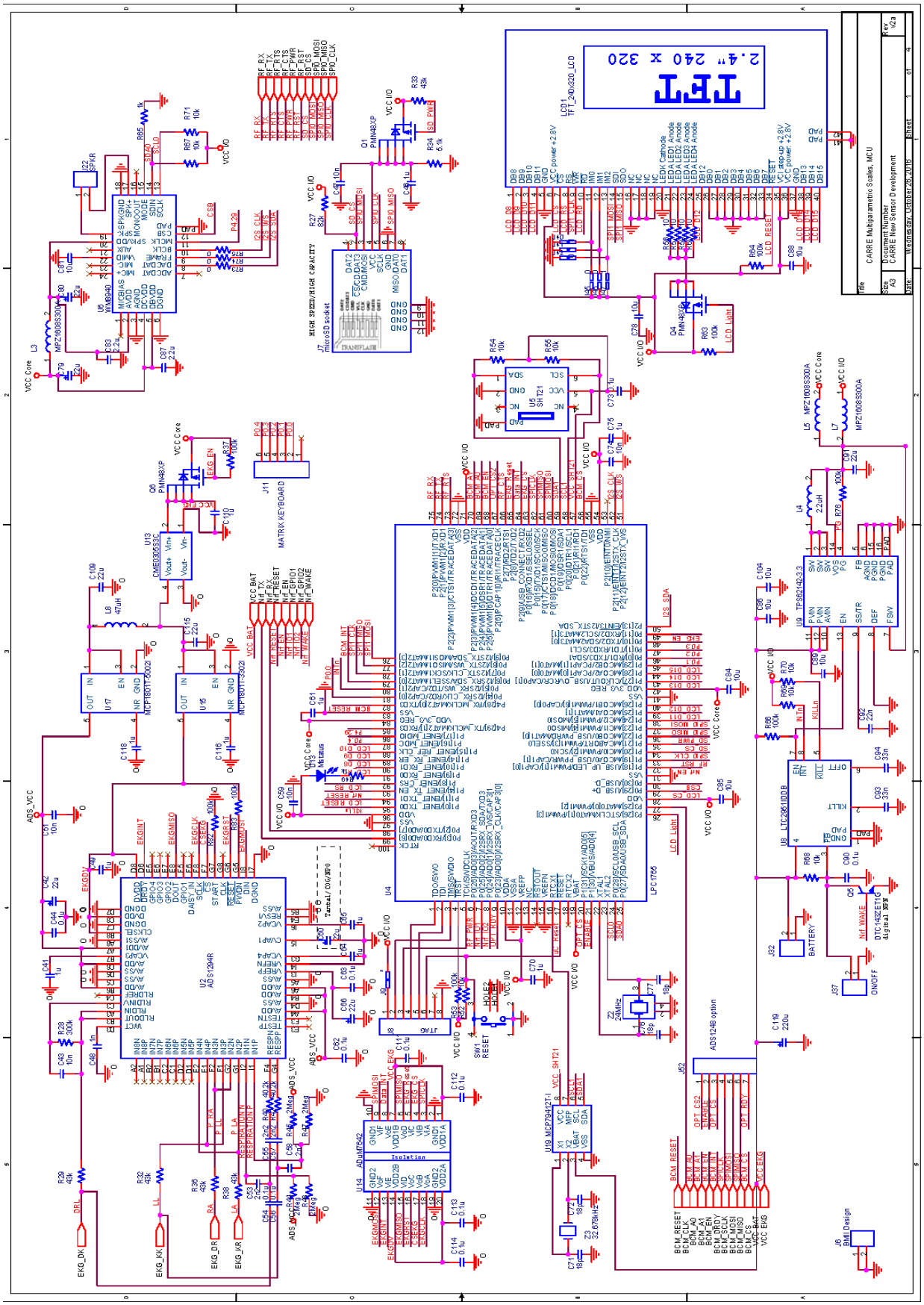

Figure 57. Schematics of ECG & main microcontroller block

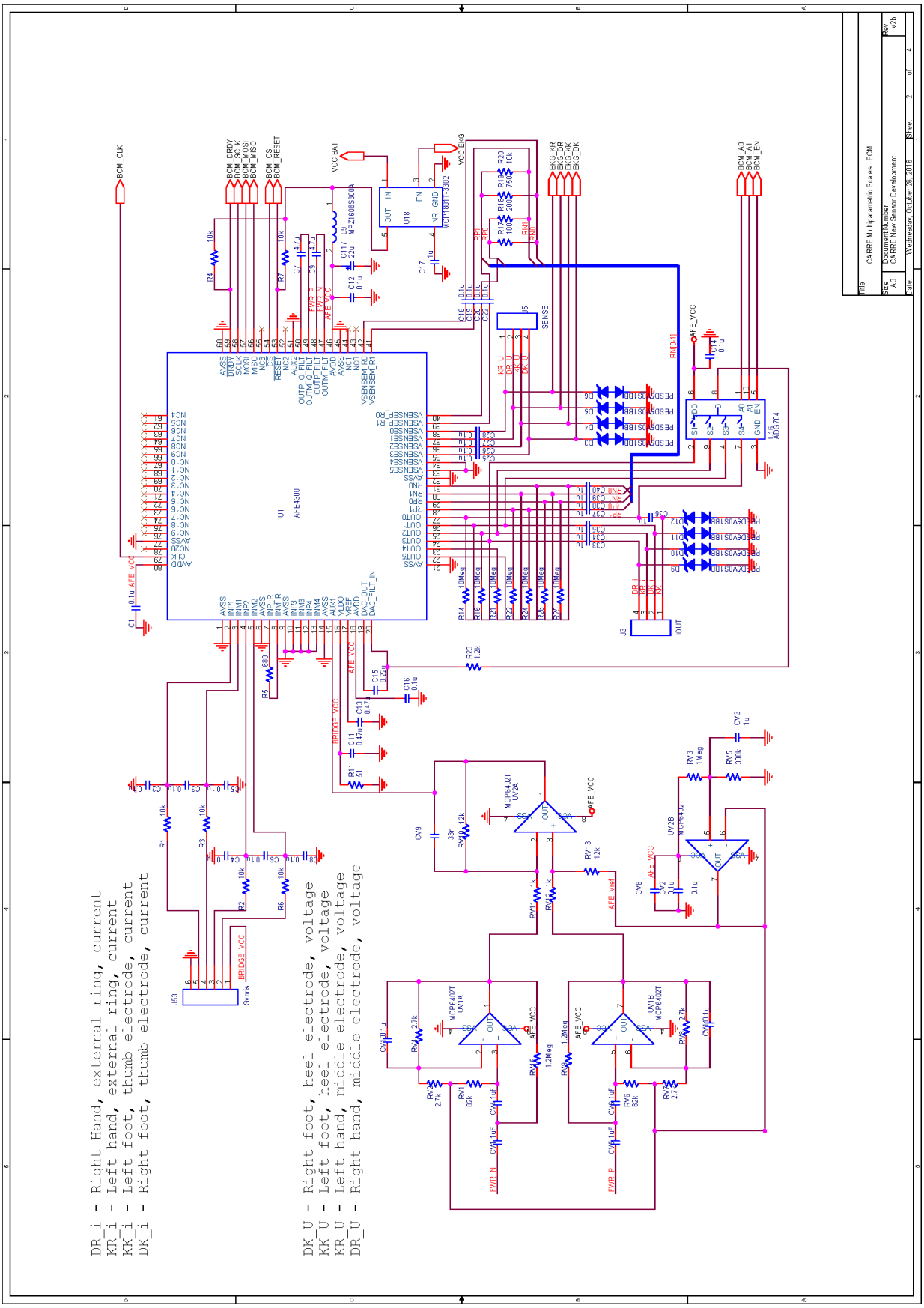

Figure 58. Schematics of Weight & Body composition frontend block

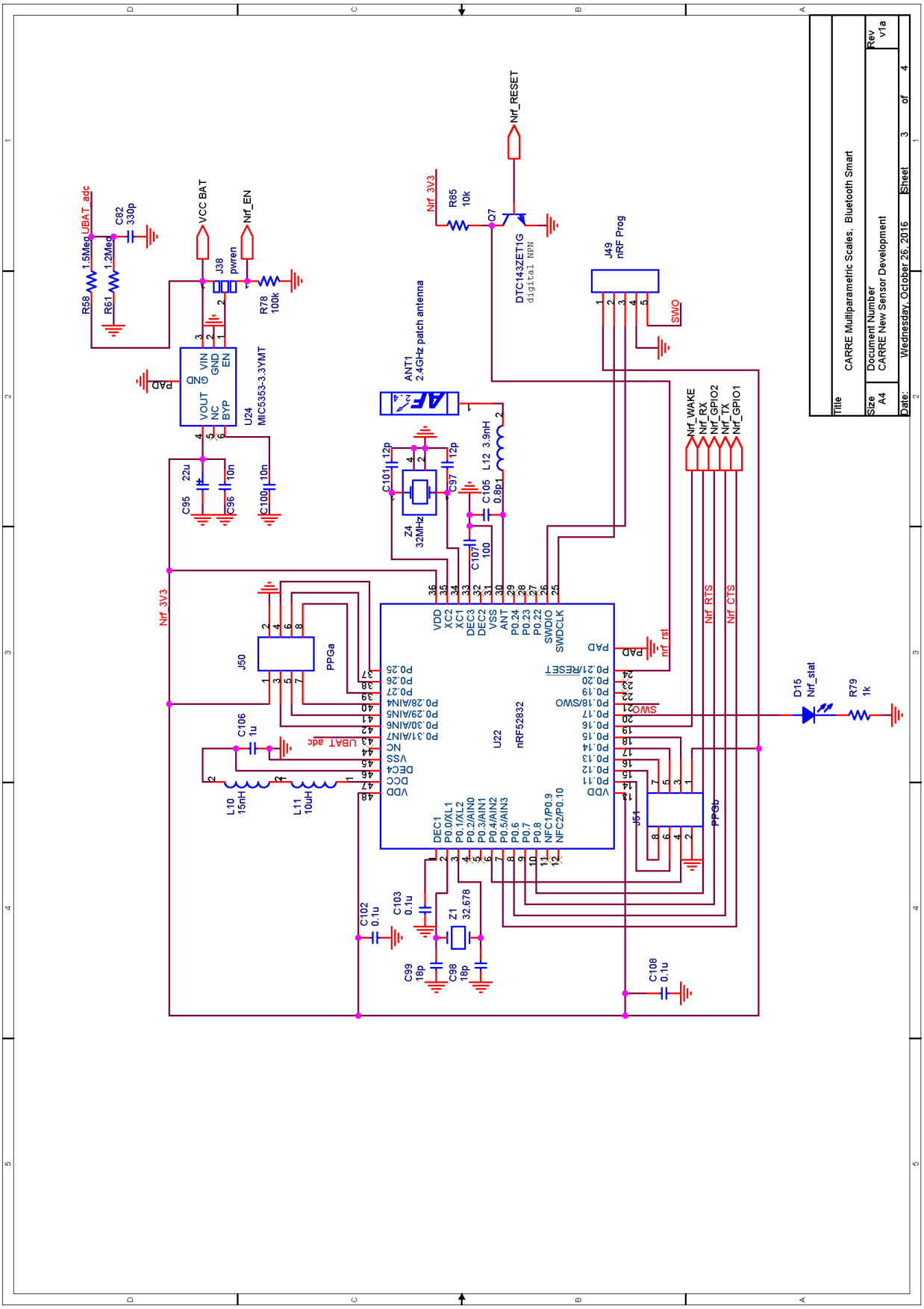

Figure 59. Schematics of Bluetooth Smart block

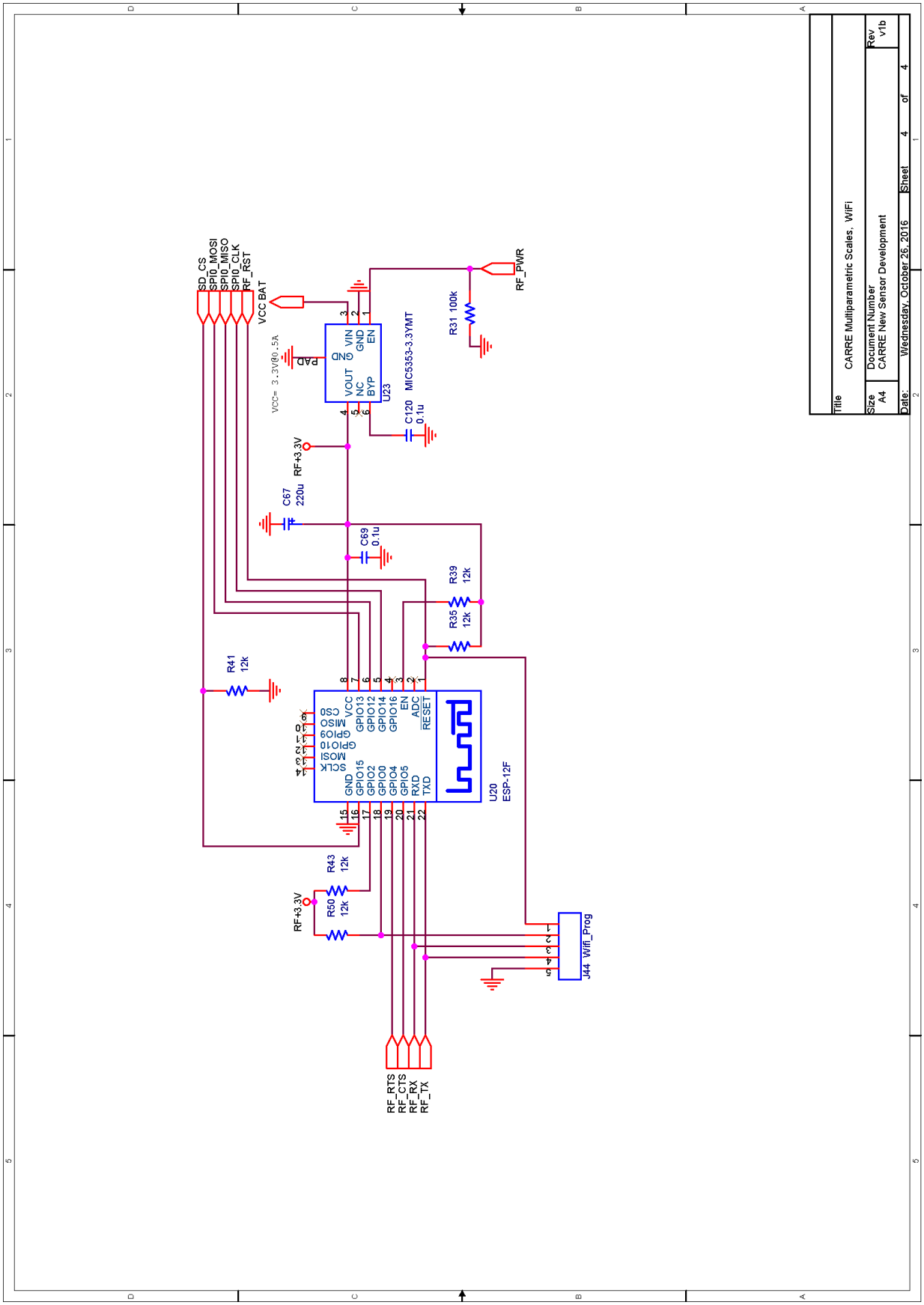

Figure 60. Schematics of Wifi block